Design and Evaluation of a Data-distributed Massively Parallel Implementation of a Global Optimization Algorithm—DIRECT

by

Jian He

The dissertation submitted to the Faculty of the
Virginia Polytechnic Institute and State University
in partial fulfillment of the requirements for the degree of

DOCTOR OF PHILOSOPHY

in

Computer Science

APPROVED:

Layne T. Watson (Chair)	Christopher Beattie
Joel A. Nachlas	Calvin J. Ribbens
Adrian Sandu	Clifford A. Shaffer

November 15, 2007
Blacksburg, Virginia

Keywords: DIRECT, dynamic data structures, global optimization, load balancing, massively parallel schemes, performance evaluation

Design and Evaluation of a Data-distributed Massively Parallel Implementation of a Global Search Algorithm—DIRECT

Jian He

(ABSTRACT)

The present work aims at an efficient, portable, and robust design of a data-distributed massively parallel DIRECT, the deterministic global optimization algorithm widely used in multidisciplinary engineering design, biological science, and physical science applications. The original algorithm is modified to adapt to different problem scales and optimization (exploration vs. exploitation) goals. Enhanced with a memory reduction technique, dynamic data structures are used to organize local data, handle unpredictable memory requirements, reduce the memory usage, and share the data across multiple processors. The parallel scheme employs a multilevel functional and data parallelism to boost concurrency and mitigate the data dependency, thus improving the load balancing and scalability. In addition, checkpointing features are integrated to provide fault tolerance and hot restarts. Important algorithm modifications and design considerations are discussed regarding data structures, parallel schemes, error handling, and portability.

Using several benchmark functions and real-world applications, the present work is evaluated in terms of optimization effectiveness, data structure efficiency, memory usage, parallel performance, and checkpointing overhead. Modeling and analysis techniques are used to investigate the design effectiveness and performance sensitivity under various problem structures, parallel schemes, and system settings. Theoretical and experimental results are compared for two parallel clusters with different system scale and network connectivity. An analytical bounding model is constructed to measure the load balancing performance under different schemes. Additionally, linear regression models are used to characterize two major overhead sources— interprocessor communication and processor idleness, and also applied to the isoefficiency functions in scalability analysis. For a variety of high-dimensional problems and large scale systems, the data-distributed massively parallel design has achieved reasonable performance. The results of the performance study provide guidance for efficient problem and scheme configuration. More importantly, the generalized design considerations and analysis techniques are beneficial for transforming many global search algorithms to become effective large scale parallel optimization tools.

ACKNOWLEDGMENTS

I am thankful that I was not alone on the long journey to finish this work. Accompanying by my side were my dear families, friends, professors, and collaborators who have given me tremendous support, encouragement, and help in the past five years.

First of all, I would like to thank my advisor, Dr. Layne T. Watson for his continued support and guidance on the journey that has not always been straight and easy. His penetrative observation and critical thinking helped keep this work on the right track. I am also grateful that he introduced me to his formal student, Dr. Masha Sosonkina at the Scalable Computer Ames Laboratory. As one of the few women in scientific fields, Masha served as a role model to me. We became not only collaborators who exchange ideas and co-author papers, but also friends who chat about nature and life.

I also would like to thank Drs. Clifford A. Shaffer, Calvin J. Ribbens, Christopher Beattie, Joel A. Nachlas, Adrian Sandu, and Eunice Santos for serving on my committee. Dr. Shaffer always asked good questions that helped me look at problems from different angles. Dr. Ribbens' enlightening and inspiring teaching on parallel computing granted me all the basic knowledge and hands-on skills for this work. I also enjoyed Dr. Beattie's training on numerical computation, Dr. Nachlas' discussion on generalization for optimization algorithms, and Dr. Sandu's presentation on interesting research topics. Due to unfortunate scheduling issues, Dr. Santos had to leave my committee two years ago. However, her advice on course selections and research directions was invaluable to this work.

Special thanks go to the JigCell research group for providing a precious real world testbed for this work. Jason W. Zwolak and Tom D. Panning applied this work to cell cycle modeling problems and gave me timely feedback that greatly improved the program functionality and usability.

Thanks must also be extended to Peter Haggerty, Rob Hunter, Luke Scharf, and Geoff Zelenka, who administrated and maintained the computing resources used in this work, including the System X and Anantham clusters.

Financial support for this work was provided in part by NSF Grant EIA-9974956, NSF Grant MCB-0083315, National Institutes of Health Grant 1 R01 GM64339-01, Air Force Research Laboratory Grant F30602-01-2-0572, and Department of Energy Grant DE-FG02-06ER25720.

Finally, my greatest thanks go to my families. To my parents, who came far away to help me in the busiest time of my life. To my husband, Alex Verstak, who collaborated with me on the S^4W project and provided insightful suggestions throughout the journey, which has become an unforgettable part of our lives. Wish the finish line of this journey would become the beginning of another exciting one for the years to come.

TABLE OF CONTENTS

List of Figures vi

List of Tables vii

1. Introduction 1
   - 1.1 Motivation 1
   - 1.2 Research Work Summary 3

2. The DIRECT Algorithm 5
   - 2.1 Algorithm 5
   - 2.2 Modification 6
   - 2.3 Related Work in DIRECT's Modification 8

3. Data Storage and Sharing 9
   - 3.1 Data Structures 9
   - 3.2 A Memory Reduction Technique 14
   - 3.3 Efficiency Study 15
   - 3.4 Related Work in Distributed Data Structures 17

4. Parallel Schemes 19
   - 4.1 Implementation Evolution 19
     - 4.1.1 pDIRECT_I 21
     - 4.1.2 pDIRECT_II 26
   - 4.2 Performance Comparison of pDIRECT_I and pDIRECT_II 33
     - 4.2.1 Selection Efficiency 34
     - 4.2.2 Task Partition 34
     - 4.2.3 Worker Assignment 38
   - 4.3 Related Work in Parallel Design for Global Optimization 41
     - 4.3.1 Direct Search Methods 41
     - 4.3.2 Combinatorial Optimization Methods 42

5. Error Handling 46
   - 5.1 Error Sources 46
   - 5.2 Checkpointing Method 47
   - 5.3 Overhead Evaluation 48

6. Performance Study, Modeling and Analysis 50
   - 6.1 Problem Configuration 51
     - 6.1.1 ϵ Tuning Parameter 51
     - 6.1.2 Problem Scale Parameter 52
     - 6.1.3 Memory Usage Comparison 52

6.2 Scheme Configuration 53
6.2.1 Parameter N_b 53
6.2.2 Subdomain Parameter m 54
6.2.3 Parameter n 59
6.2.4 Parameter k 61
6.3 Parallel System Parameters 63
6.3.1 Objective Function Cost 64
6.3.2 Network Characteristics 66
6.4 Scalability Analysis and Experiments 74
6.4.1 Vertical Scheme Scalability 74
6.4.2 Horizontal Scheme Scalability 81
6.4.3 Scalability Experiments 84

7. Real World Applications 87
7.1 Cell Cycle Modeling in Systems Biology 87
7.2 Simulation Results 89

8. Conclusion 91

References 93

Appendix A: Test Functions 98

Appendix B: VTDIRECT95 100
B.1 Package Organization 100
B.2 Portability Issues 101
B.3 Usage Guide 102

Appendix C: Shared Modules 104

Appendix D: Comments for VTdirect_MOD 137

Appendix E: Comments for pVTdirect_MOD 141

Vita 147

LIST OF FIGURES

Figure 1.1. The growth of number of boxes for a test problem. 2
Figure 1.2. Research work summary. 3
Figure 2.1. The sample points of DIRECT. 6
Figure 3.1. An example of a box scatter plot. 9
Figure 3.2. Box column lengths at the last iteration $I_{\max}$. 14
Figure 3.3. Growth of execution time with LBC or NON-LBC. 16
Figure 4.1. Three functional components. 19
Figure 4.2. The parallel scheme of pDIRECT_I. 21
Figure 4.3. Data structures in GPSHMEM. 24
Figure 4.4. The parallel scheme for pDIRECT_II. 26
Figure 4.5. Task partition schemes. 28
Figure 4.6. Comparison of the parallel efficiencies with different partition schemes and objective function costs. 35
Figure 4.7. The plot of N_i for Test Function 6 with $N = 150$. 37
Figure 4.8. Comparison of the workload (WL) patterns among workers. 40
Figure 6.1. Parallel efficiency comparison for the RO function. 52
Figure 6.2. Comparison of box memory usage without LBC or with LBC. 53
Figure 6.3. Comparison of the normalized workload on 99 workers. 54
Figure 6.4. Comparison of function minimization on FE and BY for a single domain and four subdomains. 55
Figure 6.5.(a) The 1-D view of the GR function. 55
Figure 6.5.(b) Comparison of function minimization on a 150-dimensional GR function for a single domain and four subdomains. 55
Figure 6.6. Comparison of the normalized workload bounds based on the model and the experiments on the GR function. 57
Figure 6.7. Comparison of the workload ranges based on the model and the experiments on all test problems. 57
Figure 6.8. Comparison of the average selection cost per master. 60
Figure 6.9. Comparison of the average box memory size. 60
Figure 6.10. Coefficient of variation of convex box and function evaluation shares for the horizontal scheme. 61
Figure 6.11. Coefficient of variation of the function evaluation shares for the vertical scheme. 63
Figure 6.12. Comparison of parallel efficiency as T_f changes using a small number of processors. 64
Figure 6.13. Parallel efficiency differences from that on System X to that on Anantham corresponding to the results in Figure 6.12. 64

Figure 6.14. Comparison of parallel efficiency as T_f changes using a large number of processors. 65
Figure 6.15. Parallel efficiency differences from that on System X to that on Anantham corresponding to the results in Figure 6.14. 66
Figure 6.16. Comparison of point-to-point latency test results. 67
Figure 6.17. Comparison of master response delay. 68
Figure 6.18. Comparison of the ratio R^2/e for different breakpoints of the piecewise T_{cp} model. 69
Figure 6.19. Histogram of residual errors of the linear regression models for T_{cp}. ..69
Figure 6.20. Comparison of broadcast latency result. 71
Figure 6.21. Comparison of the ratio R^2/e for different breakpoints of the piecewise T_{ca} model. 71
Figure 6.22. Comparison of broadcast latency growth pattern. 73
Figure 6.23. Histogram of residual errors of the linear regression models for T_{ca}. ..73
Figure 6.24.(a) Worker idle cycles. 76
Figure 6.24.(b) The function evaluations for all test problems. 76
Figure 6.25. The scatter plot of residuals $\delta_p(k)$. 77
Figure 6.26. The overhead measurement on a master and a worker. 79
Figure 6.27. The total master idle cycles. 81
Figure 6.28. The scatter plot of residuals $\delta'_p(n)$. 82
Figure 6.29. The growth of $\overline{T_e}$ as N and p increase. 85
Figure 6.30. Comparison of the fixed and scaled speedups. 86
Figure 7.1. Single-start DIRECT result: time lag for MPF activation. 89
Figure 7.2. Multistart DIRECT result: time lag for MPF activation. 89
Figure 7.3. Single-start DIRECT result: phosphorylation of Wee1. 90
Figure 7.4. Multistart DIRECT result: phosphorylation of Wee1. 90
Figure A.1. Griewank Function and Quartic Function. 98
Figure A.2. Rosenbrock's Valley Function and Schwefel's Function. 99
Figure A.3. Michalewicz's Function and Six-hump Camel Back Function. 99
Figure A.4. Branin rcos Function. 99
Figure B.1. The module/file dependency map. 100

LIST OF TABLES

Table 3.1. Execution time of the versions SL, HL, and HNL. 15
Table 3.2. The crossover point N_x and the threshold L_x. 16
Table 4.1. Test functions. 33
Table 4.2. Comparison of N_{gc}, N_{lc}, and N_d. 34

Table 4.3. Parallel timing results for different T_f. 35
Table 4.4. Comparison of theoretical execution time and timing results. 37
Table 4.5. Comparison of T_a, T_b, and T_c. 38
Table 4.6. Comparison of total number of subdomain function evaluations. 38
Table 4.7. Normalized workload ranges of experiments listed in Table 4.5. 39
Table 5.1. Comparison of serial checkpointing overhead. 49
Table 5.2. Comparison of parallel checkpointing overhead. 49
Table 6.1. Parameters and characteristics under study. 50
Table 6.2. N_I and N_e required for convergence with ϵ varying in (0.0, 1.0E-02). 51
Table 6.3. Comparison of I_{out} without (NON-LBC) and with LBC. 53
Table 6.4. Comparison of T_p and WR_p. 58
Table 6.5. Comparison of $\overline{N_{box}}$ and $\overline{N_f}$. 62
Table 6.6. Model formula, coefficients, e, and R^2 for T_{cp}. 70
Table 6.7. Model formula, coefficients, e, and R^2 for T_{ca}. 73
Table 6.8. Comparison of θ, e, and R^2 for the estimated linear growth of the worker idle cycles. 78
Table 6.9. Comparison of C_m, T^x_{oc}/k, T^a_{oc}/k, and T_{od}/k. 78
Table 6.10. The experimental results of T_{sk} and T_e. 80
Table 6.11. Comparison of θ', e, and R^2 for the estimated linear growth of the master idle cycles. 82
Table 6.12. Comparison of T^x_{ou}, T^a_{ou}, T^x_{oh}, T^a_{oh}, and T'_{od}. 83
Table 6.13. Verification experimental results of C_{cp}, C_{ca}, and T'_{od}. 83
Table A.1. Test functions selected from GEATbx [77]. 98

‘

CHAPTER 1: Introduction

1.1. Motivation

Global search algorithms have been increasingly applied to large scale optimization problems in many fields, including multidisciplinary engineering design, biological science, and physical science. Compared to local methods, these global approaches are more likely to discover the global optimum instead of being trapped at local minimum points for complex nonconvex or nonlinear problems with irregular design domain. The DIRECT algorithm [55] is one such global optimization algorithm that has been applied to large scale engineering design applications such as aircraft design [7] [8][21] [22], pipeline design [17], aircraft routing [10], surface optimization [98], transmitter placement [42] [47] [48], molecular genetic mapping [61], and cell cycle modeling [99] [74]. The complexity of these applications ranges from low dimensional with 3–20 variables to high dimensional with up to 143 variables.

Many global optimization problems require both supercomputing power and large data storage. For example, the parameter estimation problem for the budding yeast cell cycle [74] has 143 parameters with 36 stiff ordinary differential equations. A reasonable solution entails tens of thousands of function evaluations, requiring days to weeks of computation on a single processor. This type of application motivated this work, and many other massively parallel implementations, which also distribute data among processors to share the memory burden imposed by such high dimensional problems.

Since the birth of the first Beowulf 16-node cluster [12], numerous commodity-based cluster systems have been developed in academia and industry to provide cost-effective alternatives to expensive mainframe supercomputers. With the rapid expansion of problem scale and system size, adaptive and dynamic algorithms are being actively proposed to optimally harness the abundant computing resources. There are a few such examples in the field of global optimization algorithms, including parallel versions of direct search [25], branch-and-bound [19], Tabu search [86], and genetic algorithms [65]. These sophisticated parallel schemes take into account both algorithm characteristics and system attributes, thus producing reasonable parallel efficiency and scalability.

The nature of the DIRECT algorithm presents both potential benefits and difficulties for a sophisticated and efficient parallel implementation. At a high level, DIRECT performs two tasks— maintaining data structures that drive its selection of regions to explore and evaluating the objective function at chosen points. The multiple function evaluation tasks give rise to a natural functional parallelism. However, one of the limitations of DIRECT lies in the fast growth of its intermediate data. Jones [56] comments that DIRECT suffers from the "curse of dimensionality" that limits it to low dimensional problems (< 20). Figure 1.1 shows the growth of the number of search subregions ("boxes") for a standard test problem with dimensions $N = 10$, 50, 100, and 150. The amount of data grows rapidly as the DIRECT search proceeds in iterations, especially for high dimensional problems.

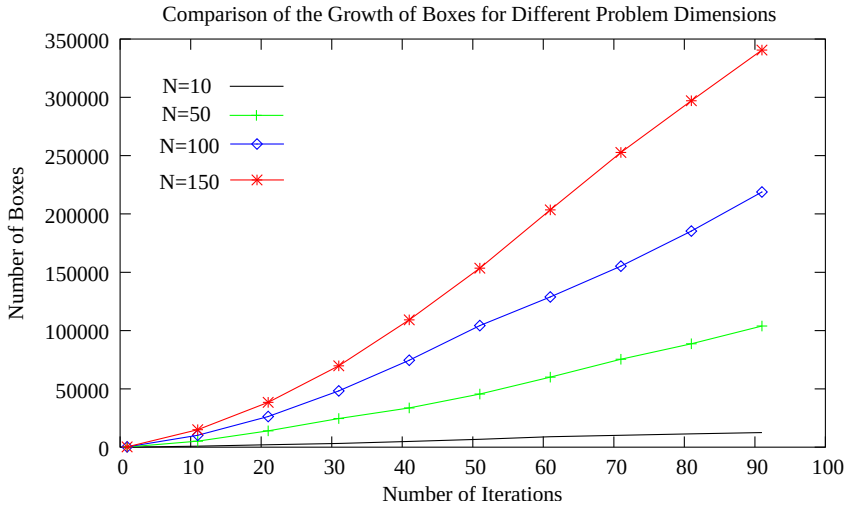

Figure 1.1. The growth of number of boxes for a test problem with dimensions $N = 10$, 50, 100, and 150.

This dictates techniques to reduce the size of data structures, thus the number of machines required to hold the distributed data in memory. The second task of evaluating the objective function at sample points presents its own challenges. The selection of sample points in the current iteration depends on all the points that have been sampled previously. This is so-called "data dependency", a design obstacle shared by many global search algorithms.

Previous parallel DIRECT implementations in the public domain include a FORTRAN 77 implementation [29] and a FORTRAN 90 implementation [93]. The data structures that they employ are static, thus inducing inefficiencies in handling an unpredictable memory requirement due to different problem structures and the nature of DIRECT's exploratory strategy. The parallel schemes have evolved from a classical master-slave paradigm in [29] to a fully distributed version with dynamic load balancing in [93]. In [29], Gablonsky adopts the master-slave scheme to parallelize the function evaluations, but little discussion is given to performance issues, such as intermediate data storage, load balancing, and communication, all of which raise many challenging issues related to both algorithms and running environments. Taking a step forward, Watson et al. [93] designed dynamic load balancing schemes for a distributed control version of DIRECT. However, other load balancing issues such as a single starting point and a distributed data structure were not considered in [93].

The design considerations absent from these earlier attempts have also motivated this work. Advanced features (derived data types, pointers, dynamic memory allocation, etc.) supplied by FORTRAN 90/95 were used to design dynamic data structures that flexibly organize the data on a single machine, effectively reduce the local data storage, and efficiently share the data across multiple processors. Moreover, a multilevel functional and data parallelism is proposed to produce multiple starting points, mitigate the data dependency, and improve the load balancing. In addition, checkpointing features are integrated to provide fault tolerance to power outage or hardware/memory failures, and enable hot restarts for large runs.

1.2. Research Work Summary

The main goal of this work is to (1) develop an efficient, portable, and robust implementation of a data-distributed massively parallel DIRECT, (2) evaluate the design effectiveness on a variety of problems, schemes, and systems, (3) guide the proper choice of optimization parameters and application settings, and (4) generalize the design considerations and analysis techniques that can be applied to parallelizing other global optimization algorithms challenged by large scale applications on massively parallel systems. A bottom-up approach was taken to accomplish the goal. The essential building blocks and the corresponding publications/reports are listed below.

(1) A modified DIRECT algorithm that offers more choices for different types of applications and preserves its strengths of global convergence and deterministic solution ([49] [50]).
(2) A set of dynamic data structures that adapt to varying memory requirements. ([49])
(3) A memory reduction technique that further mitigates the memory burden. ([46])
(4) Data-distributed massively parallel schemes and portable programming models that optimize the overall performance on large scale parallel systems. ([41] [40] [46])
(5) Error handling and checkpointing methods to enhance the program robustness. ([50])
(6) Performance studies using modeling and evaluation tools on different types of parallel systems. ([43] [45] [44])
(7) Real world applications featured with both low and high dimensions. ([42] [48] [47] [39] [6] [67] [84] [91])
(8) Software documentation on organization and usage that make this work accessible to others. ([50])

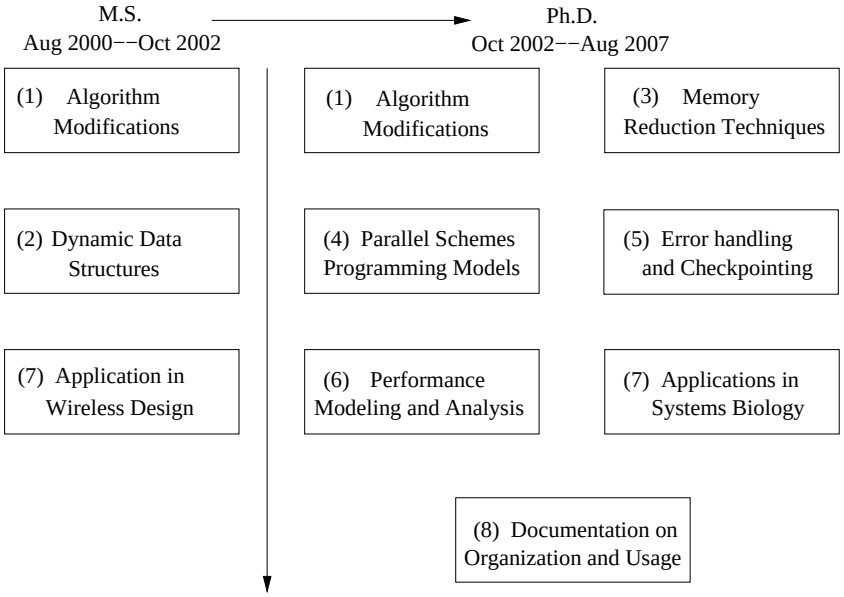

Figure 1.2. Research work summary.

The M.S. thesis [38] covers most of (1) and (2), and part of (6) and (7), which includes application examples of DIRECT in wireless communication systems. Several important improvements were made to the work in [38], so these materials are updated here. Also, a complete view of the entire body of work is shown in Figure 1.2.

(1) is described in Chapter 2, which also introduces the original DIRECT algorithm and presents a brief survey of the related work in DIRECT's modification. (2) and (3) are discussed in Chapter 3, covering the design issues, efficiency studies, and a survey of distributed data structures that inspired this work. (4) is presented in Chapter 4, where two different parallel implementations are compared. Chapter 5 describes (5) and reports the performance results of the checkpoint method under both serial and parallel computing environments. Chapter 6 presents (6) for performance study, modeling, and analysis that were done on System X, a 2200-processor Apple G5 cluster and Anantham, a 400-processor 64-bit Opteron Linux cluster. As examples for (7), real world parameter estimation problems for cell cycle modeling in systems biology are given in Chapter 7. Appendix A lists all the artificial test functions used in the study. Finally, (8) is included in Appendix B.

CHAPTER 2: The DIRECT Algorithm

Jones et al. [56] invented DIRECT (DIviding-RECTangles) as a Lipschitzian direct search algorithm for solving global optimization problems (GOPs) subject to bound constraints of the form

$$\min_{x \in D} f(x), \tag{2.1}$$

where $D = \left\{ x \in E^n \mid \ell \leq x \leq u \right\}$ is a bounded box in n-dimensional Euclidean space E^n, and $f : E^n \to E$ must satisfy a Lipschitz condition [52]

$$|f(x_1) - f(x_2)| \leq L\|x_1 - x_2\|, \quad \forall\, x_1, x_2 \in D. \tag{2.2}$$

Although DIRECT can be used for local optimization, it was designed as an effective global method that avoids being trapped at local optima and intelligently explores "potentially optimal" regions to converge globally for Lipschitz continuous optimization problems. As a direct pattern search method, DIRECT produces deterministic results and is straightforward to apply without derivative information or the Lipschitz constant of the objective function.

2.1. Algorithm

DIRECT's behavior in multiple dimensions can be viewed as taking steps in potentially optimal directions within the entire design space. The potentially optimal directions are determined through evaluating the objective function at center points of the subdivided boxes. The search is carried out through three essential operations: region selection, point sampling, and space division. [56] describes the original algorithm in six detailed steps, which are regrouped and relabeled to highlight the basic operations as below.

Given an objective function f and the feasible set D, the steps are:

1. **Initialization.** Normalize the feasible set D to be the unit hypercube. Sample the center point c_i of this hypercube and evaluate $f(c_i)$. Initialize $f_{\min} = f(c_i)$, evaluation counter $m = 1$, and iteration counter $t = 0$.
2. **Selection.** Identify the set S of "potentially optimal" boxes that are subregions of D. A box is potentially optimal if, for some Lipschitz constant, the function value within the box is potentially smaller than that in any other box (a formal definition with the tuning parameter ϵ is given by [56] and also can be found in [38]; see Section 3.1 for further explanation of ϵ.)
3. **Sampling.** For any box $j \in S$, identify the set I of dimensions with the maximum side length. Let δ equal one-third of this maximum side length. Sample the function at the points $c \pm \delta e_i$ for all $i \in I$, where c is the center of the box and e_i is the ith unit vector.

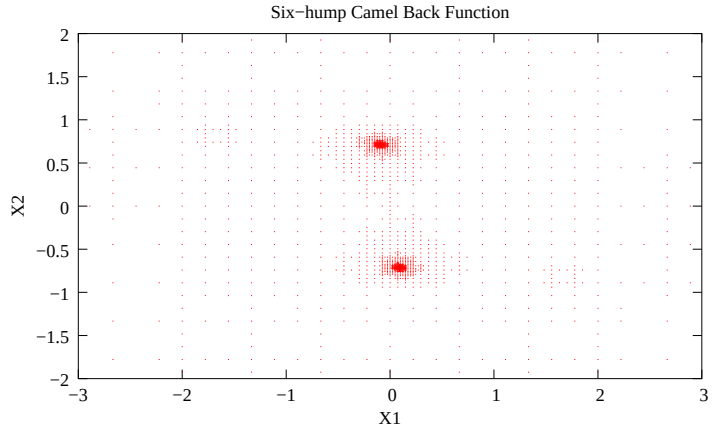

(a)

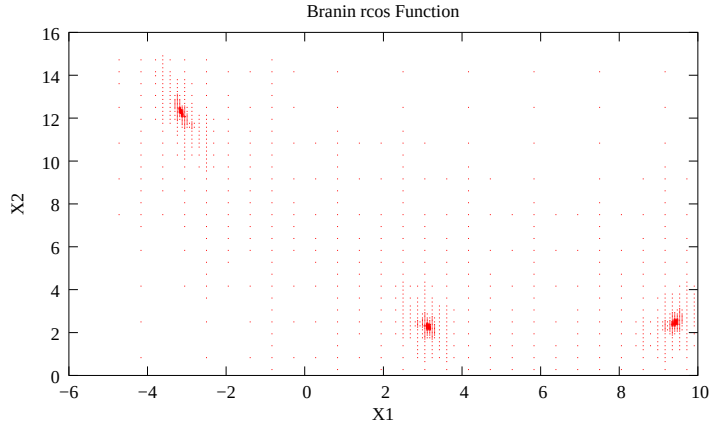

(b)

Figure 2.1. The sample points of DIRECT for (a) Six-hump Camel Back function (two global solutions) and (b) Branin rcos function (three global solutions).

4. **Division.** Divide the box j containing c into thirds along the dimensions in I, starting with the dimension with the lowest value of $w_i = \min\{f(c+\delta e_i), f(c-\delta e_i)\}$, and continuing to the dimension with the highest w_i. Update $f_{\min}$ and m.
5. **Iteration.** Set $S = S - \{j\}$. If $S \neq \emptyset$ go to **3**.
6. **Termination.** Set $t = t + 1$. If iteration limit or evaluation limit has been reached, stop. Otherwise, go to **2**.

[56] provides a good step-by-step example visualizing how DIRECT accomplishes the task of locating a global optimum. Figure 2.1 shows the sample points by DIRECT for the Six-hump Camel Back (SB) and Branin rcos (BR) two-dimensional functions (see Appendix A for a list of artificial test functions).

2.2. Modification

A few modifications were made in this work to meet the needs of various applications and improve the performance on large scale parallel systems.

For **Initialization**, an optional *domain decomposition* step is added to create multiple subdomains, each with a starting point for a DIRECT search. Empirical results have shown that this approach significantly improves load balancing among a large number of processors, and likely shortens the optimization process for problems with asymmetric or irregular structures.

The second step **Selection** has two additions. The first is an "aggressive" switch adopted from [93], which generates more function evaluation tasks that may help balance the workload under the parallel environment. The second is an adjustable ϵ, which is recommended by [56] to be within $(10^{-2}, 10^{-7})$, and "most naturally" 10^{-4} or the desired solution accuracy. The studies in [29] [31] show that $\epsilon = 0.0$ speeds up the convergence for low dimensional problems. In general, smaller ϵ values make the search more local and generate more function evaluation tasks. On the other hand, larger ϵ values bias the search toward broader exploration, exhibiting slower convergence. In the present work, the value of ϵ is taken as zero by default, but can be specified by the user depending on problem characteristics and optimization goals.

To produce more tasks in parallel, new points are sampled around all boxes in S along their longest dimensions during **Sampling**. This modification also removes the step **Iteration**, thus simplifying the loop. Differently in the serial version, **Sampling** samples one box at a time to eliminate unnecessary storage for new boxes. Another modification to **Sampling** is adding lexicographical order comparison between box center coordinates. Since box center function values may be the same or very close to each other, the parallel **Sampling** may yield a different box sequence in each box column as the parallel scheme varies. As a consequence, boxes will be subdivided in a different order, thus destroying the deterministic property of DIRECT. Hence, lexicographical order comparison is added to keep the boxes in the same sampling sequence on the same platform. Unfortunately, the deterministic property is hard to preserve across machines/compilers that produce different numerical values, so the numerical results for the same problem may vary slightly on different systems.

The last set of modifications, in **Termination**, is to offer more choices of stopping conditions. [56] commented that the original stopping condition on a limit on iterations `MAX_ITER` or evaluations `MAX_EVL` is not convincing for many optimization problems. Two new stopping rules proposed here are (1) minimum diameter `MIN_DIA` (exit when the diameter of the best box has reached the value specified by the user or the round off level) and (2) objective function convergence tolerance `OBJ_CONV` (exit when the relative change in the optimum objective function value has reached the given value).

2.3. Related Work in DIRECT's Modification

As a comparatively young method, DIRECT is being enhanced with novel ideas and concepts.

Jones has made a couple of modifications to the original DIRECT[55]. The modified version in **Division** only trisects in one dimension with the longest side length instead of in all identified dimensions in set I as above. The dimension to choose depends upon a tie breaking mechanism (e.g., random selection or priority by age).

Baker [7] first proposes the "aggressive DIRECT", which discards the convex hull idea of identifying potentially optimal boxes. Instead, it subdivides all the boxes with the smallest objective function values for different box sizes. The change results in more subdivision tasks generated at every iteration, which helps to balance the workload in a parallel computing environment.

Ljungberg et al. [61] report that DIRECT performs faster and more accurate than exhaustive grid search and a genetic algorithm. Zhu et al. [98] also found that DIRECT converges faster to a global optimum point than adaptive simulated annealing. The secret may lie in the tuning parameter ϵ defined in DIRECT to balance the global and local search efforts. Nevertheless, DIRECT still converges slowly compared to local or gradient-based algorithms, because a significant amount of time is consumed in exploring the entire design space, which is a common tradeoff between the search broadness and the convergence rate. Several modifications to DIRECT [29] [31] [28] [82] have been proposed to speed up the convergence. Gablonsky et al. [31] studied the behavior of DIRECT in low dimensions and developed an alternative version for biasing the search more toward local improvement by forcing $\epsilon = 0$. Finkel et al. developed an adaptive restart DIRECT that dynamically checks the search progress and updates the value of ϵ accordingly. Sergeyev et al. [82] proposed a diagonal partition strategy which samples two corner points of a region instead of the center in order to obtain more information about the design space and determine a set of reasonable Lipschitz constants that accelerate the convergence due to a better balanced global and local search.

Additionally, combining DIRECT with other methods has been found to be fairly successful to address the issue of slow convergence [71] [99] [74]. Nelson et al. [71] incorporated a trust region step to take advantage of the fast convergence of the local method. For noisy objective functions, Cox et al. [20] found that a combined local method with DIRECT can be stalled because it is confined by the bounds of the best box. A strategy called "box penetration" was developed in [20] to force a subset of boxes neighboring the best box to divide, thus avoiding being trapped in a local minima. Inside the global search loop of DIRECT, Zwolak et al. [99] created a local search loop using ODRPACK [14] to refine multiple sub-optimal results. Panning et al. [74] reported that the combination of DIRECT and MADS (mesh adaptive direct search) [5] discovered a better point than using either DIRECT or MADS alone.

CHAPTER 3: Data Storage and Sharing

One of the biggest design challenges of DIRECT is to break the "curse of dimensionality" first noted by its creators [56]. The approach here is to design dynamic data structures that are easily extensible to store continuously generated data from point sampling/space division and to share the data storage among multiple processors. The original design of the data structures is reported in [49] and [38], documented for the serial implementation previously named as VTDIRECT. The design has been improved by adopting a min-heap data structure and a memory reduction technique, and is used in the latest software package VTDIRECT95, a Fortran 95 implementation of DIRECT, including both serial and parallel codes (Appendix B).

3.1. Data Structures

DIRECT keeps subdividing the design space and selects potentially optimal regions according to the sampling results. The divided subregions are called "boxes". The key information for a box is stored in a derived data type `HyperBox`, containing an array of center point coordinates c, an array of box sides *side*, center point function value *val*, and box diameter *diam*. To identify potentially optional boxes, all the boxes are organized ideally by the center function values and box diameters as shown in Figure 3.1, where the vertical sequences of boxes and are called "box columns", which are sorted in the order of box diameters, while the boxes in each box column are sorted in the order of center function values. Jones et al. [56] have proved that the potentially optimal boxes are those on the lower right convex hull of the scatter plot shown in Figure 3.1, so they are also called "convex hull boxes" in this work. When $\epsilon > 0$, a line starting from $f^* = f_{\min} - \epsilon|f_{\min}|$ on the vertical axis of function values will screen out the boxes that may lead to insignificant improvement.

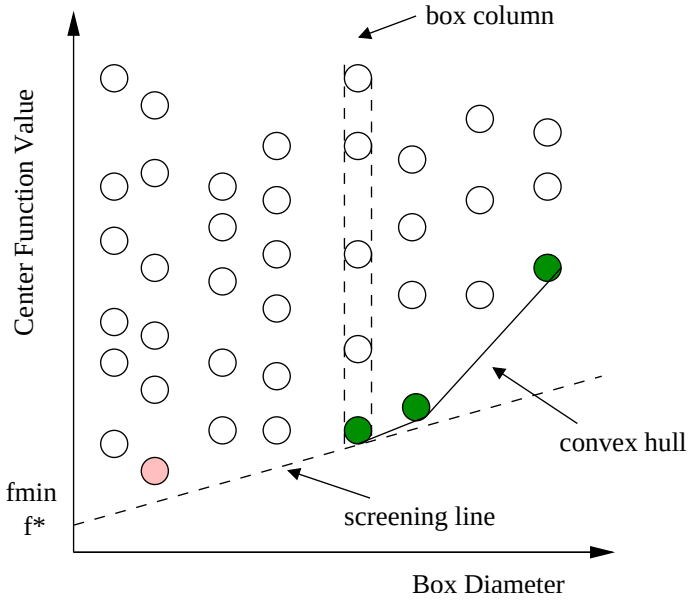

Figure 3.1. An example of a box scatter plot.

The horizontal strict order for the box diameters must be maintained to facilitate the convex hull computation. However, the vertical strict order of box center function values (implemented in the serial version described in [49]) is unnecessary for each box column, and it also incurs more operational cost such as shifting and sorting for box removal and insertion. Therefore, a min-heap data structure implements a box column, so that the lowest box owns the smallest function value and every box has a smaller function value than its left and right children if they exist. It lays out the potentially optimal box candidate at the bottom of the scatter pattern. Once this candidate box is determined to be potentially optimal, it will be removed from the heap to be subdivided, and the last box in the heap will be put to the first position and sifted down, reordering the heap in $\mathcal{O}(\log n)$ operations instead of the $\mathcal{O}(n)$ shifting operations required by a strictly increasing order of center function values. Similarly for box insertion, a new box is inserted at the end of the heap and sifted up in $\mathcal{O}(\log n)$, reduced from $\mathcal{O}(n)$, comparisons. The complexity is improved considerably, especially for large box columns.

In addition to `HyperBox`, `BoxMatrix` and `BoxLink` are the other two derived data types for storing boxes. These three are called "box structures" in [49]. `BoxMatrix` contains the following components:

(1) a two-dimensional array `M` of type `HyperBox`,
(2) an array of box counters `ind` for box columns,
(3) a pointer `child` that points to the next linked node of `BoxMatrix` needed when more box columns with new diameters are generated,
(4) an array `sibling` of pointers that point to linked nodes of type `BoxLink`, which are used to extend box columns beyond the storage afforded in `M`, and
(5) `id` to identify this box matrix among others.

Initially, a box matrix is allocated with empty box column structures (called "free box columns") according to the problem dimension and optimization scale. When currently allocated memory for a box column has been filled up, a new box link of derived type `BoxLink` is allocated dynamically adding a one-dimensional array of `HyperBox`es and associated components such as counter, pointers, and ID to extend the box column.

To maintain the strict order of box diameters for box columns, another set of "linked list structures" organizes box columns and recycles free box columns. The linked lists `setFcol` and `setInd` are of the type `int_vector`, containing a one-dimensional array *elements* of integers, an array $flags$ for marking convex hull boxes, pointers for linking nodes, and the node ID. The array $flags$ is only allocated and used for `setInd`. The third linked list `setDia` is derived from `real_vector` to hold an array of box diameters (real values), pointers, and ID. When a new box matrix is allocated, all the global IDs of its free box columns are computed based on its box matrix ID and inserted in `setFcol`. When a new box diameter is produced from **Division**, a free box column from `setFcol` is assigned to hold the box. An appropriate position for this box diameter will be found using a binary

search in `setDia`, which is sorted in decreasing order. Then, the global ID of the newly assigned box column is added in `setInd` at the corresponding position to that in `setDia`. The process is reversed when a box diameter disappears after the last box with this box diameter has been removed, so this box column becomes free. Subsequently, its diameter value and the global ID will be taken out from `setDia` and `setInd`, respectively. Finally, the free box column is recycled back to `setFcol` for later use.

Another practical issue is the sequence of dividing convex hull boxes. Because diameters are sorted in decreasing order in `setDia`, the serial version needs to start from the end of `setDia` and subdivide the box with the smallest diameter first, so that sifting up newly generated boxes would not override any existing convex hull boxes. Obviously, this potential overriding problem does not exist for the parallel version, which buffers all new boxes from subdivided convex hull boxes and inserts them all at one time. Hence, the parallel version starts from the beginning of `setDia`, thus avoiding the unnecessary cost of chasing the linked nodes of `setDia`.

A new feature is added to output multiple best boxes (MBB), which are found by searching through the box structures that hold all the information on the space partition. This feature is very useful for global optimization problems with complex structures, where local optimum points are far away from each other, thus demanding a large amount of space exploration and slowing convergence. In such a case, DIRECT is often used as a global starter to find good regions. Then, a local optimizer is applied to each region to efficiently find multiple local optimum points. Examples of this are presented in [99] and [74]. To activate the MBB option, an empty array `BOX_SET` of type `HyperBox` allocated with a user-desired size needs to be specified in the input argument list. Optionally, two more arguments `MIN_SEP` (minimal separation) and `W` (weights) can be given to specify the minimal weighted distance between the center points of the best boxes returned in `BOX_SET`. By default, `MIN_SEP` is half the diameter of the design space and `W` is taken as all ones. When the desired number of best boxes can not be found conditioned on `MIN_SEP` and `W`, the output argument `NUM_BOX` is returned as the actual number of best boxes in `BOX_SET`. The following pseudo code illustrates the MBB process and demonstrates a typical scenario of manipulating the dynamic data structures.

---

cc: the current best box center
c_b: the counter for best boxes stored in `BOX_SET`
c_m: the counter for marked boxes
$f_{\min}$: minimum function value
f_i: the current function value to be compared
i, j, k: loop counters
n_b: the desired number of best boxes
n_c: the number of columns allocated in M

n_e: the number of function evaluations
n_r: the number of rows allocated in M
p_b: the pointer to a box matrix
p_c: the pointer to a box
p_l: the pointer to a box link
sep: weighted separation between *cc* and a candidate box
x_0: minimizing vector scaled in the original design space
x_1: normalized x_0 in the unit design space

Store the first best box centered at x_0 with value $f_{\min}$;
Initialize *cc* and f_i
$c_b := 1$
`BOX_SET`(c_b)%`val` := $f_{\min}$
`BOX_SET`(c_b)%`c` := x_0
$cc := x_1$
$f_i :=$ a very large value
OUTER: **do** $k := 1$, $n_b - 1$
  Initialize p_b to point to the head of box matrices
  $c_m := 0$
  INNER1: **do while** (p_b is not NULL)
    INNER2: **do** $i := 1$, n_c
      INNER3: **do** $j := 1$, ((p_b%`ind`(i)-1) **mod** n_r) + 1
        Locate the best box with x_0 and $f_{\min}$ in the first pass.
        if ($k = 1$) **then**
          if (x_1 is the same as p_b%`M`(j, i)%`c`) **then**
            Found the best box and fill in `BOX_SET`;
            Assign the first best box with scaled p_b%`M`(j,i);
            Mark off the box at p_b%`M`(j,i);
            $c_m := c_m + 1$
            cycle
          end if
        end if
        if (box at p_b%`M`(j,i) is not marked) **then**
          Compute *sep*
          if ($sep <$ `MIN_SEP`) **then**
            mark off the box at p_b%`M`(j,i)
            $c_m := c_m + 1$
          else
            if (box at p_b%`M`(j,i)%`val`$< f_i$)

```
            f_i := p_b%M(j,i)%val
            p_c points to the box at p_b%M(j,i)
          end if
        end if
      else
        c_m := c_m + 1
      end if
    end do INNER3
    if (any box link exists for this box column) then
      p_l points to the first box link
      do while (p_l is not NULL)
        Repeat above steps in INNER3 loop for all boxes in p_l
        p_l points to the next box link
      end do
    end if
  end do INNER2
  p_b points to the next box matrix
end do INNER1
if (p_c is not NULL) then
  if (p_c is not marked) then
    Found the next best box at p_c; Scale it back to the original design
    space and store it in BOX_SET
    c_b := c_b + 1
    BOX_SET(c_b) := scaled box at p_c
    Mark it off
    c_m := c_m + 1
    Update cc
    cc := p_c%c
  end if
else
  exit OUTER since the next best box is not available
end if
Exit when all evaluated boxes have been marked
if (c_m ≥ n_e ) exit OUTER
end do OUTER
```

Pseudocode 3.1.

The MBB option is available for both serial and parallel versions except for parallel runs with multiple masters, because the communication and computation complexity of implementing MBB across multiple processors is fairly high. Also, the problem scale of locating good regions is usually much smaller than finding the global optimum, so a single master should be able to hold all the information for box subdivision.

3.2. Memory Reduction Technique

Limiting box columns (LBC) is a technique developed to reduce the memory requirements. Let $I_{\max}$ (the stopping rule `MAX_ITER`) be the maximum number of iterations allowed (a stopping criterion), I_{current} be the current iteration number, and C be one of the box columns. Each of the iterations I_{current}, ..., $I_{\max}$ can subdivide at most one box from C, because at most one box from C can be in the set of convex hull boxes at any iteration. Therefore, C only needs to contain at most $L = I_{\max} - I_{\text{current}} + 1$ boxes with the smallest function values. Boxes with larger function values are not considered by the DIRECT search limited to $I_{\max}$ iterations. However, the number of boxes generated per box column is usually much larger than L. Figure 3.2 shows the box column lengths for (1) the 10-dimensional Griewank Function (defined in Appendix A) with $I_{\max} = 400$ and (2) the 143-dimensional budding yeast parameter estimation problem [74] with $I_{\max} = 40$. Most of the box columns are longer than $I_{\max} >= L$ in both (1) and (2). When the stopping criterion $I_{\max}$ is given, storing only L boxes in box columns would significantly reduce the memory demands.

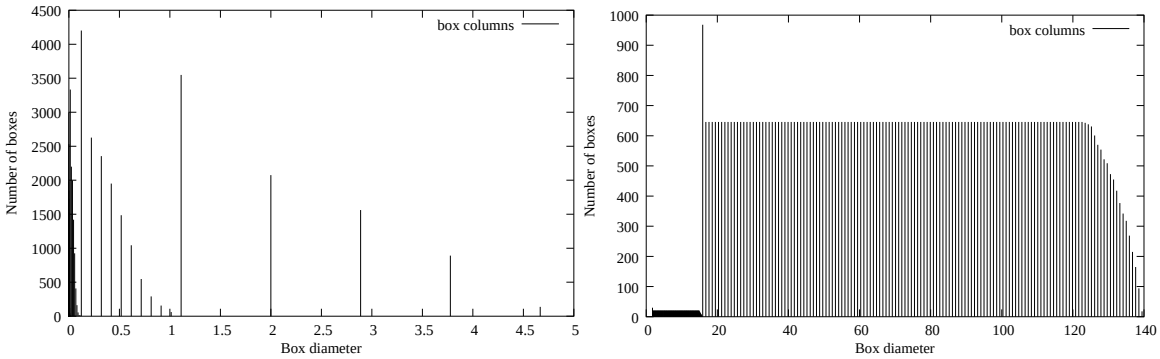

Figure 3.2. Box column lengths at the last iteration $I_{\max}$. (1) The Griewank function (left), $N = 10$ and $I_{\max} = 400$. (2) Budding yeast problem (right), $N = 143$ and $I_{\max} = 40$.

Since each box column is implemented as a min-heap ordered by the function values at the box centers, all box column operations without LBC take $\mathcal{O}(\log n)$ time and only two types of heap operations are involved—removing the lowest boxes with the smallest function values and adding new boxes. Additionally, LBC needs to remove the boxes with the largest function values ($b_{\max}$s). The min-heap data structure requires a $\mathcal{O}(n)$ time algorithm to locate the $b_{\max}$ boxes. A min-max heap [4] is considered as an ideal replacement of the min-heap data structure to locate the $b_{\max}$ boxes with constant time, which makes all operations $\mathcal{O}(\log n)$ time. The min-max heap makes a huge difference when $I_{\max}$ is large, since the number of boxes in a box column heap is very large. Also, several box columns can be taken into account to further reduce the number of boxes in the memory.

Although the extra operations of removing boxes with the largest function values in LBC are expensive, the memory requirement is reduced greatly as a result. Therefore, it is

highly recommended to enable LBC for large scale/high dimensional problems that more likely encounter memory allocation failures than small scale/low dimensional problems. LBC is enabled under three conditions: (1) the specified iteration limit $I_{\max}$ is positive, (2) the evaluation limit L_e (the stopping rule `MAX_EVL`) is not specified or is sufficiently large—$L_e \times (2N + 2) > 2 \times 10^6$, and (3) the MBB option is off. Without Condition (1), LBC would not be able to decide on the number of boxes to remove. Condition (2) is to turn off LBC to save operations for small scale runs with little concern for box storage; 2×10^6 is the threshold obtained from an empirical study. The last condition is also necessary since the MBB process demands that all boxes stay in the memory.

3.3. Efficiency Study

In terms of the execution time and memory usage, two other implementations ([29] and [93]) using static data structures were compared empirically with the serial version described in [49], which has demonstrated its strength in dealing with unpredictable memory requirements. The new improvement on data structures here is constructing box columns as heaps instead of sorted lists. In addition, lexicographical order of box center coordinates is enforced in the heap for maintaining determinism. Table 3.1 compares the execution time of an earlier version with sorted lists (SL), the current version with lexicographically ordered heaps (HL), and a version (HNL) that was built without the lexicographical order comparisons. Clearly, using heaps is much more efficient than using sorted lists. Also, the lexicographical order comparison accounts for a very tiny portion of the entire operational cost.

Table 3.1. Execution time (in seconds) of the versions with sorted lists (SL), with lexicographically ordered heaps (HL), and heaps without lexicographical order comparison (HNL). The evaluation limit is 10^5 for all test functions.

#	SL	HL	HNL
GR	233.21	10.60	10.57
QU	840.43	56.70	56.38
RO	226.52	8.12	7.92
SC	273.58	11.97	11.86
MI	468.65	29.69	29.32

The last important improvement on data structures is limiting box columns (LBC). The experimental results in Section 6.1.3 show that LBC reduces the memory usage by 10–70% for selected high dimensional test problems. The following experiments investigate the added computational cost of LBC. Figure 3.3 compares the growth of the execution time

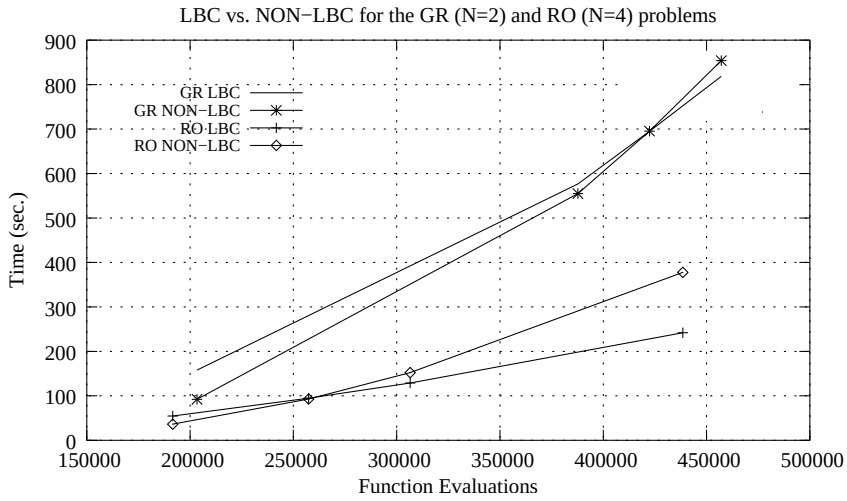

Figure 3.3. Growth of execution time with LBC or NON-LBC as N_e increases for the 2-dimensional problem GR and the 4-dimensional problem RO.

with LBC or without LBC (NON-LBC) as the number of function evaluations N_e increases for the 2-dimensional problem GR and 4-dimensional problem RO.

Regardless of the different problem structures, LBC performs slower than NON-LBC until N_e reaches a certain "crossover point", where NON-LBC begins to run slower due to less memory resource and more expensive operations on the lengthy box columns than LBC, which keeps the box columns as short as necessary. Observe that the crossover point for the 2-dimensional problem GR is approximately twice the crossover point for the 4-dimensional problem RO. This observation inspired the next set of experiments to find the approximate number of evaluations N_x at the crossover points for all five benchmark functions, and define a condition to turn off LBC if

$$L_e(2N+2) < \overline{L_x}, \tag{3.1}$$

where N is the problem dimension, $2N+2$ is the number of real values in a `Hyperbox`, L_e is the user specified limit on evaluations, and $\overline{L_x} \approx 2 \times 10^6$ is the average of the five $N_x(2N+2)$ values shown in Table 3.2. The condition (3.1) is checked only when the user specifies both stopping conditions `MAX_ITER` and `MAX_EVL`.

Table 3.2. The crossover point N_x and the threshold L_x for all five test functions.

#	GR	QU	RO	SC	MI
N	2	3	4	2	5
$N_x/10^3$	422	190	258	442	129
$L_x/10^6$	2.5	1.5	2.5	2.6	1.5

3.4. Related Work in Distributed Data Structures

Fundamental research on data structures contributed greatly to the design of distributed data structures used in parallel computing. This section presents a brief survey of several design examples related to this work.

The first example is *octree*, a three-dimensional variant of the quadtree with 2^3 branches [83]. Some octree-based methods for recursive decomposition of 3-D objects are frequently used in the construction of meshes for finite element analysis [81]. Pombo et al. [78] introduce adaptive schemes to improve the convergence rate of finite element methods. Parallel meshing avoids the computation bottlenecks, and therefore solves large-scale problems with a reasonable amount of time. The research work focuses on fast generation of tetrahedral unstructured meshes in parallel over geometric models with given refinement criteria. The meshing adaptation strategy not only automates computational methods for numerical simulations in a discrete domain, but also uses octrees to partition the geometric model and divide the workload among the processors with little overhead. The octree-based data structures maintain a hierarchical storage of the information needed in the meshing process. Thus, searching operations across large data arrays can be avoided mostly. Some special features of the octree also benefit the parallel implementations of data distribution algorithms. For example, spatial coordinates and level-tags that represent the desired depth in the branches of the octree in certain locations are stored as control points for conducting the desired mesh refinement. A weakness of this strategy, as the authors pointed out, is the load unbalance, a penalty to reduce the cost of subtree migration, which requires complex trace information for the *octree*-based data structures.

The second example is *k-d tree*, a multidimensional spatial data structure for organizing point data [81], where k denotes the dimensionality of the space being represented. Basically, it is a binary search tree with the distinction that at each level, a different attribute value is tested to determine the direction of branching. Its extension has been used in multidimensional searching in a distributed computing environment, as in [70] and [2]. Al-furaih et al. [2] study efficient parallel constructions of k-d trees on coarse-grained distributed memory parallel computers. The authors limit their studies to partial tree constructions up to a specified number of levels for the targeted applications, such as graph partitions and databases. Thus, a tree construction consists of two phases: a global construction of the first $\log p$ levels in parallel, followed by local sequential tree constructions. For both phases, three methods are discussed: median-based, sort-based, and bucket-based methods. The global construction requires distributing data structures among the processors. This generates collective communication structures. Different approaches taken by these two construction phases affect the cost of data movements involved in the inter-processor communication. Both theoretical and experimental analysis on different strategies are given to support the conclusion that using data parallelism up to $\log p$ levels of the tree followed by running

the tasks sequentially on each processor is preferable to using task parallelism for large granularity.

Unlike Al-furaih et al. [2], Nardelli et al. [70] concentrate on research work for improving the scalability of the k-d tree structures as new points are inserted dynamically. A new performance measure, distribution efficiency, was introduced to provide a means of comparing different distributed data structures. A brief literature review on the scalable distributed data structures is also given, covering from one-dimensional structures, such as distributed linear hashing and order-preserving data structures, to multidimensional ones like distributed random tree (DRT), B-trees, and R-trees. Here, k-d trees are used in the support of distributed exact, partial, and range search queries. The system consists of servers and clients. Each server manages a bucket of data for a leaf of the k-d tree. A set of "buckets" is a partition of the whole k-d space. Clients have two tasks, one for adding k-d points to certain buckets, the other for querying the structure. Data structures with dimension indices are used in both client and server sites to reduce multicast. Experimental results prove that compared with other data structures, the proposed data structure improves the efficiency of data management and querying operations on a set of multi-dimensional points in a distributed framework. In future work, the authors will extend the data structure to support dynamic point deletions.

CHAPTER 4: Parallel Schemes

The functional flow of DIRECT exposes its inherent sequential nature as seen in Chapter 2. The data dependency among the algorithm steps suggests a multilevel parallelism for **Selection** and **Sampling**. The parallel scheme for **Selection** concentrates on distributing data among multiple masters to share the memory burden. Several studies [1] [9] have shown that an appropriate configuration of multiple masters can improve the overall performance. Moreover, the data-distributed scheme naturally parallelizes the convex hull computation by merging multiple local convex hulls to a global one. Differently for **Sampling**, a functional parallelism distributes function evaluation tasks to workers. Nevertheless, function evaluations should be computed locally on masters if the evaluation cost is cheaper than the communication round trip cost. This is called the "horizontal scheme" (multiple masters without workers) to contrast with the "vertical scheme" (one master and multiple workers). These two basic schemes are conceptually described as above, but the underlying implementation can vary greatly depending on the chosen programming models and inter-processor communication patterns. Section 4.1 discusses how the overall parallel scheme has evolved from the version pDIRECT_I to the version pDIRECT_II. Section 4.2 compares the performance of these two versions. A survey of the related work in designing parallel schemes for well-known global optimization algorithms is in Section 4.3.

4.1. Implementation Evolution

The functional view of the multilevel parallelism consists of three components: domain decomposition, box subdivision, and function evaluation as shown in Figure 4.1.

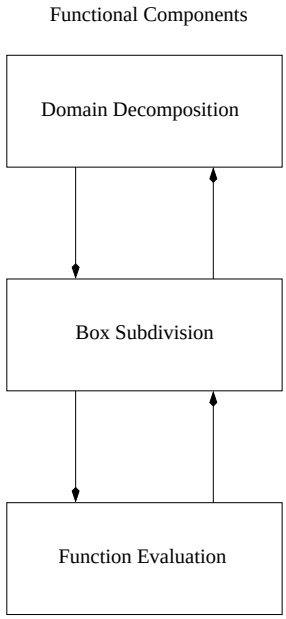

Figure 4.1. Three functional components.

Domain decomposition is an optional component that transforms the single start DIRECT into a multistart algorithm. Moreover, the resulting multiple subdomains are optimized independently, so that the objective function value may be reduced faster for problems with irregular structures (Section 6.2.2).

When multiple subdomains ($m > 1$) are used, the original feasible set delimited by upper (U_b) and lower (L_b) bounds is decomposed into m parts, each of which will be normalized to a unit box to start a DIRECT search. Theoretically, the original unscaled box is subdivided into $s = \sqrt{m}$ parts along the longest scaled dimension $D_1 = \max_i w_i(U_b - L_b)_i$, then each of these s boxes is subdivided into s boxes along the longest scaled dimension D_2 (the second longest overall). The $w_i > 0$ are user supplied component weights (dimension scalings), all one by default. In practice, s may not be an integer, so the decomposition needs to determine two reasonable divisors s_1 and s_2, where (1) $s_1 \times s_2 = m$ and (2) $s_1/s_2 \approx D_1/D_2$. The second condition on the ratio of divisors prevents the resulting subdomains from being out of proportion. For example, if $m = 12$, the acceptable divisors are (a) $s_1 = 12$, $s_2 = 1$, or (b) $s_1 = 6$, $s_2 = 2$, or (c) $s_1 = 4$, $s_2 = 3$. Whichever divisors best satisfy (2) are chosen, which best preserves the original weights on dimension bounds given by the user.

As the second component, box subdivision applies data parallelism that spreads data across multiple processors collaborating on **Selection** and **Division**. Lastly, the function evaluation component uses the classical master-slave paradigm that distributes evaluation tasks to multiple processors during **Sampling**.

In order to achieve the best performance, the implementation of the multilevel functional and data parallelism has evolved from the version pDIRECT_I to the version pDIRECT_II. In pDIRECT_I, a shared memory model (for box subdivision) is combined with a message passing model (between box subdivision and function evaluation), and processes are dynamically spawned. The data is distributed through the global data structures in the shared memory and computational tasks are distributed via messaging. This mixed paradigm improves data distribution efficiency compared to the pure functional parallel versions in [29] and [93]. However, it has its own shortcomings in program portability, processor utilization, load balancing, and termination efficiency. Therefore, the second version pDIRECT_II was developed to address these inefficiencies with a pure message passing model and more dynamic features in data structures, task allocation, and the termination process. In addition, a parallel convex hull computation is developed for pDIRECT_II to maximize concurrency and minimize network traffic.

Performance comparison results in Section 4.2 prove that pDIRECT_II is more effective for solving complex design optimization problems on modern large scale parallel systems. The following sub-sections first present pDIRECT_I and its design drawbacks, and then discuss the considerations leading to the improved version pDIRECT_II.

4.1.1. pDIRECT_I

The parallel scheme of pDIRECT_I consists of three levels as shown in Figure 4.2, each level addressing one of the functional components in Figure 4.1.

A. Topology

The processes at Level 1 form a logical subdomain master ring. The entire design domain is decomposed into multiple nonoverlapping subdomains (SDs). Each process SM_i (subdomain master i, $i = 1, \ldots, m$) on the ring starts the DIRECT search at the center of a chosen subdomain i. SM_i detects the stopping conditions, merges the results, and controls the termination at the end. SM_i is spawned at run time by MPI and joins the logical ring formed for SM processes. Level 1 uses a ring topology, because it fits the equal relationship among subdomains and represents the dependency of the stopping condition of each subdomain on other subdomains. The overall termination condition is when all subdomains have satisfied the specified search stopping criteria. In other words, a subdomain will be kept active until all search activities in other subdomains are done. This rule aims at reducing processor idleness when subdomains generate different amounts of computation. The drawback is that the stopping condition (i.e., maximum number of iterations) becomes a lower bound on the computational cost instead of an exact limit. Furthermore, the termination process is controlled by a token T passed as described in the following.

1. SM_1 issues T and passes it around the ring.
2. After the local stopping criteria are met, each SM_i checks if T has arrived at each iteration. If not, DIRECT proceeds. If yes, T is passed along in the ring.
3. After T is passed back to SM_1, a termination message is sent to all SM_i.
4. SM_1 collects the final results from all SM_i.

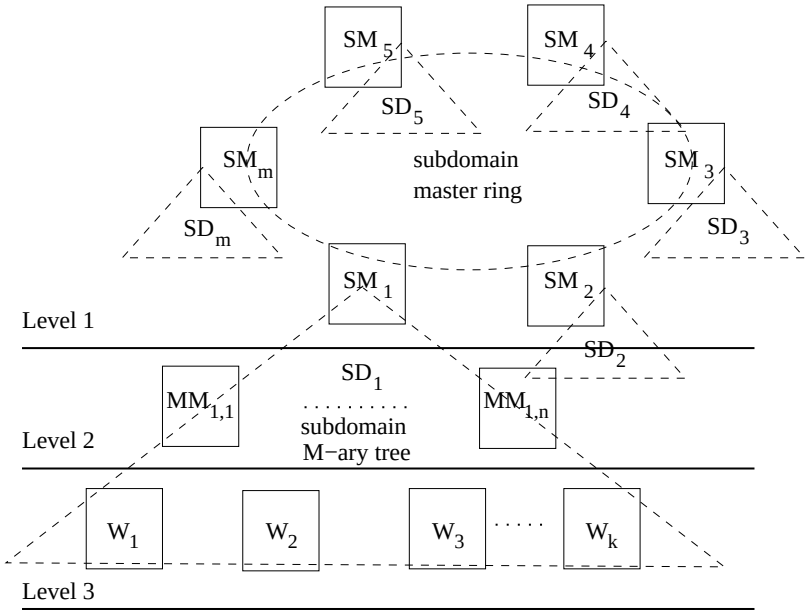

Figure 4.2. The parallel scheme of pDIRECT_I.

This process decentralizes the termination control, thus avoiding the bottleneck at SM_1 when the number of subdomains m is large. On the other hand, there are a few disadvantages of using the ring. First, the communication latency on a ring is higher than on some other topologies, such as a star or a tree. Second, the lower bound stopping condition can not provide users accurate estimates of computational cost.

Below Level 1, Level 2 uses GPSHMEM [75] to establish a global addressing space to access the data for **Selection**. This globally shared data structure corresponds to a work pool paradigm [33] that dynamically adjusts box subdivision workload among mini subdomain master (MM) processes at Level 2. Between Levels 2 and 3, a master-slave paradigm is used for distributing function evaluation tasks. Both Levels 2 and 3 take advantage of dynamic process management in MPI-2 [36] so that processors are assigned to these two levels at run time with approximately $(p-m)/m$ processors available for each subdomain (out of p total processors). In Figure 4.2, a $\lfloor M \rfloor$-ary tree structure is rooted at each SM process, where

$$M = \sqrt{\frac{p-m}{m}}.$$

Each SM process dynamically spawns $n = \lfloor M \rfloor$ mini subdomain master (MM) processes at Level 2 for box subdivision tasks. Similarly, each MM process spawns $\lfloor k \rfloor$ or $\lceil k \rceil$ worker processes for function evaluation tasks, where

$$k = \frac{p - m(1 + \lfloor M \rfloor)}{m \lfloor M \rfloor}.$$

To form the $\lfloor M \rfloor$-ary tree of processes, pDIRECT_I requires that the total number of processes $P \geq 16$. If the number of available processors $p \geq 16$, then $P = p$. Otherwise, P is set at 16, so that multiple processes may run on the same physical processor. Pseudocode 4.1 shows the interactions between $MM_{i,1}$ and $MM_{i,j}$ $(j = 2, \ldots, n)$ in subdomain i $(i = 1, \ldots, m)$ managed by SM_i.

```
done := FALSE (the search status)
MM_{i,1} receives DIRECT parameters (problem size N, domain D,
    and stopping conditions C_stop) from SM_i
broadcast DIRECT parameters to MM_{i,j}
do
    if (MM_{i,1}) then
        if (done = FALSE) then
            run one DIRECT iteration and merge intermediate results
                if (C_stop satisfied) then
                    done := TRUE
                    send done to SM_i
```

```
            end if
            cycle
        else
            receive a message from SM_i
            if (not a termination message) then
                send a handshaking message to SM_i
                broadcast a message to keep MM_{i,j} working
                run one DIRECT iteration and merge intermediate results
                cycle
            else
                broadcast a termination message to MM_{i,j}s
                terminate workers
                store the merged results
                exit
            end if
        end if
    else
        MM_{i,j} receives a message from MM_{i,1}
        if (not a termination message) then
            run one DIRECT iteration and reduce intermediate results
        else
            exit
        end if
    end if
end do
MM_{i,1} sends the final results to SM_i
```

Pseudocode 4.1.

The control mechanism is a two-level messaging—between SM_i and $MM_{i,1}$, and between $MM_{i,1}$ and each $MM_{i,j}$. The DIRECT parameters are passed from SM_i to $MM_{i,1}$, which broadcasts them again to each $MM_{i,j}$. To reduce the control overhead, no handshakes are involved between SM_i and $MM_{i,1}$ before the local stopping criteria are met. However, it is inefficient to dedicate a SM process to monitoring the search status and wrapping up the search at the end, causing significant communication overhead.

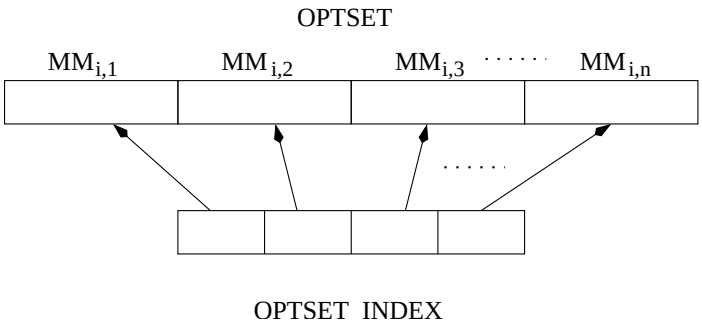

Figure 4.3. Data structures in GPSHMEM.

B. Task Allocation

At Level 2, MM processes cooperate on identifying convex hull boxes stored in a shared data structure of a global addressing space using GPSHMEM [75]. Two sets of global shared data structures `OPTSET` and `OPTSET_INDEX` (Figure 4.3) are used.

The structures `OPTSET` and `OPTSET_INDEX` are allocated and distributed across all MM processes, which use one-sided communication operations such as "put" and "get" to access shared data. These one-sided operations provide direct access to remote memory with less interaction between communicating parties. In addition, the data structure `LOCALSET` is allocated at $MM_{i,1}$ for merging the boxes with the same size. When only one MM process exists, **Selection** is the same as that in the sequential DIRECT. The following steps describe the N step implemented in pDIRECT_I.

1. $MM_{i,j}$ $(j = 1, \ldots, n)$ puts all the lowest boxes for different box sizes to its own portion in `OPTSET` and updates its index in `OPTSET_INDEX`.
2. $MM_{i,1}$ gets all boxes in `OPTSET` and merges the boxes with the same size to `LOCALSET`.
3. $MM_{i,1}$ finds convex hull boxes in `LOCALSET` and puts a balanced number of boxes for each $MM_{i,j}$ into `OPTSET` (the load balancing algorithm at $MM_{i,1}$ is described in Pseudocode 3.2).
4. $MM_{i,j}$ gets its portion of the convex hull boxes from `OPTSET`, removes some boxes (if any) that are assigned to other $MM_{i,j}$, and starts processing its convex hull boxes.

Each box is tagged with a processor ID and other indexing information to be tracked by its original owner. To minimize the number of local box operations (i.e., removals and additions) and maximize data locality, $MM_{i,1}$ restores the boxes back to their contributors before it starts load adjustment. The shared memory approach can access more memory on multiple machines than on a single machine. However, it depends on multiple software packages for global addressing, such as GPSHMEM and ARMCI [72]. Secondly, resizing the global data structures to hold an unpredictable number of lowest boxes involves expensive global operations across multiple machines. Thirdly, collecting all lowest boxes at $MM_{i,1}$ burdens local buffer storage as well as network traffic. Lastly, a global barrier is needed between steps to avoid premature "get" operations.

```
N_box: the number of global convex hull boxes
n: the number of MM processes
avgload: the average workload measured in boxes
underload: the workload shortfall from the desired avgload
overload: the workload extra over the desired avgload

merge all boxes from OPTSET to LOCALSET by the box sizes
find convex hull boxes in LOCALSET and update N_box
restore boxes given by MM_{i,j} to its portion in OPTSET
avgload := ⌈(N_box/n)⌉
d := 1 (loop counter)
OUTLOOP: do
   if (d = n) exit OUTLOOP
   if (OPTSET_INDEX(d) < avgload) then
      d_1 := d
      INLOOP: do
         underload := avgload − OPTSET_INDEX(d)
         d_1 := (d_1) mod n
         if (d_1 = d) exit INLOOP
         if (OPTSET_INDEX(d_1) > avgload) then
            overload := OPTSET_INDEX(d_1) − avgload
            if (overload ≥ underload) then
               shift enough load over
               OPTSET_INDEX(d) := avgload
               OPTSET_INDEX(d_1) := OPTSET_INDEX(d_1) − underload
               exit INLOOP
            else
               shift some and look for more
               OPTSET_INDEX(d) := OPTSET_INDEX(d) + overload
               OPTSET_INDEX(d_1) := avgload
            end if
         end if
      end do INLOOP
   end if
   d := d + 1
end do OUTLOOP
```

Pseudocode 4.2.

As shown in Pseudocode 4.2, the load adjustment is done at $MM_{i,1}$, which distributes the work to $MM_{i,j}$ by using the shared data structures in GPSHMEM. Then, each MM process subdivides its share of convex hull boxes and distributes the function evaluation tasks down to its workers. Although the control mechanism is simple, this centralized strategy suffers a common bottleneck problem. Furthermore, workers are not shared by MM processes. A worker is exclusively under the command of a particular MM that spawns it at the beginning. This fixed assignment degrades the processor utilization and load balancing among workers.

4.1.2. pDIRECT_II

The three-level hierarchy in pDIRECT_I is reshaped to be a group-pool structure with subdomain groups of masters and a globally shared pool of workers as shown in Figure 4.4. The SM and MM processes in pDIRECT_I are now grouped together to maintain data structures and perform **Selection** and **Division**, while globally shared workers perform **Sampling**. This scheme is implemented with a pure message passing model, which removes the dependency on multiple software packages, simplifies the program structure, and improves the parallel performance.

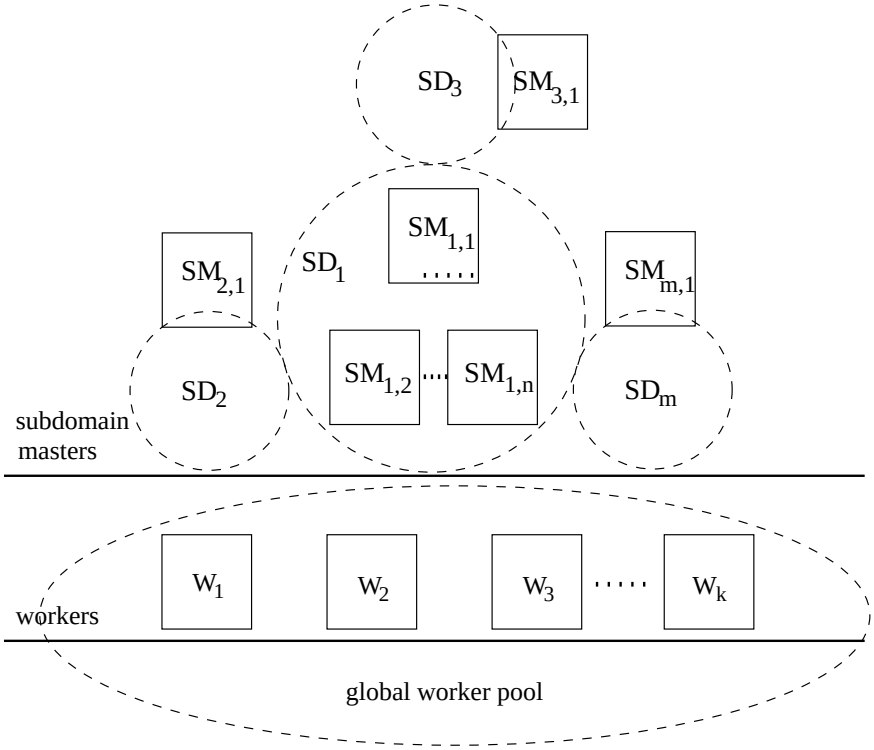

Figure 4.4. The parallel scheme for pDIRECT_II.

A. Topology

Each subdomain is served by a subdomain group of masters in lieu of the subdomain master ring. Let $SM_{i,j}$ stand for the master j in subdomain i. $SM_{i,1}$ is the root master for subdomain i. In addition to carrying out common tasks like other masters, the root masters $SM_{i,1}$ $(i = 2, \ldots, m)$ also communicate with $SM_{1,1}$ to finalize the search. This star shaped connection centered at $SM_{1,1}$ has replaced the ring topology in pDIRECT_I.

Moreover, all $SM_{i,j}$ $(j = 1, \ldots, n)$ processes except $SM_{1,1}$ become workers when they have finished all search activities for their subdomain. This dynamic feature reduces the processor idleness and offers an exact stopping condition unavailable in pDIRECT_I. When the stopping condition is satisfied, workers will receive "all done" messages from

masters and terminate themselves after confirming that no more work is available. Then, a termination message is sent from the root master (processor 0) down to a logical tree of master processors in $\log_2(n \times m)$ steps, where $n \times m$ is the total number of masters. Recall that the termination message is passed linearly along the ring and logarithmically down to the $\lfloor M \rfloor$-ary trees in pDIRECT_I. Clearly, the new termination scheme here does not require such a complicated control mechanism as in pDIRECT_I.

B. Task Allocation

Task allocation policies have strong connections to important performance metrics such as parallel efficiency and load balancing. Here, several improvements were made in allocating both box subdivision tasks in the **Selection** step and function evaluation tasks in the **Sampling** step.

In subdomain i, **Selection** is accomplished jointly by masters $SM_{i,j}$, $j = 1, \ldots, n$, where n is the total number of subdomain masters per subdomain. When $n = 1$, **Selection** is the same as that in the sequential DIRECT. When $n > 1$, **Selection** is done in parallel over the index i as follows.

1. $SM_{i,j}$, $j = 1, \ldots, n$ identify local convex hull box sets $S_{i,j}$, $j = 1, \ldots, n$.
2. $SM_{i,1}$ gathers the $S_{i,j}$ from all the $SM_{i,j}$.
3. $SM_{i,1}$ merges the $S_{i,j}$ by box diameters and finds the global convex hull box set S_i.
4. All the $SM_{i,j}$ receive the global set S_i and find their portion of the convex hull boxes.

All buffers used here are locally allocated and resized incrementally according to the updated number of boxes involved in the convex hull computation. Note that all boxes in the global convex hull box set S_i must also be in the union of the sets of local convex hull boxes ($S_{i,j}$) of the masters. Therefore, each master $SM_{i,j}$ computes $S_{i,j}$ in parallel and $SM_{i,1}$ only considers the union of all $S_{i,j}$ instead of all the lowest boxes with different diameters, as was done in pDIRECT_I. This decentralized **Selection** implementation reduces memory requirements for buffers, as well as the amount of data transferred over the network. However, a large number of subdomain masters will not perform well due to the global communication and synchronization required for finding convex hull boxes at every iteration. [97] describes a sampling technique that can further reduce the bandwidth requirements, but it comes at the expense of requiring another global communication round. Another possibility would be for $SM_{i,1}$ to gather via a d-way tree only the final merged $S_{i,j}$, where each intermediate tree node does a partial convex hull merge of its d (merged) inputs (the optimal value for d is derived in [97]). Depending on the potential memory requirement of a run, users can estimate the number of subdomain masters required to achieve a particular stopping condition. If the function evaluation cost is high, but the memory requirement is hard to assess, the checkpointing feature can be enabled to log evaluations

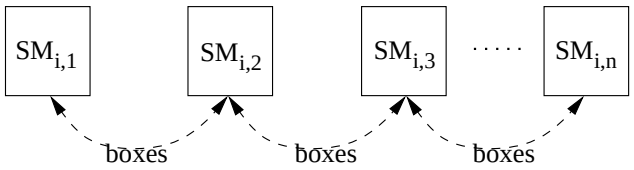

(a) Horizontal 1-D partition.

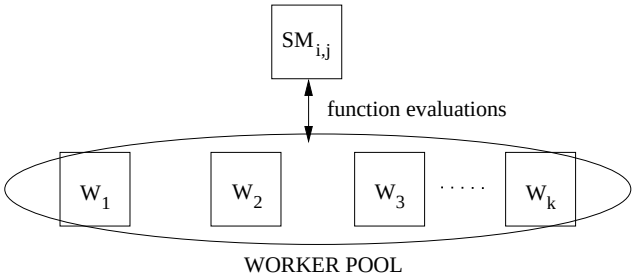

(b) Vertical 1-D partition.

Figure 4.5. Task partition schemes.

on existing masters and recover the run with more masters if memory allocation failure occurs.

Compared to pDIRECT_I, pDIRECT_II simplifies the implementation of the two basic schemes of task partitioning, namely the horizontal and vertical schemes. As discussed previously, for low computation cost, communication overhead dominates the parallel execution time and overshadows the benefits in distributing function evaluation tasks to workers. Wisely, masters would rather keep computation locally and simply share the memory burden with other masters without any worker involved in the picture. This is the horizontal scheme, also called horizontal 1-D partition for box subdivision tasks (Figure 4.5(a)). Experimental results in Section 4.2 show that this scheme achieves better speedup (for cheap function evaluations) than the vertical 1-D partition (the vertical scheme) for function evaluation tasks (shown in Figure 4.5(b)).

When these two schemes are combined, they become a hybrid 2-D partition. This hybrid scheme is usually preferred for the following reasons. First, the computation cost is higher or at least comparable to the communication cost in most real world design problems. Generally, overlapping the computation on worker processors in the vertical 1-D partition is a reasonable approach. Second, the data sharing scheme in the horizontal 1-D partition relieves the heavy memory burden on a single master processor for solving a large scale and/or high dimensional problem.

The next improved design in task allocation is on worker assignment. The worker pool is globally shared by all masters in all subdomain groups. Each worker polls all (selected) masters for evaluation tasks and returns the function values. Workers proceed in cycles that roughly correspond to the DIRECT iterations. During each cycle, a worker requests tasks from a randomly selected subset of masters until all of them are out of work. This is called

the "nonblocking" loop in Pseudocode 4.3. Once the cycle is over, the worker blocks waiting (the "blocking" loop) for further instructions from a fixed master, which is selected such that every master has a fair number of blocked workers waiting in the queue. Pseudocode 4.3 below describes how a worker W_i evaluates the objective function for masters $SM_{i,j}$ ($i = 1, \ldots, m$ and $j = 1, \ldots, n$) during **Sampling**.

C_{active}: the counter for the total number of "active" masters
    that have not reached the last iteration
C_{idle}: the counter for idle masters
converted: the flag indicating if it is converted from a master
loop: the loop status
m: the number of subdomains, given as input
n: the number of masters per subdomain, given as input
mesg: the message received from others
P_{wi}: the processor ID (PID) of W_i
sub_s: completion statuses of subdomains, given as input

loop := "nonblocking"
converted :=`FALSE`
$C_{active} := 0$
check sub_s to compute C_{active}
if ($C_{active} < nm$) *converted* := `TRUE`
$C_{idle} := 0$ (assume all masters busy initially)
OUTLOOP: **do**
  if (*loop* = "nonblocking") **then**
    send a nonblocking request to a randomly selected master $SM_{i,j}$
      from $C_{active} - C_{idle}$ busy masters
  else
    set all masters to status busy
    $C_{idle} := 0$
    send a blocking request to the master $SM_{i,j}$ that ranks as
      $(P_{wi} - C_{active})$ mod C_{active} in the list of all active masters
  end if
  INLOOP: **do**
    keep waiting for any messages
    select case (*mesg*)
      case (an evaluation task from $SM_{i,j}$)
        evaluate all points in the task
        send the results back to $SM_{i,j}$

```
            if (SM_{i,j} is responding to a blocking request) then
               loop := "nonblocking"
            end if
         case ("no point" from SM_{i,j})
            if (SM_{i,j} is at status busy) then
               set SM_{i,j}'s status idle
               C_idle := C_idle + 1
            end if
            exit INLOOP
         case ("all done" from SM_{i,j})
            if (SM_{i,j} is at status busy) then
               set SM_{i,j}'s status idle
               C_idle := C_idle + 1
            end if
            remove SM_{i,j} from the master list
            C_active := C_active - 1
            if (C_active = 0) then
               if (NOT converted)
                  exit OUTLOOP (terminate itself)
               else
                  cycle INNER (wait for "terminate")
               end if
            end if
            exit INLOOP
         case (a "non-blocking" request from a worker)
            reply "all done" to this worker (W_i was converted from a master)
         case (a "blocking" request from a worker)
            reply "all done" to this worker (W_i was converted from a master)
         case ("terminate" from the parent processor)
            pass "terminate" to the left and right children (if any)
            exit OUTLOOP
      end select case
   end do INLOOP
   if (C_active = C_idle) then
      loop := "blocking"
   else
      loop := "nonblocking"
   end if
```

end do OUTLOOP

Pseudocode 4.3.

At the same time, the master $SM_{i,j}$ is generating sample points and responding to worker requests as described in the following Pseudocode 4.4.

$S_{i,j}$: the portion of global convex hull boxes for $SM_{i,j}$
Q_w: the blocked worker queue
$A_b(1:k) := 0$ (the array of counters for tracking the number of blocking requests from workers W_1, W_2,..., W_k) for multiple subdomain cases
$C_{new} := 0$ (the counter for new points)
$C_{send} := 0$ (the counter for points that have been sent to workers)
$C_{eval} := 0$ (the counter for evaluated new points)
N_b: the upper limit on the number of evaluation tasks sent to a worker at one time
$mesg$: the message received from others

if ($S_{i,j}$ is empty) **then**
  release all blocked workers in Q_w (send them "no point" messages)
else
  find the longest dimensions for all boxes in $S_{i,j}$
  C_{new} := the number of all newly sampled points along longest dimensions
  if (Q_w is not empty) **then**
    loop sending at most N_b number of points to each worker in Q_w with a tag "responding to your blocking request"
    update C_{send}
    release the remaining blocked workers (if any)
  end if
  do while ($C_{eval} < C_{new}$)
    keep waiting for any messages
    select case ($mesg$)
      case (a "non-blocking" request from W_i)
        if ($C_{send} < C_{new}$) **then**
          send at most N_b number of points to W_i
          update C_{send}
        else
          send "no point" message to W_i.
        end if
      case (a "blocking" request from W_i)
        if ($C_{send} < C_{new}$) **then**
          send at most N_b number of points to W_i with a tag

```
                "responding to your blocking request"
            update C_send
        else
            if (A_b(i) = 0 for multiple subdomain search) then
                A_b(i) := 1
                send "no point" to W_i
            else
                put W_i into Q_w
            end if
        end if
    case (function values from W_i)
        save the values and update C_eval
        if (C_send < C_new) then
            send W_i another task with at most N_b points
            update C_send
        else
            send "no point" to W_i
        end if
    end select case
  end do
end if
```

Pseudocode 4.4.

At the beginning of each iteration, $SM_{i,j}$ sends evaluation tasks to its blocked workers. If it has more blocked workers than tasks, it signals the remaining blocked workers to start a new cycle of requesting work from other masters. Otherwise, $SM_{i,j}$ keeps receiving function values from workers and sending out more tasks. When $SM_{i,j}$ is out of tasks, it notifies workers that are requesting tasks and queues up the workers that are blocked waiting for the next iteration. In the case of multiple subdomain search, an array of blocking status (A_b) is used to track the number of times that a worker has sent a blocking request to this master during this iteration. After the first blocking request from a worker, $SM_{i,j}$ tells the worker to continue seeking work from other masters. After the second blocking request from that same worker, during this iteration, $SM_{i,j}$ queues up that worker; this gives workers a better chance to find masters who have just become busy. Observe that the subdomain masters within the same subdomain need to synchronize with each other to find global convex hull boxes during every iteration; however, no synchronization or communication is needed among workers, and masters from different subdomains also work independently, until the final termination starts. Therefore, A_b is only considered in multiple subdomain cases.

When all the masters are out of work at the end of an iteration, the next iteration begins, and the masters from different subdomains may start the next iteration at different times. Therefore, a master should encourage a worker, who has sent it the first blocking request, to seek work again from other masters. This asynchronous design allows a large number of workers to be used efficiently across masters and subdomains. Empirical results have shown that workers achieve a better load balance for a multiple subdomain search than for a single domain search. In comparison, workers in pDIRECT_I work only for a fixed master, so they have to sit idle when the master runs out of work until the next iteration starts.

This scheme also naturally distributes tasks to workers according to the speed at which they finish the work, unlike the load balancing methods that attempt to distribute an approximately equal number of function evaluation tasks to each worker. These methods assume that (1) the function evaluation at different coordinates costs the same computationally and/or (2) each worker finishes the function evaluation within the same amount of time. In fact, these two assumptions are not satisfied in many parallel systems, even though some are claimed to be homogeneous. Most importantly, many engineering design problems do have different computation cost for different regions. Therefore, the measure of a reasonable load balancing should not be the equal quantities of tasks that are distributed among workers, but the degree that all of the workers are kept busy. Note that this scheme adds a parameter N_b used for stacking function evaluations to one evaluation task. It reduces the communication overhead when the objective function is cheap. However, N_b should be set to 1 if the objective function is expensive. Otherwise, fewer tasks are available to workers and a load imbalance occurs.

4.2. Performance Comparison of pDIRECT_I and pDIRECT_II

This section presents performance results regarding the main design issues discussed in the last section. In addition to the GR, QU, and RO benchmark functions described in Appendix A, the 143 parameter estimation problem for budding yeast (BY) cell cycle modeling [74] and a few more artificial functions (Table 4.1) have been used in the evaluation. All the artificial functions have the same initial domain $[-2, 3]^N$. For some experiments, dimension $N = 150$ and an artificial time delay T_f are used to make the artificial functions comparable to the BY problem.

Table 4.1. Test functions.

#	Description
1	$f = x \cdot x/3000$
2	$f = -\sqrt{\sum_{i=1}^{N} x_i - 0.5(i-1)/N}$
3	GR
4	QU
5	$f = \sum_{i=1}^{N} \sum_{j=1}^{i} {x_j}^2$
6	RO
7	$f = 10N + \sum_{i=1}^{N} x_i^2 - 10\cos(2\pi x_i)$
8	Budding yeast parameter estimator [74]

The following experiments demonstrate the effectiveness of the **Selection** implementation, task partition, and worker assignment in pDIRECT_II.

4.2.1. **Selection** *Efficiency*

Table 4.2 compares N_{gc} (number of global convex hull boxes), N_{lc} (the combined number of local convex hull boxes), and N_d (the combined number of different box diameters) on 32 subdomain masters for all test functions at the last iteration ($I_{\max} = 1000$ for artificial test functions and $I_{\max} = 100$ for the budding yeast problem). In pDIRECT_I, $MM_{i,1}$ collects N_d boxes and finds the convex hull box set. In pDIRECT_II, N_{lc} local convex hull boxes are found by $SM_{i,j}$ ($j = 1, \ldots, n$), then gathered on $SM_{i,1}$, which identifies the global convex hull boxes. This approach increases the concurrency of the **Selection** implementation. Table 4.2 shows that it reduces the amount of data transferred over the network and the buffer size by 50–90% for all test functions.

Table 4.2. Comparison of N_{gc}, N_{lc}, and N_d at the last iteration $I_{\max}$.

#	N_{gc}	N_{lc}	N_d	$\frac{(N_d - N_{lc})}{N_d}$
1	58	2605	33358	92%
2	89	1228	6805	81%
3	145	2056	22375	90%
4	3	3201	6756	52%
5	140	1830	20276	90%
6	144	1276	28003	95%
7	144	3531	20614	82%
8	20	159	6545	97%

4.2.2. Task Partition

The following experiment is to study the parallel performance of the horizontal and vertical 1-D partition schemes. A total of $P = 288$ processors are used. In the horizontal partition, each run has all P masters that evaluate objective functions locally. In the vertical partition, a single master sends evaluation tasks to $P - 1$ workers, each task holding $N_b = 1$ set of point coordinates. Table 4.3 shows the timing results for Test Function 6 with $N = 150$, given two function evaluation costs: T_f=0.1 second (the artificial case) and the original cost $T_f \approx 0.0$ (less than 1.0E-7 second). Set $I_{\max} = 300$ for the original cost and $I_{\max} = 90$ for the artificial cost. To ensure that the two partition schemes are comparable in the number of processors, the timing results are measured from $P = 3$ processors (if $P = 1$, no workers are used in the vertical 1-D partition). Note that the horizontal 1-D partition has all P processors available for function evaluations, while the vertical 1-D partition has only $P - 1$ processors for that. Therefore, the parallel efficiency is estimated with the $base = 3$

Table 4.3. Parallel timing results (in seconds) for different function evaluation costs T_f for Test Function 6 with $N = 150$.

	Horizontal 1-D partition							
$T_f \backslash P$	3	5	9	18	36	72	144	288
0.0	21.04	15.36	12.03	12.78	14.88	40.71	23.37	31.49
0.1	6785.88	4614.23	2741.11	2633.46	2634.53	2636.03	2652.78	2644.96

	Vertical 1-D partition							
$T_f \backslash P$	3	5	9	18	36	72	144	288
0.0	49.93	41.18	40.28	41.81	45.10	45.53	65.10	55.07
0.1	8720.27	4361.30	2184.76	1033.28	507.14	256.09	149.95	79.27

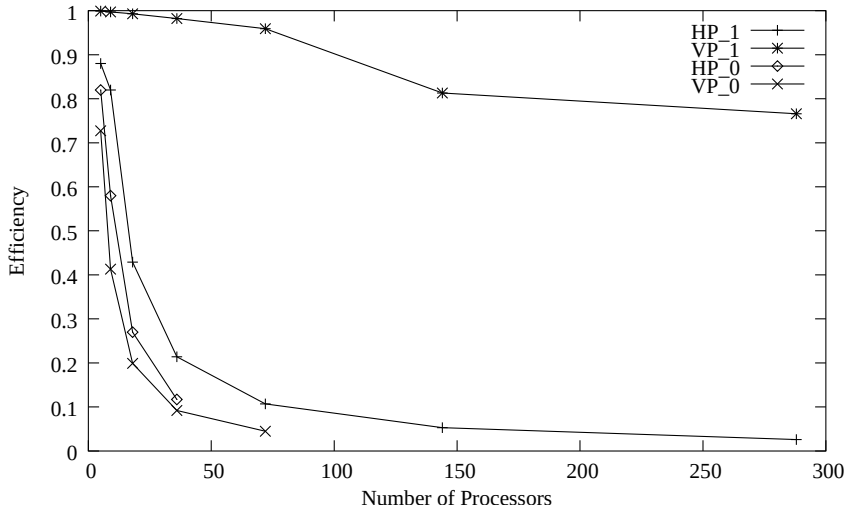

Figure 4.6. Comparison of the parallel efficiencies with different partition schemes and objective function costs.

processors for the horizontal 1-D partition and $base = 2$ for the vertical 1-D partition. The efficiency E is thus computed as $(T_{base}/T_P) \;/\; (P/base)$ as shown in Figure 4.6.

When $T_f = 0.0$ second, the horizontal 1-D partition (HP_0) runs faster than the vertical 1-D partition (VP_0). The masters in HP_0 locally evaluate the cheap objective function, thus avoiding the communication overhead for talking to workers. However, HP_0 does not achieve any speedup for $P = 72$, 144, and 288, because the number of convex hull boxes is insufficient to keep all masters busy (some masters have no convex hull boxes, thus evaluating no points locally). As for VP_0, the communication overhead always dominates the execution cost and it fails to achieve any speedup after P reaches 144. When $T_f = 0.1$ second, the vertical 1-D partition (VP_1) runs more efficiently than the horizontal 1-D partition (HP_1) (see Figure 4.6) except for $P = 3$. When $P = 3$, three masters are evaluating functions for HP_1, while only two workers are doing so for VP_1. Nevertheless, all runs with $P \geq 5$ of VP_1 take a much shorter time than those of HP_1. The first reason is that the communication overhead is negligible compared to the objective function cost

for VP_1. Secondly, when P is large, no convex hull boxes are assigned to some masters, so they have to sit idle in the case of HP_1. In general, the number of convex hull boxes is much smaller than the number of function evaluations, because DIRECT samples two new points along each longest dimension for every convex hull box. Hence, the pure horizontal 1-D partition reaches its limits when P is greater than the number of convex hull boxes. On the other hand, the memory limit on a single master makes the pure vertical 1-D partition impossible for runs with large $I_{\max}$. Therefore, a hybrid partition scheme is generally preferable to the pure partition schemes.

In the following two experiments, several hybrid partition schemes with different numbers of masters and workers are compared with the single master scheme for Test Function 6 with $N = 150$ and $T_f = 0.1$ second for a single subdomain. The first experiment varies the number of masters (2^i, $i = 0, \ldots, 5$) and fixes the total number of processors (implicitly, the number of workers also changes). The second experiment varies the number of masters and fixes the number of workers. $P = 100$ (total number of processors) is used for Experiment 1. 100 and 200 workers, respectively, are involved in Experiment 2. The measured parallel execution timing results listed in Table 4.4 are compared to a theoretical lower bound defined by

$$T_t = \sum_{i=1}^{I_{\max}} \left\lceil \frac{N_i}{k} \right\rceil T_f, \tag{4.1}$$

where T_t is the theoretical lower bound on the parallel execution time, N_i is the number of function evaluation tasks at iteration i, and k is the total number of workers. T_t depends on both the problem and the computing resource. It assumes all workers are fed continuously with evaluation tasks, distinct from reality, where finding convex hull boxes, synchronization, and communication all cost time as well. Clearly when N_i is not exactly a multiple of k, some workers are idle during the last working cycle for that iteration. A worker ideally obtains either $\delta_+ = \lceil N_i/k \rceil$ or $\delta_- = \lfloor N_i/k \rfloor$ number of tasks. The number X of idle workers can be derived from

$$\delta_+(k - X) + \delta_-(X) = N_i.$$

Here, define the overhead of function evaluation $T_o = T_p - T_t$ and the efficiency of function evaluation $E_f = T_t/T_p$, where T_p is the measured parallel execution time.

Figure 4.7 shows how the number of new evaluations per iteration (N_i) changes for Test Function 6 with $N = 150$ and $I_{\max} = 90$. Given the number of workers, T_t is then computed in Table 4.4, which shows that a wide range of hybrid task partition schemes perform reasonably well ($86.2\% \leq E_f \leq 96.3\%$). In the case of P_{100}, E_f grows slightly as the number of masters increases up to 32. Clearly, the number of convex hull boxes is sufficient to keep 32 masters busy. Moreover, smaller master-to-worker ratios seem to correspond to lower E_f values. This phenomenon may indicate a potential bottleneck problem at masters that communicate with a great number of workers, or simply more idle workers. The above

Table 4.4. Comparison of theoretical parallel execution time T_t and the parallel timing results T_p with different hybrid partition schemes for Test Function 6 with $N = 150$, $T_f = 0.1$ sec, and $I_{\max} = 90$. P_{100} stands for using a total of 100 processors. W_{100}, W_{200} stand for using a total of 100, 200 workers, respectively.

		Number of Masters					
schemes		1	2	4	8	16	32
P_{100}	T_p	203.42	204.20	207.79	215.44	234.15	282.38
	T_t	180.10	181.70	185.80	192.90	211.40	260.20
	T_o	23.32	24.10	26.09	29.64	41.25	22.18
	E_f	88.5%	88.9%	89.4%	89.5%	90.3%	92.1%
W_{100}	T_p	201.53	185.41	184.83	184.88	185.61	187.29
	T_t	178.00	178.00	178.00	178.00	178.00	178.00
	T_o	23.53	7.41	6.83	6.88	7.61	9.29
	E_f	88.3%	96.0%	96.3%	96.3%	95.9%	95.0%
W_{200}	T_p	102.32	102.06	101.56	101.55	103.14	105.86
	T_t	91.30	91.30	91.30	91.30	91.30	91.30
	T_o	11.02	10.76	10.26	10.25	11.84	14.56
	E_f	89.2%	89.5%	89.9%	89.9%	88.5%	86.2%

supposition was further investigated in the second experiment. In both W_{100} and W_{200}, E_f is improved at the beginning as the number of masters increases to a "peak point" with the best E_f. Then, it is degraded when the synchronization overhead among masters starts to dominate. Note that the peak point is 4 for W_{100} and 8 for W_{200}, while the master-to-worker ratios at these two points are the same, 1:25. Moreover, W_{200} has lower E_f values than W_{100} for the same number of masters, because masters in W_{200} deal with more workers, and more workers in W_{200} are likely to be idle. Also, the same amount of work distributed to 100 workers in W_{100} generates more communication interactions between masters and workers in W_{200}. Therefore, the search with a single subdomain will always eventually decrease E_f as more and more workers are used.

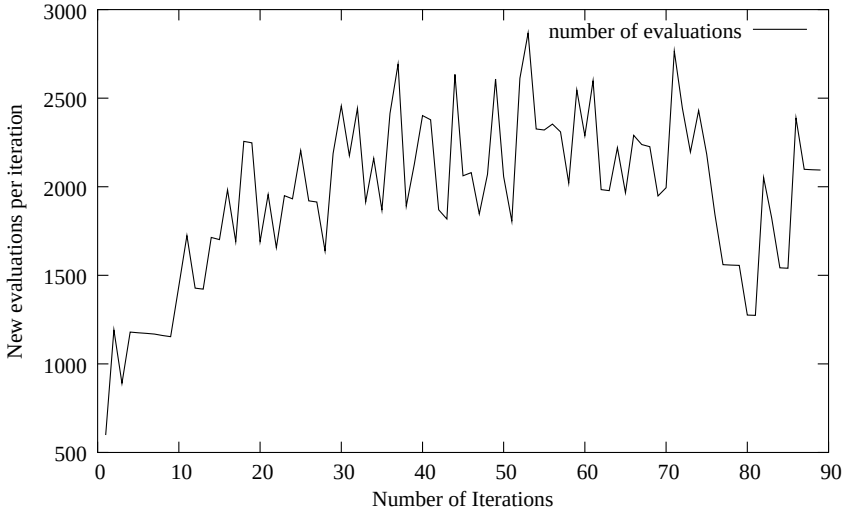

Figure 4.7. The plot of N_i ($i = 1, \ldots, 90$) for Test Function 6 with $N = 150$.

4.2.3. Worker Assignment

The following experiment demonstrates that function evaluation tasks are allocated more efficiently for a multiple subdomain search than for a single subdomain search. Load balancing among workers is improved greatly with the globally shared worker pool of pDIRECT_II, especially when masters of different subdomains generate unequal amounts of work. $P = 320$ processors were used for the budding yeast problem. $P = 200$ processors were used for the artificial test problems (Test Functions 1–7) with $N = 150$ and $T_f = 0.1$ sec.

In this experiment, the feasible domain is split into four subdomains. Note that the same test problem with four split subdomains can be solved in three different ways using P processors.

(a) All P processors are used to run a multiple subdomain search with four subdomains. The parallel execution time is T_a.

(b) Four single subdomain searches are run in parallel, each using $P/4$ processors on one of the four subdomains. The overall parallel execution time T_b is the longest duration of all four runs.

(c) Four single subdomain searches are run sequentially, each using all P processors on each of the four subdomains. The parallel execution time T_c is the total duration of these four runs.

Table 4.5. Comparison of T_a, T_b, and T_c in seconds.

#	T_a	T_b	T_c	$\frac{(T_b-T_a)}{T_a}$	$\frac{(T_c-T_a)}{T_a}$
1	382	407	441	6.2%	15.4%
2	1132	1139	1185	0.6%	4.6%
3	358	369	417	3.1%	16.4%
4	870	874	921	0.4%	5.9%
5	260	263	312	1.1%	20.0%
6	428	476	477	11.2%	11.4%
7	1142	1148	1196	0.5%	4.7%
8	8595	10643	11059	23.8%	28.7%

Table 4.6. Comparison of total number of subdomain function evaluations for experiments listed in Table 4.5. e_i is the total number of evaluations for subdomain i, which is the same for all of the ways (a), (b), and (c).

#	e_1	e_2	e_3	e_4	$\bar{e}$	s^2
1	181409	194927	194927	181463	2090.9	7789.1^2
2	550691	550691	550691	550691	6118.8	0
3	176075	176075	176075	176075	1956.4	0
4	421723	421723	421723	421723	4685.8	0
5	123685	123685	123685	123685	1374.3	0
6	228193	203635	198727	192397	2286.0	15661^2
7	555435	555435	555435	555435	6171.5	0
8	82471	44631	47531	87063	1635.6	22445^2

Table 4.5 compares T_a, T_b, and T_c for all the test problems ($I_{\max} = 90$ for Test Functions 1–7 and $I_{\max} = 40$ for the budding yeast problem). T_a is the smallest among the three. T_b is only slightly bigger than T_a for Test Functions 2, 3, 4, 5, and 7, but becomes significantly bigger ($> 5\%$) for Test Functions 1, 6, and 8, each of which has a large s^2, the variance of the total number of function evaluations for the four subdomains (in Table 4.6). Also, T_c is the largest among the three. Observe that it is only slightly bigger ($< 5\%$) than T_a for Test Functions 2 and 7. Table 4.6 shows that these two test functions have a large $\bar{e} = \sum e_i / I_{\max}$ (> 6000), the average number of function evaluations per iteration, where e_i is the total number of evaluations for subdomain i. Since more tasks are generated at each iteration for Test Functions 2 and 7 than for the other test functions, $P - 1$ workers are better load balanced in case (c).

Table 4.7. Normalized workload ranges (WR) of a, b, and c for experiments listed in Table 4.5.

#	WR_a	WR_{b1}	WR_{b2}	WR_c
1	[0.99969,1.0002]	[0.95743,1.0413]	[0.99193,1.0091]	[0.97495,1.0250]
width	5.4685E-5	8.3845E-2	1.7152E-2	5.0023E-2
2	[0.99985, 1.0002]	[0.99871,1.0014]	[0.99871,1.0014]	[0.9959,1.0049]
width	3.2897E-4	2.6460E-3	2.6460E-3	9.7536E-3
3	[0.99972,1.0001]	[0.99633,1.0038]	[0.99633,1.0038]	[0.98213,1.0138]
width	3.8E-4	7.4827E-3	7.4827E-3	3.1646E-2
4	[0.99989,1.0001]	[0.99840,1.0017]	[0.99841,1.0017]	[0.99470,1.0032]
width	2.1E-4	3.2577E-3	3.2576E-3	8.4916E-3
5	[0.99967,1.0005]	[0.99476,1.0062]	[0.99478,1.0063]	[0.98949,1.0104]
width	7.9529E-4	1.1487E-2	1.1488E-2	2.0914E-2
6	[0.99973,1.0001]	[0.93170,1.1108]	[0.99497,1.0038]	[0.98802,1.0072]
width	4.0281E-4	1.7910E-1	8.8312E-3	9.9186E-1
7	[0.99984,1.0001]	[0.99898,1.0011]	[0.99898,1.0011]	[0.99678,1.0035]
width	2.3958E-4	2.0986E-3	2.0986E-3	6.7307E-3

Figure 4.8 shows the normalized workload among workers for two runs: (1) Test Function 6 with moderate $\bar{e}$ and large s^2, and (2) Test Function 7 with large $\bar{e}$ and small s^2. Generally, workload is normalized by dividing the total evaluation time for each worker by the average evaluation time for all workers. Specially for case (b), the workload is also computed based on $P/4$ processors for each run instead of considering all P processors for the general normalization. Table 4.7 lists the normalized workload ranges, where WR_{b1} was obtained by averaging the workload based on P processors and WR_{b2} was obtained by averaging the workload based on $P/4$ processors.

Figure 4.8 plots the normalized workload among workers for Test Functions 6 and 7 in cases (a), (b), and (c). Figure 4.8 I and II use different ways of normalization for case (b). In all three pictures of Figure 4.8, case (a) has the best load balancing, i.e., the workload

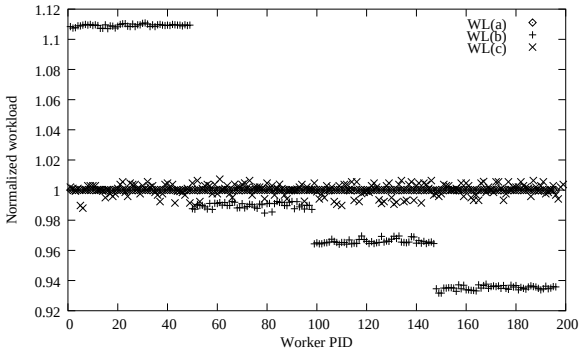

I. Normalization based on P processors for case (b).

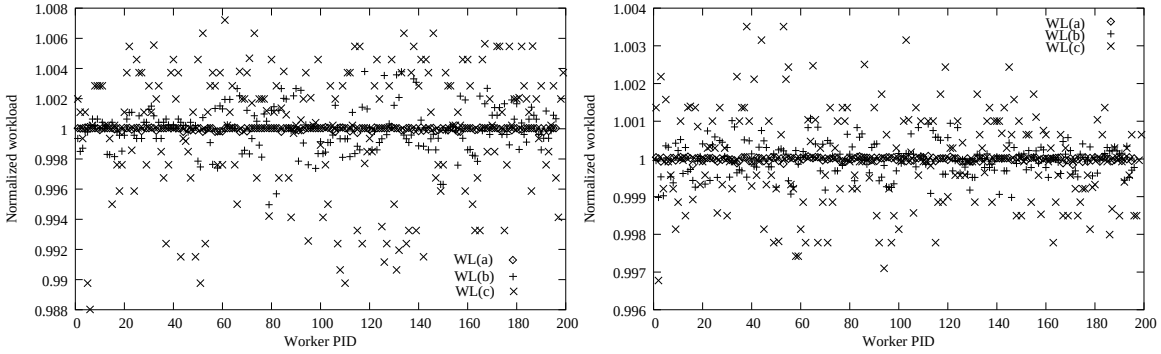

II. Normalization based on $P/4$ processors for case (b) on Test Function 6 (left) and Test Function 7 (right).

Figure 4.8. Comparison of the workload (WL) patterns among workers for cases (a) (circles), (b) ("+" marks), and (c) ("x" marks).

values fluctuate in the narrowest range around the average value 1.0 as listed in Table 4.7. In Figure 4.8 I, case (b) presents the widest range (WR_{b1}) and an interesting pattern that correlates with the variance of the number of function evaluations for the four subdomains of Test Function 6. In case (c), the workload values fall within ranges slightly wider than those in case (a). Nevertheless, if the average workload is computed separately (based on $P/4$ processors) for each run of case (b), case (b)'s *thus computed* average workload range (WR_{b2}) for Test Function 6 is slightly narrower than that of case (c), but wider than that of case (a). This explains the timing results for Test Function 6 ($T_a < T_b \approx T_c$). Since s^2 is 0 for Test Function 7, the workload pattern is regular for all four runs of case (b) as shown in Figure 4.8 II. Also, the same workload range is obtained by either averaging the workload of all workers (WR_{b1}) or of the workers within each run (WR_{b2}) of case (b). Similarly for Test Function 7, the narrower workload range implies shorter parallel execution time. This experiment concludes that the multiple subdomain search has the best parallel performance in terms of parallel execution time and load balancing. Multiple subdomain search allows masters from different subdomains to provide work to the globally shared workers at different times, especially for subdomains that generate different amounts of

work. In comparison, all masters run out of tasks at the end of each iteration in the single subdomain search. In the latter case, therefore, all workers will be idle until new tasks are available at the next iteration, a direct consequence of the DIRECT algorithm's data dependency.

4.3. Related Work in Parallel Design for Global Optimization

4.3.1. Direct Search Methods

Direct search methods are characterized by the fact that they do not use derivatives [58], thus are usually more robust in the situations where the function values are subject to noise, analytic derivatives are unavailable, or finite difference approximations to the gradient are unreliable. Torczon [89] designs parallel implementations for Intel's distributed memory parallel machines, including iPSC/2, iPSC/860, and the Intel Touchstone Delta. The author approaches the parallelism from two levels, one at the programming level for a "do-loop", the other at the compilation level where some directives are used to allow for parallelization on the Sequent Symmetry S81, a typical shared-memory parallel machine. The SPMD (single program multiple data) model is used for the parallel computation. Two sets of library subroutines are provided for constructing parallel search schemes and performing the actual optimizations respectively.

Dennis et al. [25] give a detailed algorithm design procedure for a class of parallel direct search methods. Scalability and efficiency are two major concerns for this research work. In the context of direct search methods, it is demonstrated that computing additional function values at each iteration can reduce the elapsed time to completion of an algorithm in a parallel computing environment and may actually reduce the total number of function evaluations required to produce an acceptable solution. In terms of implementation efficiency, Dennis et al. minimize the cost of communication by stacking function evaluations on each processor until the computation cost balances the communication cost. With an assumption that the dimension of the problem is smaller than the number of available processors, the parallel implementation achieves a near-linear speedup. The authors pointed out that scalability may be degraded if additional processors are added to enhance the performance of an inherently sequential algorithm. The inherently sequential nature of some algorithms like Newton or quasi-Newton methods limits the number of processors that can be successfully employed if the fundamental algorithm remains essentially unchanged. A different approach is to tailor the original algorithm to fit the new specifications given by the dimension of the problem, the number of available processors, and the relative expense of function evaluations to communication costs. Hence, different algorithms are remodeled with different performance characteristics.

4.3.2. Combinatorial Optimization Methods

Many search methods in the literature have been applied to the combinatorial optimization problems. The problem statement is similar to the general GOP given in Equation (2.1), that is, to find a solution x that minimizes (maximizes) an objective function $f(x)$ within a specified discrete set X. Holmqvist et al. [51] survey several heuristic methods, such as SA (simulated annealing), TS (tabu search), and GA (genetic algorithm). Finally, branch and bound (B&B) is discussed as the last example.

A. Simulated Annealing

The name "simulated annealing" derives from the analogy between annealing material and the strategy of solving combinatorial optimization problems. Annealing means that a solid material is heated beyond its melting point and then slowly cooled. When cooling stops, the material settles in a low energy state. In combinatorial optimization, this is represented by moving in the landscape constituted by the feasible search space, and when the algorithm stops, a feasible solution has been obtained. SA defines a series of states that are reachable from the current state. From an initial state, a random perturbation of the system generates a new state as the new solution. The change of the objective function from the new state to the old state is calculated. If the change is negative, the new state is accepted. If it is non-negative, the new state is accepted depending on a probability function controlled by the current temperature and the recent change. Thus, SA is a method of accepting small increases in the objective function value through adjusting the temperature. Stopping criteria for the SAs are generally as follows: the temperature has reached the specified lowest level, a number of iterations or temperature decreases has passed without acceptance, the proportion of accepted moves drops below a given value, or a given, maximum number of iterations has been completed.

Due to SA's inherently sequential nature, the simplest and the most straightforward parallel scheme is to let all available processors run a sequential SA on the whole problem and then select the best solution found at the end. An improved approach is to coordinate the processors for a given time period to explore the most promising areas of the design space. The third proposed strategy is to split the search area into as many parts as the number of available processors and distribute each to one processor. This approach requires the effort of decomposing the problem domain and coordinating the operations on distributed data structures. Besides the three naive approaches above, the authors survey other sophisticated approaches for parallelizing SA, such as the master-slave model, division strategy, and clustering strategy. The master-slave model has become one of the most general design patterns used in parallel computation [53]. In fact, both the division and the clustering strategies can be viewed as variants of the master-slave model. For the DIRECT algorithm, both Baker et al. [93] and Gablonsky [29] apply this model to their parallel DIRECT implementations.

B. Tabu Search

Similar to SA, TS uses a heuristic to move from one solution to the next. But it provides a better strategy to overcome the risk of getting stuck in a local minimum, in contrast to the random choice strategy of SA. First, an initial solution is constructed by using problem-specific properties. Next, the cost function values for candidate solutions in the neighborhood are computed and an attempt to move to the neighbor giving the best solution is made. To avoid getting stuck in local minima, historical information from the previous k iterations is used. The set of solutions obtained by this information forms a tabu list, which becomes the short-term memory for the recently explored directions. These directions will be disallowed in the following k moves. TS does not converge naturally, so a typical stopping rule is a specified number of iterations.

As for parallel TS, Holmqvist et al. [51] offer similar strategies to the ones for SA. An adaptive parallel scheme is proposed by Talbi et al. [86] to dynamically adjust the parallelism degree of the application with respect to the system load. A dynamic scheduling system MARS (multiuser adaptive resource scheduler) [37] is used to harness idle time and support reconfiguration of the active set of processors. Two main categories of parallel TS algorithms are given as (1) domain decomposition for the search space or the neighborhood, and (2) multiple TS task partition with independent or cooperative task execution. Additionally, Talbi et al. [86] extend this classification by introducing a new taxonomy dimension: the task scheduling scheme for processors. Non-adaptive, semi-adaptive, and adaptive are the three new categories determined by the dependency of the number and location of tasks/data on the parallel machines. Experimental results of applying MARS to the QAP (quadratic assignment problem) are shown to demonstrate the improved adaptability, efficiency, and robustness.

C. Genetic Algorithms

Unlike TS and SA, GAs have an inherent parallel nature, which has resulted in a great number of implementations and publications in this area [51]. Cantu-Paz [16] collects, organizes, and presents some representative parallel GAs. GAs are stochastic search algorithms based on an analogy to natural selection and recombination. They attempt to find the optimal solution to the problem at hand by manipulating a population of candidate solutions. The population is evaluated and the best solutions are selected to "reproduce" and "mate" to form the next generation. Over a number of generations, good traits are intended to dominate the population, resulting in an increase in the quality of the solutions. McMahon et al. [65] summarize some differences of GAs from traditional optimization and search methods. First, traditional methods mostly work on a single candidate solution instead of populations of candidate solutions. Second, a broader scope of GAs helps solve problems with noisy or discontinuous fitness values in large search spaces.

GAs and SAs are stochastic algorithms, and hence require an ensemble of runs for reliable results. McMahon et al. [65] apply this ensemble concept to partition each population into subpopulations. A ring-based migration model is proposed to separately evolve subpopulations and selectively share genetic information among them. The ring topology is used in both migration and termination detection. Load balancing is another design issue highlighted in [65], because the variation in the number of generations to converge for the distributed subpopulations will eventually lead to a load imbalance. A dynamic load balancing strategy was introduced to redistribute work to processors that finish the work early and become idle. The approach presented in [65] belongs to the most sophisticated class of multiple-population coarse-grained GAs categorized by Cantu-Paz [16]. The other two major classes are global single population master-slave GAs and single-population fine-grained GAs. The master-slave GAs have a single population, for which the evaluations of fitness are distributed among processors. They are also known as global GAs because the selection and crossover operations consider the entire population. Fine-grained parallel GAs differ from global GAs in the scope of manipulations, which are restricted to neighborhoods in one spatially structured population. Cantu-Paz [16] emphasizes that the fine-grained and coarse-grained GAs change the way the original GA works, while the global GAs do not affect the behavior of the original algorithm. A combination of some of these three classes is called hierarchical parallel GA, which promises better performance than any of the component approaches. At a higher level, it is a multiple population algorithm with single population parallel GAs (either master-slave or fine-grained) at the lower level. A new degree of complexity may be introduced to the already complicated scene of parallel GAs, but the execution time can be reduced more than any of the component methods.

D. Branch and Bound

The last example is another widely used method for solving combinatorial optimization problems—branch and bound (B&B). The B&B search starts at the root of a state space tree [95], which can be constructed dynamically depending on problem-dependent choices. The choice made at each level leads to one of the branches at the next level, therefore it reduces the cost by directing the search to only parts of the design space implicitly [19]. The tree can be explored by a best-first method instead of a depth-first or a breath-first to avoid exhaustive search in all nodes at each level, thus guide the search down to paths that most likely lead to the best solution. Pruning is another strategy of avoiding unpromising search paths by bypassing paths that can not lead to a better solution than the current best solution.

Considering a minimization problem, a B&B algorithm consists of three main components: (1) a bounding function or cut-off function provided for a given subspace of the solution space with a lower bound for the best solution value obtainable in the subspace, (2) a strategy for selecting the live solution subspace to be investigated in the current iteration,

and (3) a branching rule to be applied if a subspace after investigation cannot be discarded, hereby subdividing the subspace considered into two or more subspaces to be investigated in subsequent iterations [19]. In (2) above, a live solution subspace consists of live nodes. A "live node" is a node that has been reached but not all its children have been explored. It becomes a dead node when all of its children have been visited. Queue and stack are two common data structures for the B&B implementation.

An attractive feature of B&B is that disjoint subtrees can be dealt with independently, which makes it well suited for parallel implementations. However, several issues make the parallelization more complex and less efficient. First, the current lower bound generated by the bounding function is required by all the processors to prune their portion of the tree optimally. The level at which to prune changes during the search, as better solutions are found. In addition, the size of the state space tree in any partition is unknown in advance. Load balancing becomes a significant issue. For a shared memory model, the list of live nodes is a shared data structure, which needs synchronized access. The resultant serialization significantly limits the potential speedup. Rao et al. [79] propose a method of synchronizing a portion of the shared data structure. Additional status information has to be stored in each node to control multiple access. For a message-passing model, the data structure is distributed among processors and broadcasting is used to update the current better nodes to each other at intervals. Interprocessor communication cost can be reduced by selecting children nodes at random instead of a fixed order [54]. Three kinds of *speedup anomalies* may occur for the parallel B&B implementations: acceleration anomaly (greater than n), deceleration anomaly (less than n), and detrimental anomaly (less than 1). Theoretical studies have shown that they stem from the dynamic development of the search tree. Strategies were proposed in [19] to prevent the speedup anomalies.

CHAPTER 5: Error Handling

Program robustness requires error handling that anticipates, detects, and resolves errors at run time. The highest level of error handling capability is fault tolerance that attempts to recover from hardware or operating system failures if possible, and if not, terminates the program gracefully. The tradeoff for fault tolerance is increased program complexity. The errors encountered in this work come from several sources, including input parameters, memory allocation, files, MPI library, and hardware/power failure, etc. The error handling strategies here aim at balancing potential computation loss with implementation complexity. Therefore, simple fault tolerance features are considered only for recovering from some of the input parameter errors. The remaining errors are regarded as fatal errors, which are handled by checkpointing to save the computation as much as possible for later recovery.

5.1. Error Sources

Input parameter errors: Input parameter errors—for instance, the given lower bounds are not less than the upper bounds or none of the four stopping rules is specified—are recognized in the initialization phase. The function `sanitycheck` verifies all input parameters and assigns values to the derived local variables. Some input parameter errors are recoverable when the parameters are also in the output list. In this case, the default parameter values are set or the desired features are disabled, and the revised parameter values will be reported to the user upon return. Examples of such errors include nonpositive values of `MAX_ITER`, `MAX_EVL`, or `MIN_DIA` for stopping conditions. Also, if the box structures in (the subroutine argument) `BOX_SET` are not allocated, the missing pointers are recovered by allocating them with the correct problem dimension. For an irrecoverable error, the error code is returned in `STATUS`, which is an integer in the serial version, or an array of integers to hold return statuses for all subdomains in the parallel version. All masters and workers will check the sanity of input parameters and handle such errors in the same way.

MPI errors: The MPI function calls in the parallel version may also return errors at run time. By default, any error that MPI encounters internally for the global communicator `MPI_COMM_WORLD` is set as `MPI_ERRORS_ARE_FATAL` whose default action aborts the entire program. In this work, `MPI_ERRORS_RETURN` is set in place of the default error handler to notify the user of errors during the initialization phase, and reset to the default one to reduce the overhead after all processors have passed the initialization. `MPI_ALLTOALL` is used to collect initialization status on each processor from all others. If a fatal error occurs on a subset of processors during initialization, every processor is notified that the initialization failed. Then, the program terminates gracefully with a defined error code. The fatal errors here include those related to MPI and also all the irrecoverable errors discussed in this section.

Memory allocation errors: The next source of errors is memory allocation that aborts the program when the virtual memory is exhausted. The behavior of the program depends on the virtual memory management under a particular operating system. It may simply quit or may become intolerably slow because of the heavy disk paging. The ultimate solution for this type of error is checkpointing (see the next section).

5.2. Checkpointing Method

This work adopts a user level and nontransparent checkpointing method that records or recovers function evaluation logs via file I/O. [76] categorizes such a method as "user level" and "nontransparent" because it is visible in the source code and is implemented outside the operating system without using any system level utilities. It requires more programming effort than simply applying system level transparent tools (e.g., MPICH-V by [15], FT-MPI by [27], LAM-based MPI-FT by [62], or model based fault tolerance MPI middleware by [11]), but it is flexible and precise in choosing what to save, instead of dumping all the relevant program and even system data. Another drawback of using fault tolerance enhanced tools in a parallel program is the dependence on a particular implementation of the MPI standard. For MPI based programs, Gropp et al. [35] also recommend "user-direct" checkpointing with which it is easier to extract all the necessary state information than with "system-direct" methods. In the present work, function data points $(x, f(x))$ are chosen as the checkpointing state information for both serial and parallel versions.

The checkpointing switch `RESTART` can be 0 ("off"), 1 ("saving"), or 2 ("recovery"). During checkpointing, the errors are mainly related to the file in the process of opening, reading, writing, verifying the file header, or finding checkpoint logs. For "saving", the program will report an opening error if the default checkpoint file already exists, in order to prevent the saved checkpoint logs from being overwritten. Hence, an old checkpoint file should be either removed or renamed before starting another "saving" run. The opening error also occurs when "recovery" can not find the needed checkpoint file. Note that the checkpoint file has a fixed name (`vtdirchkpt.dat`) in the serial version, while in the parallel version, the file name on each master is tagged with its subdomain ID and master ID (i.e., `pvtdirchkpt.000.001` is saved by $SM_{1,2}$ in SD_1).

Each checkpoint file has a header containing important parameters that must be validated in the recovery run to ensure that **Sampling** will produce the same sequence of logs as in the file. For the serial version, the header includes the problem dimension, upper and lower bounds, ϵ, and the aggressive switch. Changing any of these parameters will result in different point sampling. However, other input parameters such as `MAX_ITER` or `BOX_SET` can be modified for the recovery run. Some applications may use checkpointing as a convenient probing tool to find a good stopping condition or a reasonable set of best boxes. In the parallel version, m (the number of subdomains) and n (the number of masters per subdomain) are added in the header. m must be the same in the recovery run, but n is permitted to be changed in order to adjust the number of masters. This makes it possible to recover a crashed run due to memory allocation failure.

In the serial version, a checkpoint log consists of the current iteration number t, a vector c of point coordinates, and the function value val at c. The "saving" run records each evaluation as a checkpoint log in the file. Assuming the computing platform is the same,

the points are sampled in the same sequence for the same number of iterations/evaluations, because of the deterministic property of DIRECT. Therefore, the recovery run loads all the checkpoint logs, or those that are within the iteration limit if specified. These logs are stored in a list in the same order as in the file, and will be recovered in that order as the program progresses. Recall that in the serial version, **Sampling** samples around one convex hull box at a time, but in the parallel version, it samples around all the convex hull boxes to produce as much work for the workers as possible. As the serial program generates new points, N_t (the number of points at iteration t) is unknown. Therefore, t is required for each checkpoint log in the serial version. However, N_t is known under the parallel version. Hence, the checkpoint file has a different form for the parallel version—in addition to a file header, a subheader consisting of t and N_t is followed by N_t logs, each with c and val.

When the number of masters n is the same as the "saving" run, the recovery run proceeds on each master similarly as in the serial version. If n is changed, the masters in the recovery run read in the checkpoint logs from all the files generated by all the masters during the saving run. Since the total number of logs aggregated from all masters may become very large, the masters load the logs only for the current iteration. The original deterministic sequence on a single machine breaks into pieces on multiple masters, so it is better to organize the logs for easy searching. In the present work, these logs are sorted in lexicographical order of the point coordinates, which are looked up using a binary search to retrieve the corresponding function values. When the checkpoint file is corrupted or is from a different platform, some point coordinates may be missing—a fatal error that aborts the recovery run.

5.3. Overhead Evaluation

The following experiments measure the checkpointing overhead under the serial and parallel running environments. The evaluation limit is 10^5 and the original cost $T_e \approx 0.0$ is used for the five test functions. Table 5.1 reports the execution time without checkpointing T_{nc}, the time for "saving" T_{sv}, and the time for "recovery" T_r. First, note that T_{sv} is always greater than T_{nc}, but T_r is sometimes less than T_{nc}. This means the recovery overhead is very tiny even for the cheap functions. Second, the saving overhead depends heavily on the number of iterations, because the checkpoint logs are flushed to the file at the end of each iteration. The average saving overhead per iteration is approximately 0.003 second. For real-world applications, T_e is usually much greater (e.g., $T_e \approx 3.0$ and 11.0 for the cell cycle parameter estimation problems presented in Chapter 7). In such cases, the saving overhead would be insignificant compared to the cost of function evaluations.

Under the parallel environment, all processors are masters since the function evaluation cost is too low to justify distribution to workers. Table 5.2 shows the timing results of saving and recovering the checkpoint logs saved by a single master and recovered using multiple masters, and both saving and recovery with multiple masters. The checkpointing overhead on a single master in the parallel version is slightly more than that in the serial version. Recovering with multiple masters costs more than that with a single master, but the overhead does not grow dramatically as the number of masters doubles. In some cases, the recovery overhead even drops with more masters. The saving and recovery overhead with three masters is also comparable to that with the single master. In summary, checkpointing overhead is very insignificant compared to the benefit of saved computation for expensive function evaluations.

Table 5.1. Comparison of serial checkpointing overhead (in seconds) for five test functions. I is the number of iterations upon termination with the stopping rule $L_e = 10^5$, T_{nc} is the execution time without checkpointing, T_{sv} is the execution time with saving, and T_r is the execution time for recovery.

#	I	T_{nc}	T_{sv}	T_r
GR	3057	10.58	18.85	11.50
QU	12238	56.70	87.38	57.28
RO	1198	8.12	11.61	9.22
SC	3637	11.97	21.43	12.96
MI	1968	29.69	34.61	24.05

Table 5.2. Comparison of parallel checkpointing overhead (in seconds) when saving with a single master (m1) and saving with three masters (m3) for five test functions. The stopping rule is evaluation limit $L_e = 10^5$. T_{nc} is the execution time without checkpointing, T_{sv} is the execution time with saving, and $T_r(m)$ is the execution time for recovery with m masters.

#	T_{nc}	T_{sv}	$T_r(1)$	$T_r(2)$	$T_r(3)$	$T_r(4)$	$T_r(5)$	$T_r(7)$	$T_r(8)$
GR m1	13.22	21.06	14.43	26.11	–	22.76	–	–	27.86
GR m3	11.95	21.07	–	–	12.71	–	23.49	27.24	–
QU m1	55.87	109.15	57.42	76.27	–	86.51	–	–	104.47
QU m3	68.58	83.04	–	–	49.52	–	95.78	107.46	–
RO m1	9.33	12.80	10.70	16.89	–	13.74	–	–	14.50
RO m3	6.61	10.47	–	–	7.02	–	13.28	13.89	–
SC m1	14.44	23.38	15.37	30.05	–	26.11	–	–	30.39
SC m3	14.49	25.59	–	–	13.68	–	34.40	29.87	–
MI m1	30.31	35.58	23.30	21.57	–	18.87	–	–	20.68
MI m3	14.40	17.84	–	–	11.74	–	18.28	20.03	–

CHAPTER 6: Performance Study, Modeling, and Analysis

Several optimization parameters and system characteristics listed in Table 6.1 are selected for the performance sensitivity study. In fact, more input parameters are required to define the optimization problem. For example, the upper and lower bounds of the design domain define the search region. Varying the bounds certainly affects the convergence rate as well as the total computational cost to reach the solution, so the proper bounding for a particular problem deserves a thorough application-oriented study by researchers in that field. In this section, upper and lower bounds are fixed for each problem as in Appendix A.

Table 6.1. Parameters and characteristics under study.

#	Description
ϵ	Search tuning parameter
N_d	Problem dimension
$I_{\max}$	maximum iterations
N_b	number of evaluations per task
m	number of subdomains
n	number of masters per subdomain
k	number of workers
T_f	objective function cost, seconds
T_{cp}	point-to-point round trip cost, microseconds
T_{ca}	one-to-all broadcast cost, microseconds

The first three parameters affect problem configuration. The parameter ϵ tunes the search broadness as discussed in Chapter 2. The parameters N_d and $I_{\max}$ directly affect the problem scale. $I_{\max}$ is also required to enable the local memory reduction technique discussed in Chapter 3. Section 6.1 studies the parameters for problem configuration. The parallel scheme parameters N_b, m, n, and k have great impact on both minimization performance and parallel performance such as load balancing. In Section 6.2, these performance metrics are analyzed theoretically and experimentally. The next subset $\{T_f,\ T_{cp},\ T_{ca}\}$ determines the task granularity defined as the ratio of the computation time to communication time per task. These parameters are addressed in Section 6.3, followed by detailed discussions of the influence of these parameters on overhead and scalability in Section 6.4.

6.1. Problem Configuration

6.1.1. ϵ Tuning Parameter

The convergence speed certainly depends on the problem structure, but the parameter ϵ also plays an important role as reported by [56], [28], [29], and [31]. The following tests demonstrate how ϵ affects the convergence speed on the benchmark functions. The convergence is defined as when both the global optimum value $f_{\min}$ and global optimum solution x_0 are achieved within less than 0.1% error, thus the desired accuracy is $\alpha =$ 1.0E-03. [56] recommends ϵ to be the desired solution accuracy to find good optimization results with a reasonable amount of work. Table 6.2 lists the number of iterations (N_I) and evaluations (N_e) needed to converge to the solution for the benchmark functions with ϵ values in (0.0, 1.0E-02).

When ϵ is between 1.0E-03 and 1.0E-07, all benchmark function optimizations converge with a reasonable number of iterations and evaluations. $\epsilon = \alpha$ yields the smallest number of evaluations for QU, SC, and MI, and the second smallest for RO. The problem GR prefers ϵ as small as possible to minimize the amount of work. However, observe that the MI optimization fails to converge when $\epsilon = 0.0$, because the search is biased to be so local that the search has to stop since the minimum box diameter 1.26E-15 has been reached after 235 iterations and 25301 evaluations. Moreover, using $\epsilon =$ 1.0E-02 $> \alpha$ increases the number of evaluations a thousand fold for the problem QU. Therefore, the desired accuracy is proved to be a reasonable choice for ϵ, unless the optimization goal is to find a local solution, in which case $\epsilon = 0.0$ can improve local convergence, or to broadly explore the feasible set, when $\epsilon > \alpha$ is appropriate.

Table 6.2. The number of iterations N_I and evaluations N_e required for convergence with ϵ varying in (0.0, 1.0E-02).

	GR		**QU**		**RO**		**SC**		**MI**	
ϵ **value**	N_I	N_e	N_I	N_e	N_I	N_e	N_I	N_e	N_I	N_e
1.0E-02	259	3561	$> 12 \cdot 10^3$	$> 10^5$	151	6567	33	285	892	16771
1.0E-03	25	295	57	563	146	6883	22	151	312	10890
1.0E-04	15	143	57	587	146	7217	21	157	318	14559
1.0E-05	14	135	57	613	146	7423	21	157	319	17629
1.0E-07	14	135	57	637	146	7485	21	157	319	23059
0.0	14	135	57	679	146	7485	21	173	—	—

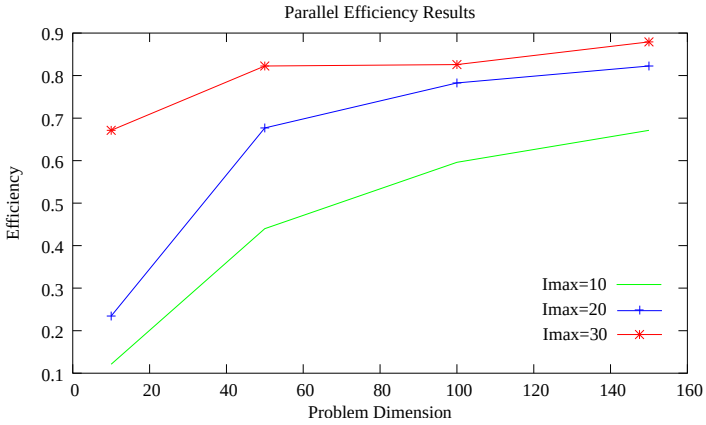

Figure 6.1. Parallel efficiency comparison for the RO function using 100 processors. $N_d = 10$, 50, 100, and 150. $I_{\max} = 10$, 20, and 30.

6.1.2. Problem Scale Parameters

As N_d grows, the memory requirement imposed by the intermediate data increases dramatically as shown in Figure 1.1. A local memory reduction technique—LBC (limiting box column)—has been discussed in Section 3.2 and is evaluated in the next section.

Large scale problems with higher dimensions (larger N_d) and larger $I_{\max}$ are intended to generate more work that keeps a large number of processors busy. Figure 6.1 shows the comparison of parallel efficiencies with various N_d and $I_{\max}$ for the RO function using $p = 100$ processors. The parallel efficiency E is the ratio of (algorithmic) speedup $S = T_s/T_p$ to p, where T_s is the execution time with a single processor and T_p is the parallel execution time with p processors. E is improved with both increasing N_d and increasing $I_{\max}$, because higher N_d and larger $I_{\max}$ yield more function evaluations. Better load balancing is the real reason behind the improved parallel efficiency as the problem scale grows. A workload model bound is discussed later to analyze the performance influence of the parallel scheme parameters.

6.1.3. Memory Usage Comparison

The bar plot in Figure 6.2 compares the memory allocated for holding boxes with and without LBC for all test problems. The first five artificial functions set $N_d = 150$ to generate an amount of intermediate data comparable to that for the BY problem. Memory usage for the FE problem is the smallest, because it has the lowest N_d. All tests were run on a single machine until (1) the stopping condition $I_{\max} = 1000$ was reached, or (2) the diameter of the box holding the best solution became smaller than the problem precision, or (3) the run crashed due to memory allocation failure. Table 6.3 compares the number of iterations I_{out} for all test problems on a single processor before it halts due to one of the above three conditions. The LBC technique reduces the memory usage by 10–70% for the test problems so that the program can run longer without memory allocation failure on a single processor.

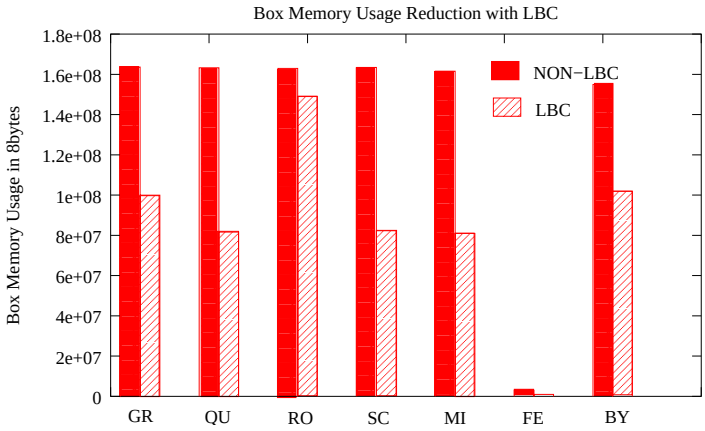

Figure 6.2. Comparison of box memory usage without LBC (NON-LBC) or with LBC for all the test problems.

Table 6.3. Comparison of I_{out} (the number of iterations before the program halts on a single processor) without (NON-LBC) and with LBC for all test problems. $I_{\max} = 1000$.

#	NON-LBC	LBC
GR	206	467
QU	90	1000
RO	105	122
SC	95	453
MI	82	936
FE	316	316
BY	185	477

6.2. Scheme Configuration

6.2.1. Parameter N_b

Extending Equation (4.1) in Chapter 4, a theoretical lower bound on the parallel execution time T_t for the parallel scheme with k workers is:

$$T_t(N_b) = \sum_{i=1}^{I_{\max}} \left\lceil \frac{F_i}{k} \right\rceil (N_b T_f), \tag{6.1}$$

where F_i is the number of function evaluation tasks at iteration i, and N_b is the number of point evaluations per task. Implicitly, such a lower bound assumes $T_f > T_{cp}$, a necessary condition for achieving reasonable speedup when distributing tasks to remote workers. It considers the computation time of function evaluations and the idle time of workers waiting for new tasks to become available at the beginning of each iteration.

With P_i being the number of point evaluations required at iteration i, the number of tasks $F_i = \lceil P_i/N_b \rceil$, and thus the theoretical lower bound for iteration i is

$$\left\lceil \frac{F_i}{k} \right\rceil (N_b T_f) = \left\lceil \frac{\lceil P_i/N_b \rceil}{k} \right\rceil (N_b T_f).$$

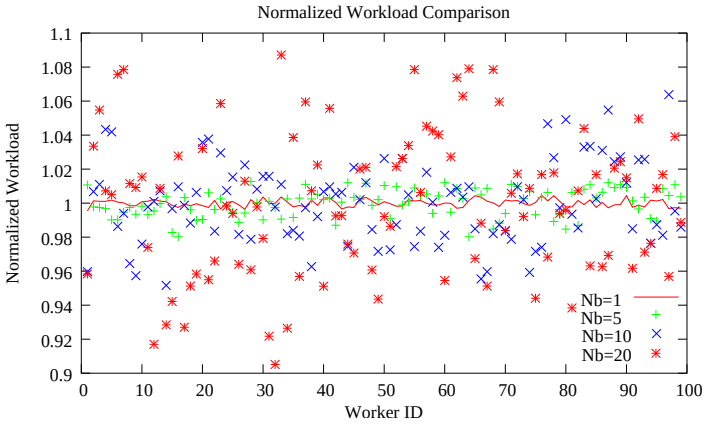

Figure 6.3. Comparison of the normalized workload on 99 workers with $N_b = 1$, 5, 10, and 20 for the 150-dimensional GR function.

This is clearly minimal when both $N_b \mid P_i$ and $k \mid (P_i/N_b)$, but lacking this divisibility, the minimum expected value occurs for $N_b = 1$, since

$$\left\lceil \frac{\lceil P_i/N_b \rceil}{k} \right\rceil N_b = \left(\frac{P_i}{N_b k} + \frac{a}{N_b k} + \frac{b}{k} \right) N_b$$
$$= \frac{P_i}{k} + \frac{a}{k} + \frac{bN_b}{k},$$

where $0 \le a < N_b$ and $0 \le b < k$, is clearly minimal (in expected value) for $N_b = 1$. (Note: (6.1) is valid except for the special case where $F_i \bmod k = 1$ and one task has $0 < N_{b-} = P_i \bmod N_b < N_b$ point evaluations. In this case the optimal choice for N_b is the value that minimizes N_{b-}. Since for $k \gg 1$, $F_i \bmod k = 1$ is a rare event, this special case is ignored here.)

Figure 6.3 compares the normalized workload on 99 workers with increasing $N_b = 1$, 5, 10, and 20. A better load balance is achieved when $N_b = 1$, so $N_b > 1$ should only be used to stack cheap function evaluations to achieve $N_b T_f > T_{cp}$. Detailed analysis for load balancing is given in the following subsection.

6.2.2. Subdomain Parameter m

The scheme parameter m, the number of subdomains, is specified according to the computational budget and optimization goal. With more function evaluations generated across multiple subdomains, the same $I_{\max}$ likely yields a better solution than the single domain search. Figure 6.4 compares the function minimization progress with a single domain ($m = 1$) and four subdomains ($m = 4$) for FE [99] and BY [74], the cell cycle parameter estimation problems. In both cases, the single subdomain search results in higher minimum function values. This behavior indicates an irregular or asymmetric problem structure, a common case for many science and engineering problems. If the problem structure is symmetric or the global minimum is near the center, a single domain DIRECT search may

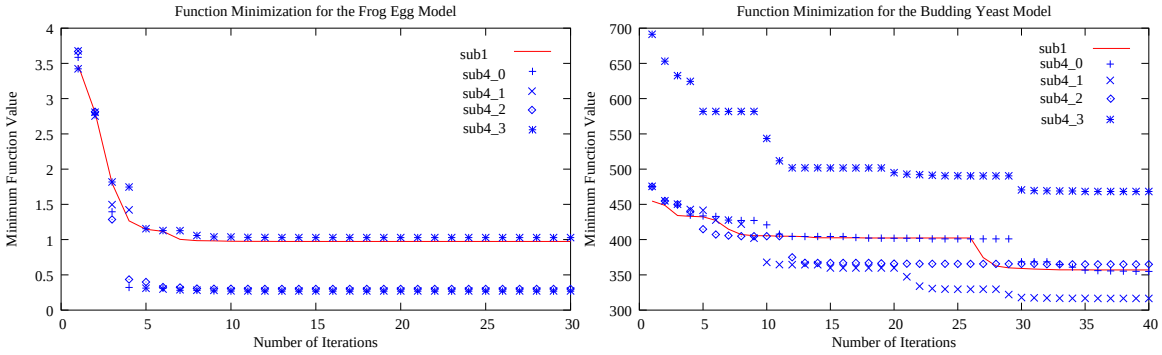

Figure 6.4. Comparison of function minimization on FE and BY for a single domain (sub1) on left and four subdomains (sub4_i) on right, where i is the subdomain ID.

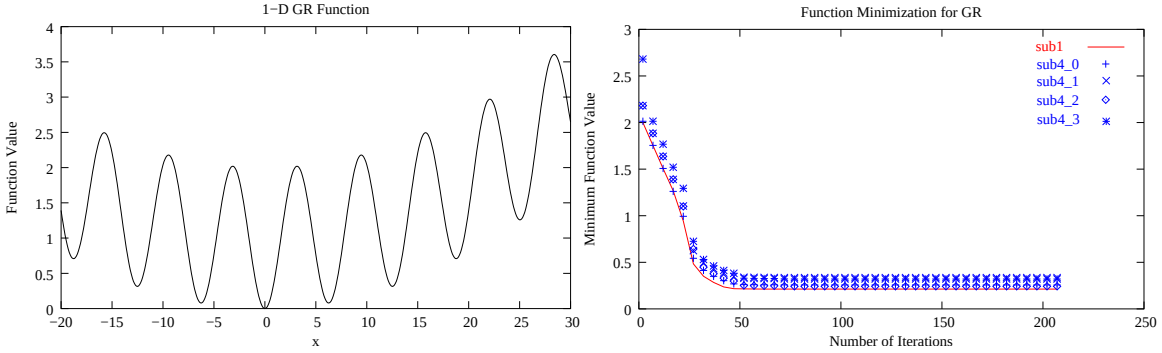

Figure 6.5. (a) The 1-D view of the GR function (left). (b) Comparison of function minimization (right) on a 150-dimensional GR function for a single domain (sub1) and four subdomains (sub4_i), where i is the subdomain ID.

converge to the target faster than the multiple subdomain search. The GR function is such an example shown in Figure 6.5. The single domain search progresses slightly better than the four subdomain search, since the global solution is located close to the center of the design domain.

The second advantage of the multiple subdomain search is improved load balancing among workers. Section 4.2.3 shows that function evaluation tasks are distributed more efficiently to workers with a multiple subdomain search than a single domain search, especially when subdomains have unequal amounts of work. The globally shared workers have a better chance to find work if the subdomain masters are not synchronized due to the data dependency in a single domain. An analytical workload model is constructed here to interpret the experimental observations. For simplicity, the objective function cost T_f is assumed to be constant. Again, $T_f > T_{cp}$ is assumed so that the workload model can ignore all the communication overhead.

The model is developed from the simplest case with one subdomain $m = 1$, one master $n = 1$ and extended to cases with $m = 1$, $n > 1$ and $m > 1$, $n > 1$. The potential communication bottleneck at masters is not considered in this section assuming the message buffers

on master processors are sufficiently long and the service time for each message is negligible. Due to the variability of workload distribution among workers, a bounding analysis is applied to capture the lower and upper workload bounds. Bounding techniques require less computation and weaker assumptions than exact solution techniques, but sufficiently characterize the system performance under variability and uncertainties [63].

At every iteration, each master dispatches function evaluation tasks to workers upon request during **Sampling**, each task defined by the coordinates of N_b points. As before, let P_i be the total number of point evaluations during iteration i, and $F_i = \lceil P_i/N_b \rceil$ the total number of function evaluation tasks. When P_i is not exactly a multiple of N_b, the last task has $N_{b-} = P_i - \lfloor P_i/N_b \rfloor N_b < N_b$ points, but all the remaining tasks have N_b points. A task costs either $T_b = N_b T_f$ or $T_{b-} = N_{b-} T_f$. At iteration i, each of k workers obtains either $\delta_{i-} = \lfloor F_i/k \rfloor$ or $\delta_{i+} = \lceil F_i/k \rceil$ tasks. The workload on each worker is defined as the total computation time for function evaluations. When F_i is a multiple of k and P_i is not a multiple of N_b, the worker that obtains the last task with N_{b-} points reaches the lower bound $WL_{li} = (\delta_{i-} - 1)T_b + T_{b-}$. In other cases, the workload lower bound is $WL_{li} = \delta_{i-} T_b$. Note that $\delta_{i-} = 0$ when $F_i < k$. Summing over all $I_{\max}$ iterations, the workload lower bound is

$$WL_l = \sum_{i=1}^{I_{\max}} WL_{li},$$

where $WL_{li} = (\delta_{i-} - 1)T_b + T_{b-}$ if $k \mid F_i$ and N_b does not divide P_i; $WL_{li} = \delta_{i-} T_b$ otherwise.

Following the same reasoning, the workload reaches the upper bound when a worker obtains δ_{i+} tasks, all of which have N_b points to compute or one of which has $N_{b-} > 0$ points if the remainder of F_i/k is 1. So the upper bound

$$WL_u = \sum_{i=1}^{I_{\max}} WL_{ui},$$

where $WL_{ui} = (\delta_{i+} - 1)T_b + T_{b-}$ if $F_i - \lfloor F_i/k \rfloor k = 1$ and $N_{b-} > 0$; otherwise, $WL_{ui} = \delta_{i+} T_b$.

To compare workload balance for different problems, the workload is normalized by dividing by the average workload $\overline{wl} = \sum_{i=1}^{I_{\max}} (P_i/k) T_f$. Hence, the normalized workload WL_j on worker j (j = 1, 2, ..., k) is within the range $(WL_l/\overline{wl}, WL_u/\overline{wl})$. Let $WR = WL_u/\overline{wl} - WL_l/\overline{wl}$ be the measure of workload balance, so smaller WR is better. Observe that WL_l would be closer to WL_u with $N_b = 1$, because then $N_b \mid P_i$ always, yielding a

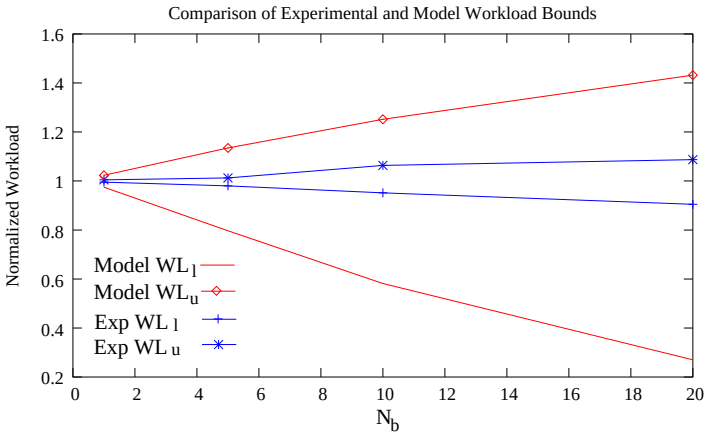

Figure 6.6. Comparison of the normalized workload bounds based on the model and the experiments with 99 workers and $N_b = 1$, 5, 10, and 20 for the 150-dimensional GR function.

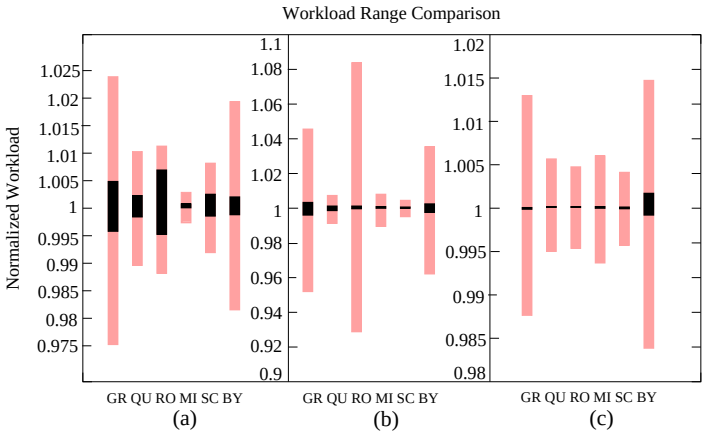

Figure 6.7. Comparison of the workload ranges based on the model (grey) and the experiments (black) for (a) a single domain search with 1 master and 99 workers, (b) a single domain search with 4 masters and 196 workers, and (c) a four subdomain search with 1 master per subdomain and totally 196 workers. $N_b = 1$. The vertical bars, left to right, correspond respectively to problems GR, QU, RO, SC, MI, BY. $I_{max} = 90$ and $N_d = 150$ for the artificial problems. $I_{\max} = 40$ and $N_d = 143$ for the BY problem.

larger WL_l. Recall that $N_b = 1$ also gives the smallest possible $WL_u = \sum_{i=1}^{I_{\max}} \lceil P_i/k \rceil T_f \leq \sum_{i=1}^{I_{\max}} \lceil \lceil P_i/N_b \rceil /k \rceil N_b T_f$.

Figure 6.6 plots the workload ranges estimated with the model and the actual workload ranges measured from experiments for different N_b values. All the experimental workload bounds are within the model estimation, but the difference between the experimental bounds and the model estimation becomes larger as N_b increases. The model sums up the lowest workload among workers over all iterations, while in reality, the workload on a particular worker has a fair chance to be the lowest at every iteration. Therefore, the load balancing measurement is better than the model estimation because of the inherent randomness of the parallel scheme.

For high dimensional test problems, Figure 6.7(a) compares the workload ranges based on the model and the experiments for a single domain search using one master and 99

workers. Consider only $N_b = 1$ for simplicity in the remaining analysis and discussion. The model estimations in Figure 6.7(a) are all within 2.1% of the measured workload bounds from experiments.

The above model can be easily extended to the case $n > 1$ with multiple masters sharing the memory burden and the computation involved in the parallel **Selection**. Since workers randomly select masters to request work, each master initially has an approximately equal number (k/n) of workers to compute its function evaluation tasks. Although masters may have different numbers of tasks, the global shared worker pool balances the workload by assigning workers to masters with work. A weight variable $w_{i,j} = F_{i,j}/F_i$ is introduced, where $F_{i,j} = w_{i,j}F_i$ is the number of tasks on master j for iteration i. Master j has $w_{i,j}F_i$ tasks, thus $w_{i,j}k$ workers are assigned to it. Each worker obtains $\delta_{i-} = \lfloor w_{i,j}F_i/(w_{i,j}k) \rfloor$ or $\delta_{i+} = \lceil w_{i,j}F_i/(w_{i,j}k) \rceil$ tasks. It turns out that $w_{i,j}$ is canceled out for the workload estimation. Hence, the number of masters n in a single domain search has little impact on the workload bounds. Table 6.4 shows the experimental results for the parallel execution time T_k and the normalized workload range (WR_k) using $k = 100$, 200 workers in a single domain search with the number of masters n varying from one to eight. The timing and load balancing results are very close to each other for all n.

Table 6.4. Comparison of the parallel execution time T_p and the measured normalized workload range WR_p for the RO function with $N_d = 150$, $T_f = 0.1$, and $I_{\max} = 90$ using 100 and 200 workers.

		Number of Masters			
k		1	2	4	8
100	T_k	348.56	346.90	351.39	348.04
	WR_k	0.013	0.015	0.018	0.019
200	T_k	200.30	183.00	184.20	182.59
	WR_k	0.018	0.026	0.024	0.032

The random worker assignment strategy plays an important role in balancing the workload among workers. If fixed worker assignment is used instead, each master would have a fixed number of workers (k/n) to compute the function evaluations for all iterations. Workers assigned to master j would obtain either $\delta'_{i+} = \lceil (w_{i,j}F_i)/(k/n) \rceil$ or $\delta'_{i-} = \lfloor (w_{i,j}F_i)/(k/n) \rfloor$ tasks. Note that $w_{i,j} = 1/n$ produces the same assignment as in the case of random worker assignment. With some $w_{i,j} < 1/n$ (implying $\delta'_{i-} \leq \delta_{i-}$) and some $w_{i,j} > 1/n$ (implying $\delta'_{i+} \geq \delta_{i+}$) under the fixed worker assignment, the lower bound WL_l becomes smaller and the upper bound WL_u becomes greater, but the average workload $\overline{wl}$ is the same, so the workload range $(WL_u - WL_l)/\overline{wl}$ becomes larger, indicating a worse balanced workload.

In the previous two cases, the masters in a single subdomain $m = 1$ serve as a single work source for workers. Multiple subdomains $m > 1$ serve as multiple work sources,

because the masters from different subdomains are not synchronized to update intermediate results or to compute the global convex hull boxes. A similar weight variable w'_j is used in this case to estimate the number of workers assigned for the subdomain j:

$$w'_j = \sum_{i=1}^{I_{\max}} F_{i,j} \Big/ \sum_{j=1}^{m} \sum_{i=1}^{I_{\max}} F_{i,j}, \tag{6.2}$$

where $F_{i,j}$ denotes the number of tasks at iteration i for subdomain j. w'_j is based on the overall tasks from all iterations because subdomains are asynchronous. In contrast, $w_{i,j}$ in the single domain case is defined for each iteration due to the global synchronization inside a subdomain. For subdomain j, the average workload is $\overline{wl_j} = \sum_{i=1}^{I_{\max}} F_{i,j}/(w'_j k)T_b$. The workload lower bound in subdomain j is $WL_{lj} = \sum_{i=1}^{I_{\max}} \lfloor F_{i,j}/(w'_j k) \rfloor T_b$, where $T_b = T_f$ because $N_b = 1$; the workload upper bound is $WL_{uj} = \sum_{i=1}^{I_{\max}} \lceil F_{i,j}/(w'_j k) \rceil T_b$. Hence, the overall normalized workload range is

$$\left(\min_{1 \le j \le m} (WL_{lj}/\overline{wl_j}), \max_{1 \le j \le m} (WL_{uj}/\overline{wl_j}) \right)$$

across all m subdomains. Figure 6.7(c) compares the model estimated workload ranges with the experimental results for a four subdomain search using 196 workers and four masters, one per subdomain. All the experimental workload results fall within the 1.5% ranges estimated by the model. Due to the randomness of workers' requests to masters, the experimental workload is better balanced than the (worst case) model estimation. For comparison, the workload ranges based on the model and experiments for a single domain search using the same number of masters and workers are shown in Figure 6.7(b). To keep the problem the same as in the four subdomain search, the single domain search is applied to each of the four subdomains sequentially using 49 workers and one master. The workload is normalized over the total workload of the four runs. The model estimated range for the single domain is wider than that for the four subdomains. This estimation is verified by the experimental results, which present smaller ranges for the four subdomain search (dark bars in Figure 6.7(c)) than for the single domain search (dark bars in Figure 6.7(b)).

6.2.3. Parameter n

The number n of masters affects the efficiency of **Selection** and data distribution. Convex hull computation is the key component in **Selection**. The parallel **Selection** involves both local and global computation of convex hull boxes. First, each subdomain master computes the local convex hull boxes. Next, the root subdomain master gathers all the local convex

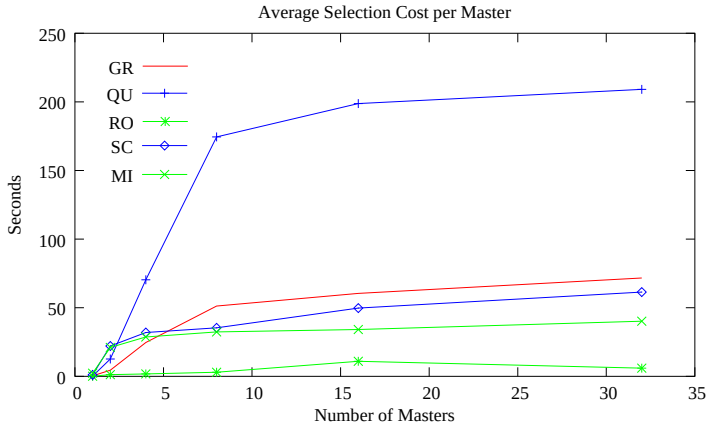

Figure 6.8. The average **Selection** cost per master increases as n grows from 1 to 32 for test problems. $I_{\max} = I_{out}$ with LBC support listed in Table 3.3 in Section 3.3.5.

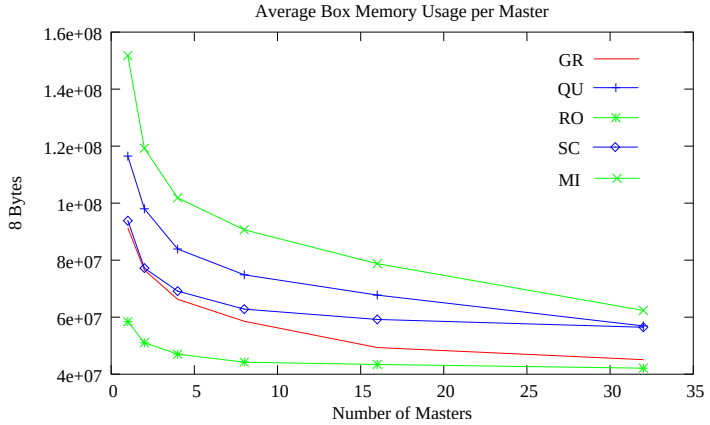

Figure 6.9. The average box memory size decreases as n grows from 1 to 32 for test problems. $I_{\max} = I_{out}$ with LBC support listed in Table 4.2.

hulls to find a global convex hull set of boxes. Finally, each subdomain master starts **Sampling** on its own portion of the convex hull boxes.

Recall that for the local convex hull computation, the gift-wrapping algorithm with complexity $\mathcal{O}(N^2)$ [64] is preferred because it requires no extra space. A faster algorithm, Graham's scan [34], is used for the global convex hull computation at the root subdomain master. It takes $\mathcal{O}(N)$ operations because the gathered local convex hull boxes are already sorted, saving $\mathcal{O}(N \log(N))$ operations required for sorting at the root subdomain master. Although the Graham's scan needs a stack for back-tracking, the buffer for merging local convex hull boxes also serves as a stack of boxes, which are indexed by integer pointers for back-tracking. As n increases, the number of sets of local convex hull boxes grows, and more boxes are merged at the root subdomain master for the final global computation. Since the root needs to gather from all and broadcast to all at each iteration, the communication overhead may overshadow the benefit of sharing the memory burden. Therefore, the value of n should be large enough to accommodate the intermediate data, yet no larger to minimize the network traffic for global communication.

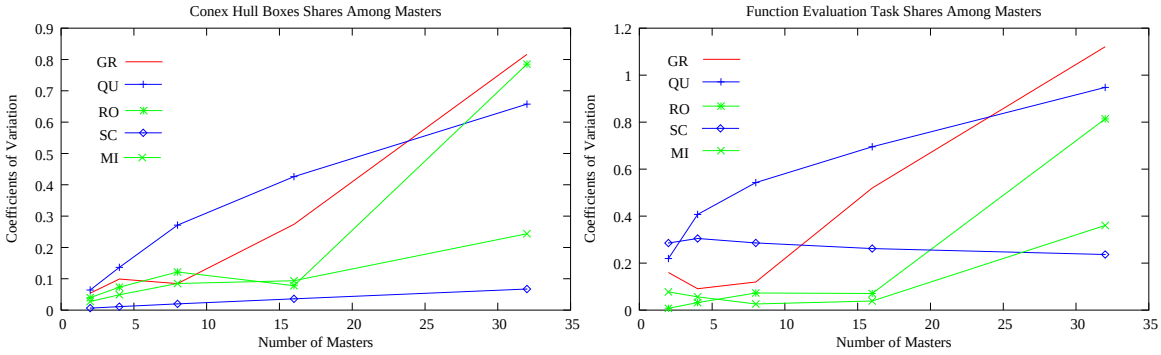

Figure 6.10. Coefficient of variation of (a) convex box shares (left) and (b) function evaluation task shares (right) as p grows from 2 to 32 for the horizontal scheme for test problems with $N = 150$.

To investigate the performance impact of n, other scheme parameters need to be fixed. The horizontal scheme with a single domain ($m = 1$), no workers ($k = 0$), and a varying number n of masters is employed to study the computational complexity of **Selection** and the balance of data distribution among masters. The analysis of n's influence on the communication overhead is presented in detail in Section 6.3, which discusses parameters related to system settings. Let LD_i be the number of different box diameters and LC_i the number of local convex hull boxes on master i ($i = 1, \ldots, n$). At the root subdomain master, $GD \leq \sum_{i=1}^{n} LC_i$ is the merged number of distinct box diameters and $GC \leq GD$ is the final number of convex hull boxes. The total convex hull computation includes n local gift-wrappings $\left(\mathcal{O}\left(\sum_{i=1}^{n}(LD_i)^2\right)\right)$, n global merges $\left(\mathcal{O}\left(\sum_{i=1}^{n} LC_i\right)\right)$, and one global Graham's scan ($\mathcal{O}(GD)$). Figure 6.8 shows how the average **Selection** cost per master grows as n increases for five test problems. Here, the cost includes the communication overhead and the convex hull computation. The motivation for using multiple masters is not to reduce the **Selection** cost, but to share the memory burden. As n grows from one to 32, the average memory storage for boxes is decreased significantly (shown in Figure 6.9).

6.2.4. Parameter k

In the previous section, the number of workers $k = 0$ forms a horizontal scheme of pure masters. In the vertical scheme, $k \geq 2$ workers are used with a single master. High objective function cost is one of the factors that favor the vertical scheme, where a large number of workers can be utilized efficiently. More importantly, the poor load balancing in the pure horizontal scheme becomes the major obstacle to using a large number of masters that compute function evaluations locally. At each iteration, convex hull boxes are assigned to masters using a simple balancing heuristic that apportions the boxes into approximately equal shares. However, the number of function evaluation tasks on a master depends on the number of longest dimensions contained by its share of the convex hull boxes. So the function evaluation tasks on masters are still very likely to be unbalanced even if all masters obtain the same number of convex hull boxes.

Finding an optimal convex hull box assignment that minimizes the variance of the combined number of longest dimensions on all masters is an NP-complete problem similar to the knapsack or bin packing problems [64]. Although a polynomial time approximate solution is available (i.e., dynamic programming), it does not solve all the balancing problems. Even if a supposedly optimal box assignment is found, a load imbalance still occurs when (1) an insufficient number of convex hull boxes is generated, or (2) T_f varies at different sample points. The first cause is inevitable in early stages of the DIRECT search, and it also happens more often for low dimension problems or problems with certain structures that produce a small number of convex hull boxes. The second cause is also common in many engineering design problems, such as the ray-tracing technique and WCDMA simulation in wireless communication system design [42] [47] [48].

Figure 6.10 shows the coefficient of variation (a) c_b for the convex hull box shares per processor and (b) c_f for the function evaluation task shares per processor with $p = 2$, 4, 8, 16, 32 for test problems with $N = 150$ and $I_{\max} = I_{out}$, the maximum number of iterations before the program halts on a single processor with the LBC support (see Table 6.3). The general trend is that both the convex hull and the function evaluation shares become less balanced as p grows except for the problem SC. For c_b shown in Figure 6.10(a), the problems GR, QU, and RO have a sharp increase, but the problems SC and MI increase slightly, because a larger number of convex hull boxes are generated per iteration for the last two problems (see Table 6.5, a list of the average convex hull boxes $\overline{N_{box}} = \sum_{i=1}^{I_{out}} C_i/I_{out}$ and function evaluation tasks per iteration $\overline{N_f} = \sum_{i=1}^{I_{out}} F_i/I_{out}$, where C_i is the number of convex hull boxes and F_i is the number of function evaluation tasks at iteration i). As the only exception, the problem SC has an improved function evaluation task balance even though its convex hull box balance becomes worse as p grows. However, if more than the necessary number of processors are used, i.e., $p > \overline{N_{box}}$, the problem SC will eventually become unbalanced on convex hull box and function evaluation task distribution among master processors.

Table 6.5. Comparison of the average number of convex hull boxes $\overline{N_{box}}$ and function evaluation tasks $\overline{N_f}$ per iteration for test problems.

#	$\overline{N_{box}}$	$\overline{N_f}$
GR	13.341	2990.2
QU	10.197	2007.8
RO	16.025	4234.7
SC	103.52	17152.0
MI	26.521	5942.0

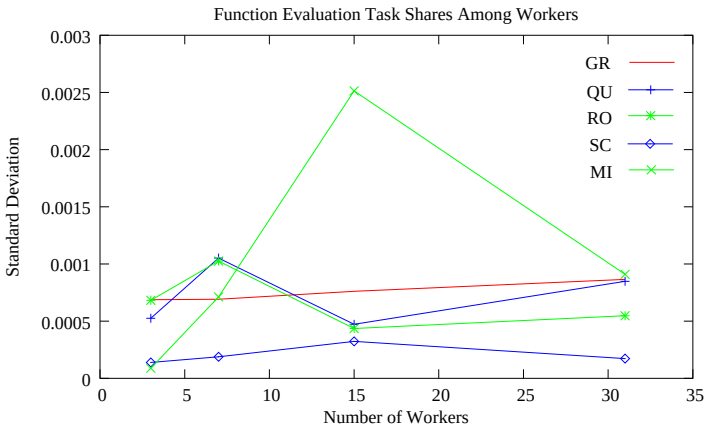

Figure 6.11. Coefficient of variation of the function evaluation task shares as p grows from 4 to 32 for the vertical scheme for test problems with $N = 150$.

For the vertical scheme, a similar set of experiments with $p \geq 4$ demonstrates a significant improvement on the function evaluation task balance among worker processors as shown in Figure 6.11. Not only does c_f decrease by two orders of magnitude, but the narrower range of values of c_f indicates better scalability. The drawback of the pure vertical scheme is the limited memory capacity on the single master processor that is dedicated to dispatching function evaluation tasks instead of carrying out the actual function evaluations as the masters do in the horizontal scheme. Therefore, the ultimate solution is the hybrid scheme that shares the memory burden on more than one master if necessary ($n \geq 1$), and dynamically assigns k workers to task-loaded masters. The number k of workers should be at least twice the number of masters, that is, $k \geq 2mn$.

6.3. Parallel System Parameters

All the analysis so far in this work is based on an ideal computing environment ignoring any communication overhead. This section addresses in detail the system configuration characterized by T_{cp}, T_{ca}, and T_f. An Apple Xserve G5-based system with 2,200 processors (System X) and an AMD Opteron-based system with 400 processors (Anantham) provide two different types of parallel computing environment.

Both System X and Anantham are cluster systems of dual CPU nodes located at Virginia Tech. On System X, 10 Gbps InfiniBand switches connect 1,100 nodes, each of which has two 2.3 GHz processors and 4 GB of main memory. On top of the 32-bit Mac OS X operating system, MVAPICH (MPI-1 implementation over VAPI [60]) software is used to communicate via the InfiniBand interconnect. On Anantham, 200 nodes running the 64-bit Linux operating system, each with two 1.4 GHz processors and 1 GB of main memory, are interconnected over 2 Gbps Myrinet [13] interfaces underlying a GM (General Messaging) communication platform. Both System X and Anantham have Ethernet as a secondary network. A detailed performance comparison of VAPI/InfiniBand and Myrinet/GM on a 32-node cluster can be found in [59].

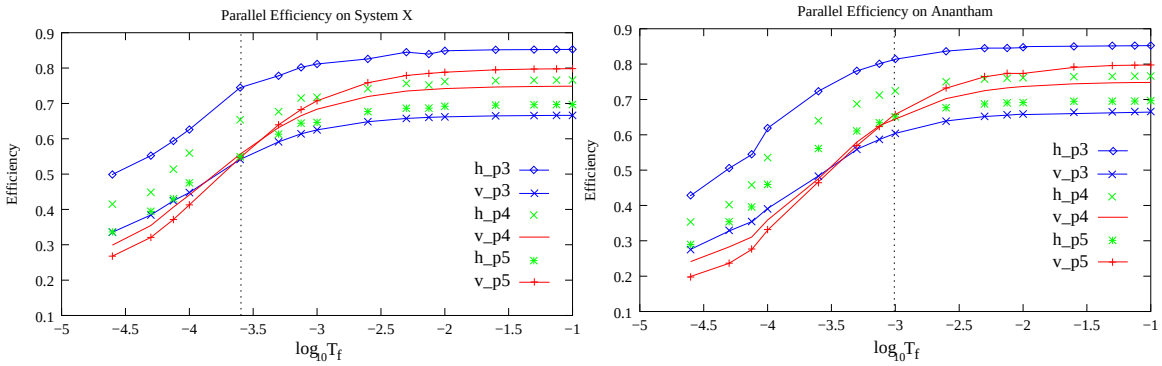

Figure 6.12. Comparison of parallel efficiency as T_f changes in the range $(0, 0.1)$ using $p = 3$, 4, and 5 processors for the 150-dimensional GR function with $I_{\max} = 90$ on System X (left) and Anantham (right). "v_" stands for the vertical scheme and "h_" for the horizontal scheme.

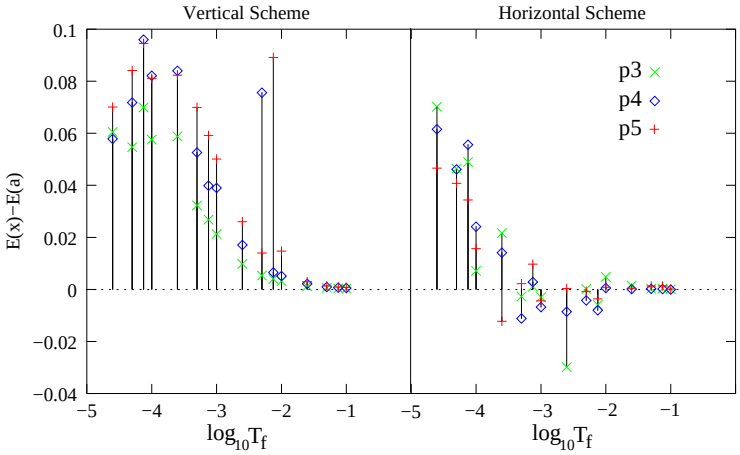

Figure 6.13. Parallel efficiency differences from that on System X to that on Anantham (marked as "E(x)-E(a)") corresponding to the experimental results in Figure 6.12.

6.3.1. Objective Function Cost

The objective function cost T_f is the key parameter that affects parallel performance under different parallel schemes. The empirical study in Section 4.2.2 concluded that the horizontal scheme outperforms the vertical scheme when $T_f \approx 0.0$, but performs worse than the vertical scheme when $T_f = 0.1$. The performance impact of $T_f \in (0.0, 0.1)$ was further investigated using the 150-dimensional GR function under both the vertical and horizontal schemes on System X and Anantham.

The first experiment used a small number of processors $p = 3$, 4, and 5 with T_f being adjusted in 15 small time intervals from $T_1 = 0.1$ to $T_{16} =$ 2.5E-05. Since the 150-dimensional GR function originally costs about 1.5E-05 on System X and 2.5E-05 on Anantham, T_{16} is chosen as the smallest objective function cost to make the test cases comparable on System X and Anantham. Figure 6.12 shows that the parallel efficiency increases sharply as T_f grows from T_{16} to T_{mid} (called "performance boundary" marked as the dotted lines with x coordinates being 2.5E-04 and 1.0E-03 on System X and Anantham,

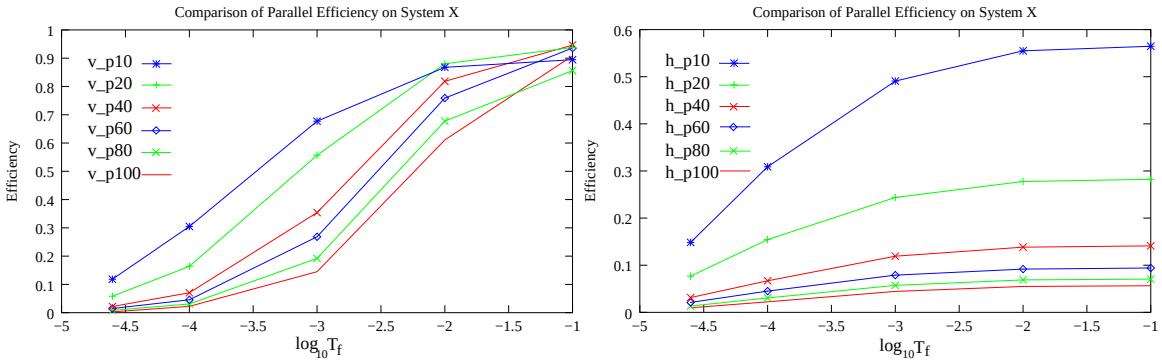

Figure 6.14. Comparison of parallel efficiency as T_f changes in the range $(0, 0.1)$ using $p = 10$, ..., and 100 processors on System X for the 150-dimensional GR function with $I_{\max} = 90$ for vertical (left) and horizontal (right) schemes.

respectively), then grows slightly up to T_1, which gives the highest efficiency for a particular setting specified by the parallel scheme, the number of processors, and the computing platform system. Because $T_f < T_{mid}$ is comparable with the communication cost under either vertical or horizontal scheme, the communication overhead dominates and degrades the efficiency significantly. When $p = 3$ and 4, the horizontal scheme outperforms the vertical scheme regardless of the value of T_f because one processor is dedicated as the master in the vertical scheme. When $p = 5$ and $T_f \geq T_{mid}$, the vertical scheme starts to perform better than the horizontal scheme. The turning point T_{mid} is different for System X and Anantham due to the different underlying network properties characterized by T_{cp} and T_{ca}, which are considered in the next subsection.

A smaller value of T_{mid} suggests a lower T_{cp} and/or a higher T_{ca}. The point-to-point communication, characterized by T_{cp}, happens more often in the vertical scheme than in the horizontal scheme, while the global one-to-all communication, with the cost T_{ca}, is a feature of the horizontal scheme. Moreover, the common overhead caused by data dependency and problem structure becomes more dominant than the communication overhead when $T_f > T_{mid}$ and eventually levels off the efficiency growth to the highest possible value for a particular setting.

The difference from $E(x)$ (the efficiency on System X) to $E(a)$ (the efficiency on Anantham) is marked as $E(x) - E(a)$ in Figure 6.13. Observe that $E(x) \geq E(a)$ for the vertical scheme, but for horizontal scheme, there are a few cases when $E(x)$ is worse than $E(a)$ for $T_f \in$(2.5E-04, 1.0E-02). More importantly, the difference becomes very small as T_f grows beyond 1.0E-02. However, the conclusion should not be drawn without a further study that compares the performance impact of T_f using a larger number of processors.

The second experiment uses $p = 10$, 20, 40, ..., and 100 processors with T_f being adjusted from the largest $T_1 = 0.1$ to $T_i = T_{i-1} \times$ 1.0E-01 ($i = 2$, 3, and 4), and to the smallest value of $T_5 =$ 2.5E-05. As expected, the results on System X (Figure 6.14) show that the parallel efficiency of the vertical scheme is greatly improved reaching 80-90% for

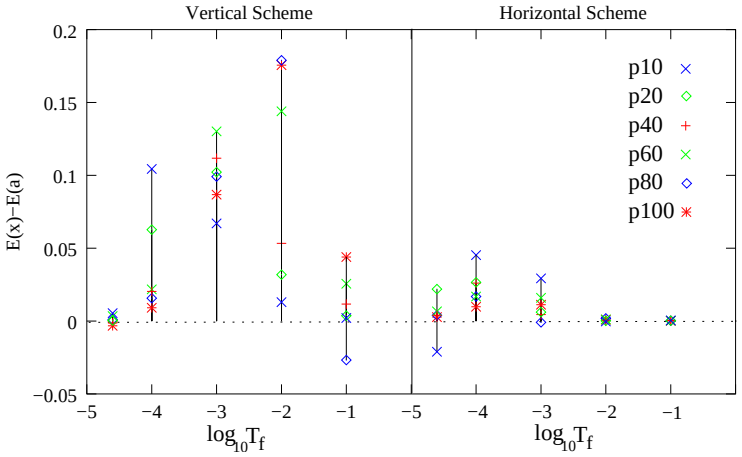

Figure 6.15. Parallel efficiency differences from that on System X to that on Anantham (marked as "E(x)-E(a)") corresponding to the experimental results in Figure 6.14.

all p numbers of processors when T_f grows from T_5 to T_1. However, the efficiency of the horizontal scheme is improved slightly except for $p = 10$, when it still does not surpass 60% for the largest T_1. For the vertical scheme on System X, smaller p results in higher efficiency when $T_f \in (T_5, T_2)$. For the rest of the T_f values, reasonable efficiency is attained ranging from the lowest $E = 0.85$ to the highest $E = 0.94$ on 80 and 40 processors, respectively. In the horizontal scheme, all the cases perform less efficiently than in the vertical scheme, especially when a large number of processors are used. On Anantham, similar results were produced as observed in Figure 6.15, which plots the differences of the parallel efficiency for both vertical and horizontal schemes on System X and Anantham. For most cases, System X gives a higher or equal efficiency. The next subsection studies the system-dependent parameters that may cause the performance variance on different systems.

6.3.2. Network Characteristics

Network connections are affected by many factors and characterized mostly by the classical metrics such as point-to-point latency, broadcast latency, and bandwidth. Here empirical studies of the network performance are presented for the point-to-point round trip cost T_{cp}. Although the one-way broadcast cost T_{ca} is also recognized as major network characteristic [96], its detailed modeling is beyond the scope of this work, which simplifies the modeling and analysis regarding T_{ca}.

The OSU benchmark library [73] provided in the MVAPICH software distribution was used to measure the MPI-level point-to-point and broadcast latencies. Small simulation programs were also used to quantize the other delays (i.e. host overhead, bottleneck, and network contention) involved in the messaging via MPI. Based on the benchmark and simulation results, both network characteristics T_{cp} and T_{ca} may be modeled as linear functions of the message size and the number of processors. For all the experiments in this section, the timing results were measured in microseconds. For small messages (less than 8 Kbytes), the results were the average of 10,000 runs, before which 1,000 runs were skipped as the network warm-up period; for large messages, 110 runs were done with the first 10 runs skipped.

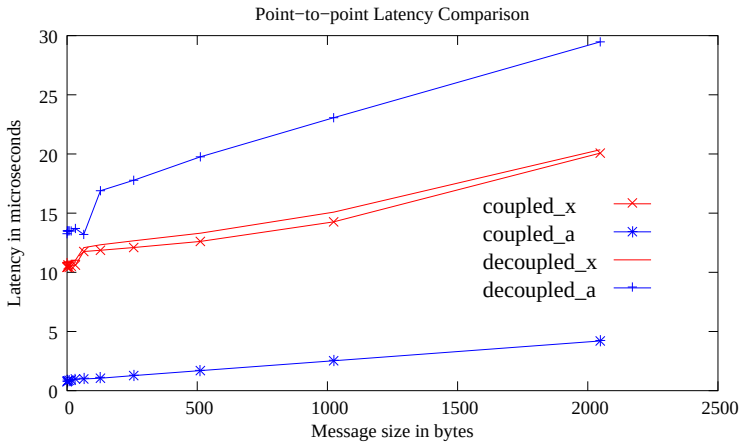

Figure 6.16. Comparison of point-to-point latency test results. The processors are either coupled or decoupled on System X ("_x") and Anantham ("_a").

A. Round Trip Cost T_{cp}

T_{cp}, the message point-to-point round trip cost, can be measured as the time for a master to receive from and reply to a worker. All the point-to-point messages for a same problem have the same size, so the transmission time for these messages over the network theoretically is the same.

Figure 6.16 shows the latency benchmark results between two processors on System X and Anantham as the message size S_m grows up to 2048 bytes. The two processors are either "coupled" on the same node or "decoupled" on two different nodes. The latency benchmark is a typical ping-pong test, where the sender calls `MPI_Send` to send a certain size message to the receiver and waits for a reply; the receiver calls `MPI_Recv` to receive the message and sends it back as the reply. The average latency results shown in Figure 6.16 are the one-way message transmission delays.

The timing results show that using decoupled processors yields a much higher latency on Anantham than on System X. Furthermore, using coupled processors reduces the latency significantly on Anantham but causes almost no change on System X. Observe that the Myrinet intra-node latency is lower than that of VAPI for InfiniBand, which has been also pointed out in [59]. The reason behind such a poor performance of MVAPICH is that its particular Mac OS X implementation used on System X takes no advantage of the shared memory available to the coupled processors and all the communications may involve the network interface on a given node. In fact, the disregard or poor usage of the shared memory may actually *increase* communication latencies as has been shown, e.g., in [18]. On the other hand, the MPI implementation over Myrinet is more mature now and has been well tuned to exploit the shared memory access provided by the Linux operating system.

On System X, InfiniBand is still an attractive communication medium compared with using the Gigabit Ethernet over TCP/IP because InfiniBand delivers a much better communication performance for both decoupled and coupled processors. For instance with the

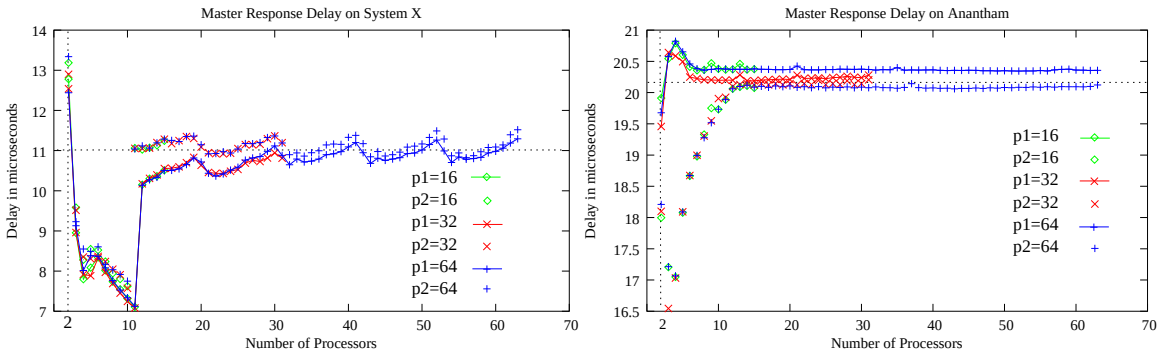

Figure 6.17. Comparison of master response delay using $p = 16$, 32, and 64 processors on System X (left) and Anantham (right). "p_i" means it uses i processors per node.

message size $S_m = 1024$ bytes, $T_{cp} = 37.58$ and 225.19 when MPICH-2 is used between two coupled (over the shared memory) and decoupled processors (over the Gigabit Ethernet), respectively. Conversely, $T_{cp} = 14.26$ μs when MVAPICH is used via VAPI/InfiniBand instead.

When a large number of processors are used, T_{cp} may also include a certain amount of response delay due to the host buffer latency, bottleneck effect, and network contention at the receiver. Such a delay is called "master response delay" because it is more likely to happen at a master that handles the messages exchanged with workers and other masters than at a worker that only communicates to one master at a time. A small MPI program was written to simulate the same communication pattern between a master processor and a group of processors, either as other masters or workers that communicate with this master simultaneously. With p processors, the master processor repeats the receive-and-reply of a small handshaking message ($S_m = 112$ bytes, a typical message size for a 10-dimensional problem with $N_b = 1$ function evaluation per task) 11,000 times initiated by other processors in one of the $p - 2$ subsets of the total $p > 2$ processors. The first 1,000 handshakes are considered as the network warm-up period as in the other experiments, thus not counted in the timing results. Six groups of simulation results shown in Figure 6.17 are the average timing results with $p = 16$, 32, and 64 processors either coupled or decoupled on System X and Anantham.

On both systems, the curves for different p numbers are overlapped very well. Similarly to the latency benchmark results, using coupled processors reduces the master response delay significantly on Anantham especially for small number of processors, but slightly increases the delay on System X. On System X, no matter whether the processors are coupled or decoupled, the delay drops dramatically at the beginning until $p = 10$ (coupled) or $p = 11$ (decoupled), then suddenly reaches up to a saturated level ≈ 11.0 μs. On Anantham, the delay of using coupled processors drops slightly at the beginning, then increases significantly until $p = 10$, from which point it starts leveling off at the saturated level ≈ 20.0 μs. If using decoupled processors instead, the delay increases slightly at the

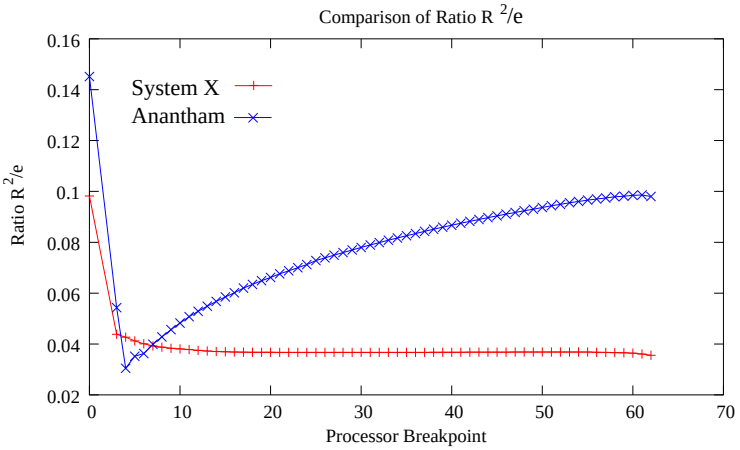

Figure 6.18. Comparison of the ratio R^2/e for different breakpoints of the piecewise T_{cp} model on System X and Anantham.

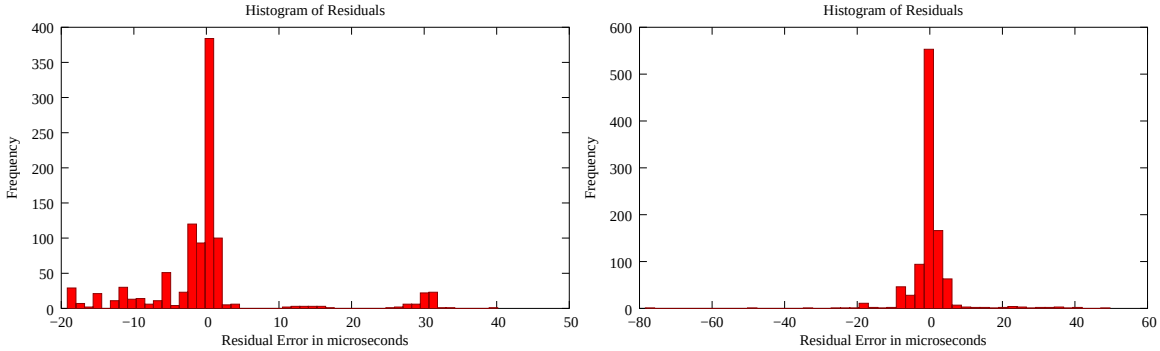

Figure 6.19. Histogram of residual errors of the linear regression models for T_{cp} on System X (left) and Anantham (right).

beginning from $p = 2$ to $p = 4$, then drops to a level $\approx 20.3\ \mu s$. The narrower bandwidth on Anantham yields a longer delay because the network contention occurs when a large number of processors are communicating to each other simultaneously. In the following experiments, coupled processors are used primarily because the cluster is utilized more efficiently (when decoupled processors are used, 50% of the processors are idle). Secondarily, it makes a minor difference on System X and even reduces the latency on Anantham.

The above experiments conclude that the T_{cp} between a master and a group of processors is affected by two factors: (1) the message size S_m and (2) the number of processors p that communicate with the master. T_{cp} increases as S_m grows, but varies when p is small and levels off at a certain value when p is sufficiently large depending on computing system. Therefore, T_{cp} is formed as a multivariate function of S_m and p as follows:

$$T_{cp}(p, S_m) = T_L(S_m) + T_d(p),$$

where $T_L(S_m)$ is defined as the point-to-point latency function in terms of S_m without the response delay and $T_d(p)$ as the pure response delay function in terms of p. In Figure 6.16,

the data points for decoupled processors essentially depict $T_{cp}(S_m, p)$ as the point-to-point latency $T_L(S_m)$ with a response delay $T_d(p = 2)$, so $T_L(S_m)$ is fairly likely a linear function of S_m. In addition, the data points for coupled processors in Figure 6.17 show that the delay function $T_d(p > 2)$ with $T_L(S_m = 112\text{bytes})$ may be a piecewise linear function with one breakpoint around $p = 10$, which disconnects the two pieces on System X but connects them on Anantham. The optimal breakpoints of a piecewise linear model can be determined systematically as in [92]. For this work, a series of piecewise linear T_{cp} models were estimated using R statistic package [23] at every possible breakpoint that forms either a single linear model or a two-piece piecewise linear model, each piece containing at least two different p numbers from the experimental data. For each piecewise linear model, define the ratio of the average correlation coefficient $R^2 = (R_1^2 + R_2^2)/2$ and the sum of the residual standard errors $e = e_1 + e_2$ as the objective function to find the optimal breakpoint. Clearly, the ratio is simply R_1^2/e_1 for the single model case. When either R_1 or R_2 is below 0.5, the model is considered invalid and sets the objective function value to zero. The shortest point-to-point message is 48 bytes in the present work, so the data points were collected with message size $S_m = 2^i$ bytes ($i = 6, \ldots, 14$) using $p = 64$ coupled processors on System X and Anantham.

For each system, Figure 6.18 shows that the single model maximizes the ratio of R^2/e, thus a single linear model is used for T_{cp} on both systems. Table 6.6 lists the model formula, coefficients, residual standard errors e, and correlation coefficient R^2.

Table 6.6. Model formula, coefficients, residual standard errors e, and correlation coefficient R^2 for T_{cp} on System X (X) and Anantham (A).

#	$T_{cp}(S_m, p)$ Linear Models
X	$9.917 + 0.007S_m + 0.001p$
	$e = 9.435,\ R^2 = 0.926$
A	$18.76 + 0.007S_m - 0.017p$
	$e = 6.587,\ R^2 = 0.956$

The values e and R^2 are very reasonable for both systems. The model coefficients suggest that T_{cp} is affected only slightly by S_m and p. Ignoring S_m and p, T_{cp} is about twice smaller on System X than on Anantham. The histograms of residual errors are plotted in Figure 6.19 using 50 bins for the total of 1,008 data points. The residual errors fall in a narrower range [-20,50] on System X than the range [-80,60] on Anantham. However, residuals are skewed with more data points located away from zero on System X than on Anantham, where residual errors follow an approximate normal distribution. Because System X has maximum 2,200 processors, the maximum impact of the term $0.001p$ is 2.2 μs. Also, the maximum value of $-0.017p$ on Anantham is 6.8 μs. Therefore, the impact of p on T_{cp} is negligible on both systems. Since the factor S_m has a large range of values depending on the problem dimension, the number of function evaluations per node, and the scheme configuration, S_m is kept in the final model of T_{cp}:

$$T_{cp}(S_m) = 0.007S_m + L_{cp}, \tag{6.3}$$

where $L_{cp} = 9.917$ on System X and 18.76 on Anantham.

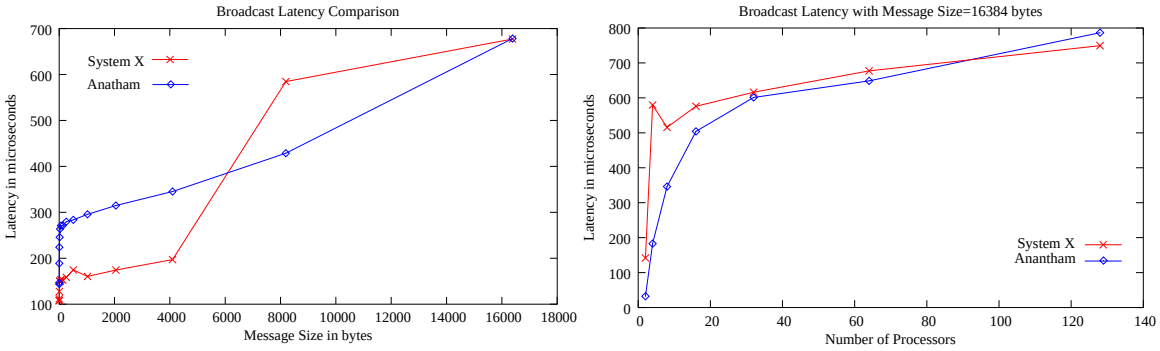

Figure 6.20. Comparison of broadcast latency results (in microseconds) on System X and Anantham. (a) The message size increases with $p = 32$ coupled processor nodes (left). (b) A fixed size message (S_m=16K bytes) is broadcast on an increasing number of processors $p = 2, \ldots, 128$ (right).

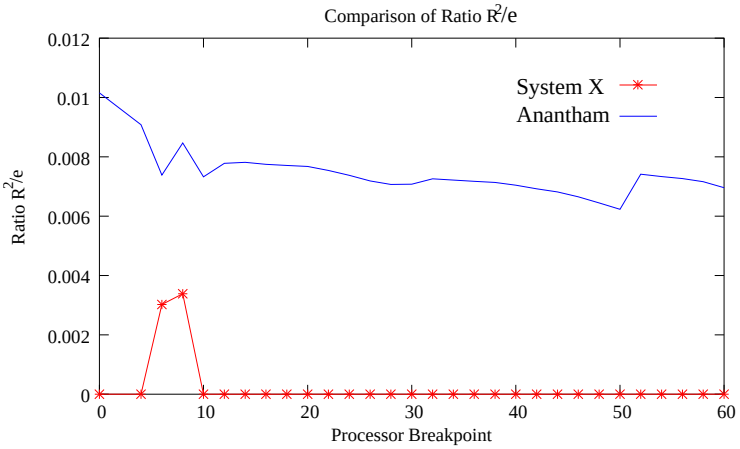

Figure 6.21. Comparison of the ratio R^2/e for different breakpoints of the piecewise T_{ca} model on System X and Anantham.

B. Broadcast Cost T_{ca}

T_{ca} measures the global one-to-all communication cost among master processors that collaborate on the parallel **Selection**, one of the main steps of the DIRECT algorithm. From the second iteration, the associated global operations occur in the following five phases:

1. BARRIER: All masters prepare local convex hull boxes and counters, then wait at a barrier.
2. GATHER_I: The root master m_0 gathers the counters of the local convex hull boxes to prepare the buffer.
3. GATHER_II: m_0 gathers the local convex hull boxes to the buffer.
4. BCAST_I: m_0 broadcasts the counter of the global convex hull boxes.
5. BCAST_II: m_0 broadcasts the global convex hull boxes.

Essentially, BARRIER can be approximated as an all-to-one GATHER followed by an one-to-all BCAST operations for a small message. The complexity and efficiency of these global operations in different MPI implementations depend on the chosen algorithms.

Vadhlyar et al. [90] give comprehensive discussions on the algorithms and modeling techniques for collective communications. Here, a simplified empirical approach was taken to measure the communication cost for BCAST, which is used to approximate the cost of the GATHER and BARRIER operations. Intuitively, T_{ca} is a function of the message size S_m and the number of processors p —$T_{ca}(S_m, p)$. Hence, the approximate communication cost in terms of T_{ca} for the global operations at iteration i are listed below:

1. BARRIER: $2 \times T_{ca}(8, p)$,
2. GATHER_I: $T_{ca}(8 \times p, p)$,
3. GATHER_II: $T_{ca}(\sum_{j=1}^{p} LC_{i,j} \times S_{box}, p)$,
4. BCAST_I: $T_{ca}(8, p)$,
5. BCAST_II: $T_{ca}(GC_i \times S_{box}, p)$,

As above,

$$S_{box} = (2 \times N_d + 5) \times 8 \tag{6.4}$$

is the size of a box in bytes, $LC_{i,j}$ is the number of local convex hull boxes on master j ($j = 1,\ldots,n$), and GC_i is the final number of global convex hull boxes at iteration i.

Figure 6.20(a) shows the broadcast latency benchmark results with 64 coupled processors on System X and Anantham. For messages with $S_m < 6K$ bytes, System X yields a significantly lower latency than Anantham. As S_m grows, the broadcast latency on System X increases more dramatically than Anantham, then starts leveling off at $S_m = 8K$ bytes, and eventually becomes less than that on Anantham. Figure 6.20(b) shows the growth of broadcast latency with a fixed size message in terms of the number of processors. For small numbers of processors ($p \leq 64$), the broadcast tends to cost more on System X than Anantham, but it costs less on System X when $p = 128$. Since the processors are coupled, more efficient intra-node communication lowers the latency on Anantham, but it can not overcome the limitation of the narrow bandwidth for larger messages and more processors.

To formulate $T_{ca}(S_m, p)$, 480 data points were collected with message sizes $S_m = 2^j$ bytes ($j = 0,\ldots,14$) and $p = 2 \times i$ ($i = 1,\ldots,32$) coupled processors on both systems. Observe in Figure 6.20(b), $p = 8$ and $p = 16$ appear to be reasonable breakpoints for the T_{ca} piecewise linear models for System X and Anantham respectively. A series of piecewise linear T_{ca} models were estimated to find the optimal breakpoint. Figure 6.21 shows that most of the breakpoints would result in R^2 values below 0.5 on System X, but yield reasonable R^2 values on Anantham. The ratio reaches the maximum value at $p = 8$ on System X and at $p = 0$ for Anantham. Therefore, a piecewise linear model with the breakpoint at $p = 8$ for System X and a single linear model for Anantham were built as shown in Table 6.7, which

Table 6.7. Model formula, coefficients, residual standard errors e, and correlation coefficient R^2 for T_{ca} on System X (X) and Anantham (A).

#	$T_{ca}(S_m, p)$ Linear Models
X	$2 \leq p \leq 8$:
	$-76.193 + 0.004S_m + 69.874p$
	$e = 128.3,\ R^2 = 0.613$
	$p > 8$:
	$65.886 + 0.025S_m + 1.144p$
	$e = 70.11,\ R^2 = 0.730$
A	$65.142 + 0.026S_m + 3.756p$
	$e = 75.15,\ R^2 = 0.763$

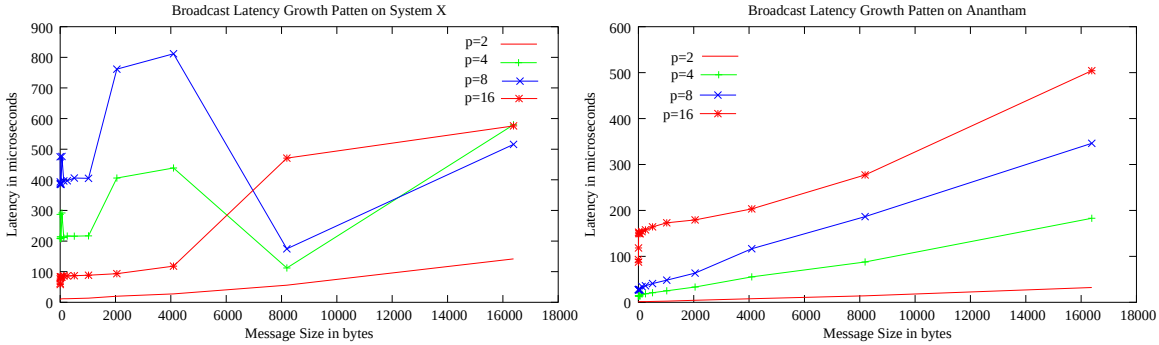

Figure 6.22. Comparison of broadcast latency growth pattern (in microseconds) with $p = 2$,4, 8, and 16 coupled processors on System X (left) and Anantham (right).

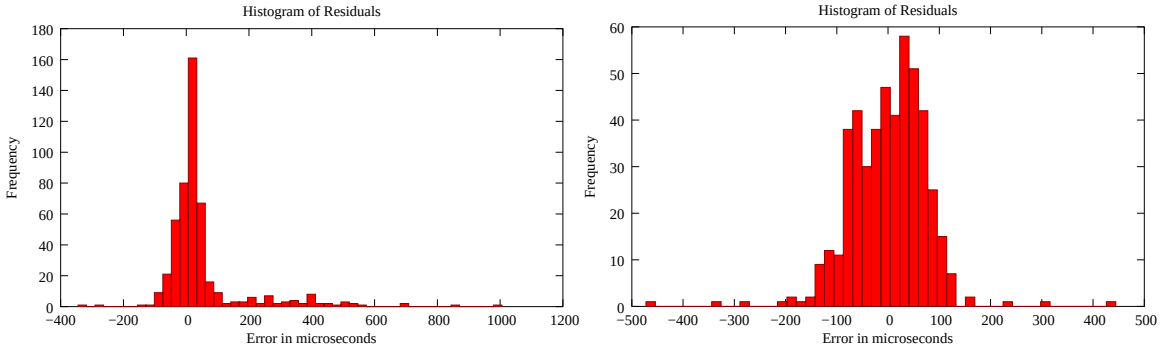

Figure 6.23. Histogram of residual errors of the linear regression models for T_{ca} on System X (left) and Anantham (right).

lists the model formula, coefficients, residual standard error e, and correlation coefficients R^2.

The T_{ca} model on Anantham offers a slightly better fit with a smaller e and a larger R^2. Most of the fitting error for System X is from the data points for $p = 4$, 6, and 8, which do not follow the common pattern that the broadcast latency should increase as the message size S_m grows (Figure 6.22). This unusual behavior of broadcast latency on System X was likely caused by the different port speed of 4 core and 64 leaf switches that connect 4 and 8 processors during a temporary period of network upgrade. The histogram of residual

errors are shown in Figure 6.23 with 50 bins for the total 480 data points. On Anantham, the narrower range and approximately normally distributed errors implies a better fit for T_{ca} than that on System X. Based on the models for $p > 8$, p yields a three times greater impact on T_{ca} on Anantham than that on System X, but S_m affects T_{ca} approximately the same on both systems. When $p \leq 8$, the models also describe the unusual influence of p on T_{ca} on System X as well as the consistent broadcast latency growth patten on Anantham. The final model of T_{ca} is generalized as below:

$$T_{ca}(S_m, p) = L_{ca} + C_s S_m + C_p p, \tag{6.5}$$

where L_{ca}, C_s, and C_p are the system-related parameters given in Table 6.7.

6.4. Scalability Analysis and Experiments

Scalability is the capacity to increase speedup in proportion to the number of processors p for a parallel system including a parallel implementation of an algorithm and a particular execution environment. The crucial step is to identify the overhead as the function of problem scale and system scale. The scalability is evaluated with a realistic tool—isoefficiency function [57] based on the characterized communication patterns and overhead sources.

Kumar et al. [57] point out that if the parallel efficiency can be maintained constant as the total work grows at least linearly with p, then the parallel implementation is scalable. The authors have previously used the isoefficiency function to analyze the performance of restarted Generalized Minimum Residual (GMRES) method [80] for iterative solution of large-scale sparse linear systems [85]. Decker and Krandick [24] have generalized the concept of isoefficiency function to be used in search algorithms and showed its application in the analysis of a search algorithm that computes isolating intervals for polynomial real roots. Here, the overhead terms are analyzed in great detail in order to identify the ones with significant weight under different circumstances. The derivation of the isoefficiency function is shown for both the vertical ($n = 1$, $k > 1$) and the horizontal ($n > 1$, $k = 0$) schemes.

6.4.1. Vertical Scheme Scalability

In the vertical scheme, three sources of overhead are present. The first is the communication involved in distributing tasks to remote workers. The second is the idleness due to task imbalance among workers due to the data dependency of algorithm steps. $N_b = 1$ (one function evaluation per task) is assumed, since Section 6.2.1 has proved that it minimizes the data dependency overhead especially for expensive objective functions. The third is the idle time when workers wait for **Division** and **Selection** to be finished at the master. Since **Division** and **Selection** are necessary steps of DIRECT, and the cost does not vary

with k, the third source of overhead is considered as a constant for a particular problem with a specified stopping condition.

Let W be the total number of function evaluations over $I_{\max}$ iterations,

$$W = \sum_{i=1}^{I_{\max}} F_i, \tag{6.6}$$

where F_i denotes all the function evaluation tasks at iteration i. The total overhead for k workers is

$$T_o(W, k) = k \times T_k - W \times T_f, \tag{6.7}$$

where T_k is the parallel execution time with k workers. Define the parallel efficiency E_p as

$$E_p = \frac{W \times T_f}{k \times T_k}. \tag{6.8}$$

If E_p can be maintained constant as W grows at least linearly with k, then the vertical scheme is scalable. The isoefficiency function is derived from Equation (6.7) and (6.8) as follows:

$$W = \frac{E_p}{1 - E_p} \times (T_o(W, k)/T_f). \tag{6.9}$$

It describes the total work W in terms of T_o, the total overhead function given a desired E_p and the constant objective function cost T_f. To find if W is a linear function of k, $T_o(W, k)$ as a function of W needs to be extended by accumulating over all $I_{\max}$ iterations. All the costs, except for the function evaluation, are included in $T_o(W, k)$. So it has three terms: T_{oc}^1 (communication overhead), T_{od} (data dependency overhead), and a constant T_{os} (the **Division** and **Selection** cost).

The interaction between masters and workers is described in full detail in Section 4.1.2. Here, the communication phases are only outlined.

(1) Each of k workers sends a non-blocking request to a random selected master.

(2) For each worker that has sent a non-blocking request or that is in the queue, a master sends a task if any. If no more tasks, the master sends a "no point" message, or if no more iterations, sends a "all done" message.

(3) The workers who received tasks send values back to the master. Those who received the "no point" notice check with other masters, who may have tasks, and if none have tasks, send blocking requests and wait. Those who received the "all done" notice terminate. For each value received, a master sends a task if any; If no more tasks, sends a "no point" notice; For each blocking request, queues up the worker.

Only one master distributes tasks, so if it runs out of tasks at the end of an iteration, all workers will block waiting in its queue. So, Phase (1) happens only at the first iteration

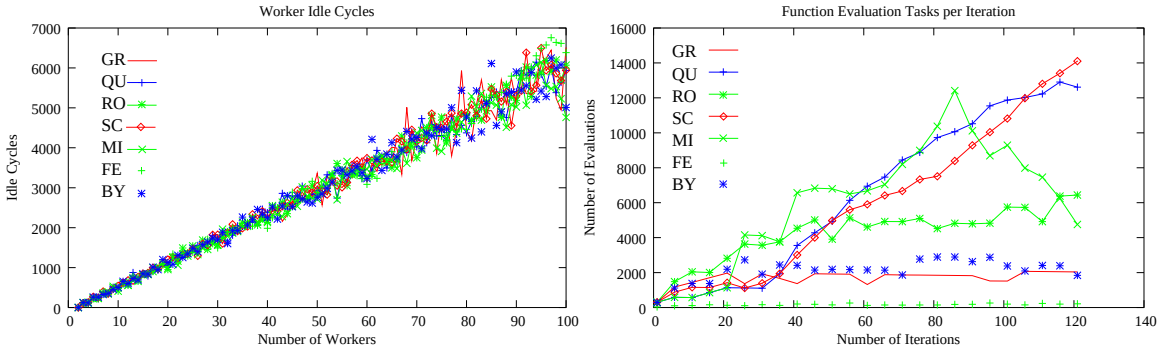

Figure 6.24. All the worker idle cycles, shown in (a) on the left, are calculated using $k = 2, \ldots, 100$ workers and the function evaluations are shown in (b) on the right for all the test problems on System X. $I_{\max} = 122$.

because the workers are all in the queue of the master from the second iteration. Phases (2) and (3) are repeated at every iteration. To sum up the communication overhead, consider the message types and the frequency of these messages exchanged between a master and a group of workers:

(a) $T_1 = k \times T_{cp}/2$ (k workers send nonblocking requests),

(b) $T_2 = F_i \times T_{cp}/2$ (workers receive F_i tasks),

(c) $T_3 = F_i \times T_{cp}/2 + k \times T_{cp}$ (the master receives all function values and sends "no point" messages at end of each iteration to k workers; all workers then send blocking requests to the master),

(d) $T_4 = k \times T_{cp}/2$ (workers receive "all done" messages from the master at the last iteration).

The communication overhead over all iterations is

$$T_{oc}^1 = T_1 + \sum_i^{I_{\max}} T_2 + \sum_i^{I_{\max}} T_3 + T_4.$$

Represent it as a function of W (Equation 6.6) and k with $T_{cp}(S_m)$ (Equation 6.3):

$$\begin{aligned} T_{oc}^1(W,k) &= (k(1+I_{\max}) + W)T_{cp}(S_m) \\ &= (0.007S_m + L_{cp})W \\ &+ (1+I_{\max})(0.007S_m + L_{cp})k. \end{aligned} \tag{6.10}$$

For point-to-point messages, the message size S_m (in bytes) depends on the problem dimension N_d:

$$S_m = (N_d + 4) \times 8. \tag{6.11}$$

Therefore, $T_{cp}(S_m)$ is a constant for the same problem on a particular system. Because T_{oc}^1 depends linearly on k, it grows linearly as $\mathcal{O}(k)$ for a fixed size problem specified by $I_{\max}$ and W. On System X, the twice smaller L_{cp} (Table 6.6) gives a slower growth of T_{oc}^1 in terms of k than that on Anantham.

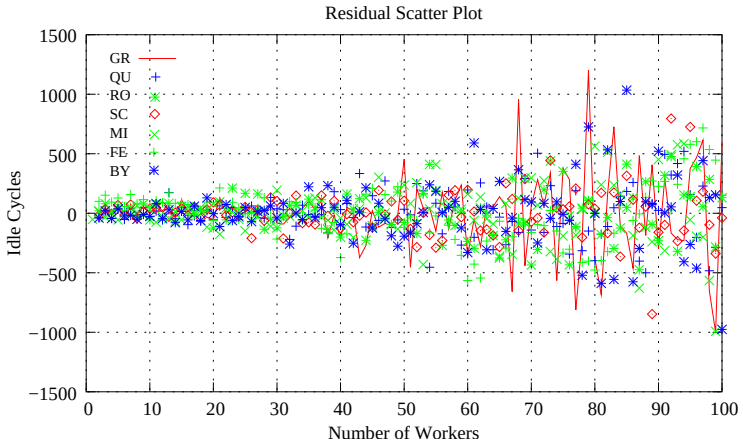

Figure 6.25. The scatter plot of residuals $\delta_p(k)$ for test problems on System X.

The second source of overhead—data dependency—is as important as the communication. It causes task imbalance among workers. At iteration i, if some workers obtain no tasks, when the number of tasks F_i is less than the number of workers k, or obtain fewer tasks than others, idle cycles will appear, each of which lasts about T_f. The number X_i of such cycles can be derived from the equation:

$$\delta_{i+} \times (k - X_i) + \delta_{i-} \times (X_i) = F_i,$$

where $\delta_{i+} = \lceil F_i/k \rceil$ and $\delta_{i-} = \lfloor F_i/k \rfloor$ are the workers' task shares defined in the workload model of Section 6.2.2. Because $\delta_{i+} - \delta_{i-} = 1$,

$$X_i = \frac{\delta_{i+} \times k - F_i}{\delta_{i+} - \delta_{i-}} = \delta_{i+} \times k - F_i,$$

yielding the total data dependency overhead:

$$\begin{aligned} T_{od} &= \sum_{i}^{I_{\max}} X_i \times T_f \\ &= \sum_{i}^{I_{\max}} \left(\left\lceil \frac{F_i}{k} \right\rceil \times k - F_i \right) T_f. \end{aligned} \tag{6.12}$$

Observe that T_{od} becomes 0 when F_i is a multiple of k. Figure 6.24(a) shows the results for $\sum_{i=1}^{I_{\max}} (X_{i,j})$, which is the total number of worker idle cycles over $I_{\max}$ iterations using $j = 2,\ldots, k$ workers.

Interestingly, each curve for the total idle cycles presents a linear function of k with a fluctuation, which falls in a larger range when more workers are used. Note that the wall clock duration of data dependency overhead is actually

$$\sum_{i=1}^{I_{\max}} sgn(X_{i,j}) T_f \geq \sum_{i=1}^{I_{\max}} (X_{i,j}) T_f / k,$$

Table 6.8. Comparison of the growth rate θ, the residual standard error e, and the correlation coefficient R^2 for the estimated linear growth of the worker idle cycles for test problems.

#	θ	e	R^2
GR	61.093	327.6	0.966
QU	60.724	202.5	0.986
RO	61.816	194.1	0.988
SC	61.879	200.1	0.987
MI	59.186	241.2	0.980
FE	64.613	234.9	0.984
BY	60.658	269.7	0.976

and this average—rather than total—overhead per worker and is considered for experimental verification here.

The growth rate of the number of idle cycles was estimated by the same linear regression tool used in the previous subsection. Although the QU, SC, and MI problems generate more function evaluation tasks per iteration than other problems do so (Figure 6.24(b)), the growth rates are very close to each other for these test problems as shown in Table 6.8. Hence, T_{od} grows approximately linearly with k with a fluctuation that can be described by the residual error function $\delta_p(k)$ (Figure 6.25).

Table 6.9. Comparison of C_m, T_{oc}^x/k (on System X), T_{oc}^a/k (on Anantham), and T_{od}/k (in seconds) for all test problems using $k = 99$ workers. $I_{\max} = 122$ with first 12 iterations skipped for estimation. $N_b = 1$. $N_d = 150$ and $T_f = 0.1$ for artificial functions, $N_d = 16$ and $T_f = 2.66$ for FE, and $N_d = 143$ and $T_f = 11.02$ for BY.

#	C_m	T_{oc}^x/k	T_{oc}^a/k	T_{od}/k
GR	413332	0.039	0.057	4.450
QU	1598908	0.149	0.221	5.371
RO_x	1021480	0.097	–	5.101
RO_a	1017544	–	0.141	5.540
SC	1487836	0.139	0.206	5.368
MI	1508052	0.141	0.209	4.957
FE	59604	–	0.006	156.860
BY	528468	0.048	–	616.790

Table 6.9 compares the number of one-way messages C_m, the theoretical communication overheads per worker T_{oc}^x/k and T_{oc}^a/k on System X and Anantham, respectively, and the wall clock data dependency overhead T_{od}/k for all test problems with $k = 99$ workers. On both System X and Anantham, $I_{\max} = 122$ iterations were run, such that the first 12 iterations skipped, so the number of one-way messages is $C_m = 2(k(I_{\max} - 12) + \sum_{i=13}^{I_{\max}} F_i)$. Both T_{oc}^x and T_{oc}^a were estimated using the formula for T_{oc}^1 in Equation 6.10 given C_m, F_i (the number of function evaluation tasks per iteration collected from the runs), the linear

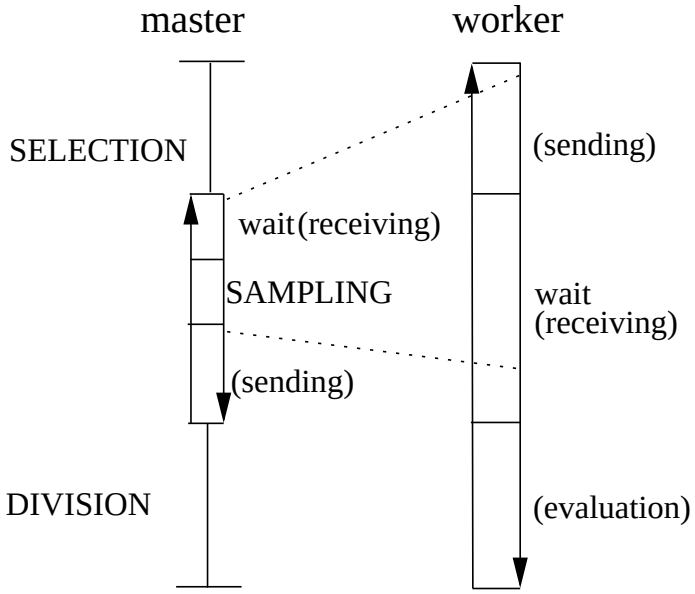

Figure 6.26. The overhead measurement on a master and a worker.

models of T_{cp} in Equation (6.3), and S_m in Equation (6.11). The wall clock time T_{od}/k is calculated with Equation (6.12) given the collected data for F_i using 99 workers. The data for the BY problem were collected only on System X and that for the FE problem were collected only on Anantham, because the versions of these applications used require specific execution environments. A reasonably large objective function cost $T_f = 0.1$ is assumed for artificial functions while $T_f \approx 2.66$ for the FE problem and $T_f \approx 11.02$ for the BY problem were measured with experiments. In addition, the RO problem generates different numbers of function evaluation tasks on System X and Anantham because the 64-bit registers on System X and the 80-bit registers on Anantham give slightly different computation precision. During the **Selection** step, the RO problem yields different results depending on the floating point hardware. Therefore, the estimation of the communication and data dependency overhead differs on these two systems.

When T_f is taken into account, the data dependency overhead becomes more significant for expensive functions, such as FE and BY, than for cheap objective functions. Although System X has lower communication overhead, the common overhead T_{od} still dominates because $T_f \geq 0.1$ is sufficiently large. On the other hand, if $T_f \leq$1.0E-03, T_{od} would become less dominant than the communication overhead. This explains the observed values of the parallel efficiency as T_f changes (Section 6.3.1).

To verify the above theoretical analysis, T_{sk} (total sampling time with k workers) and T_e (total evaluation time) were measured by the phases depicted in Figure 6.26. T_{sk} is the same for the master and the worker. T_{oc}^1 is verified by counting messages instead of directly timing the duration because it is hard to separate sending and receiving costs from **Sampling**. However, it is expected that the estimated overhead $T_{ot} = (T_{oc}^1 + T_{od})/k$

Table 6.10. The experimental results of the Sampling cost T_{sk} and the evaluation cost T_e for all test problems on System X ('_x') and Anantham ('_a'). The combined experimental overhead $T_{oe} = T_{sk} - T_e/k$ is compared to the estimated overhead $T_{ot} = (T^1_{oc} + T_{od})/k$.

#	T_{sk}	T_e	T_{oe}	C_m	T_{ot}
GR_x	202.44	19578.0	4.68	413332	4.50
GR_a	203.28	19578.0	5.52	413332	4.51
QU_x	802.48	78857.0	5.94	1598908	5.52
QU_a	803.73	78858.0	7.18	1598908	5.59
RO_x	510.46	49987.0	5.54	1021480	5.20
RO_a	509.65	49789.0	6.73	1017544	5.68
SC_x	746.46	73306.0	5.99	1487836	5.51
SC_a	748.85	73304.0	8.41	1487836	5.57
MI_x	756.44	74316.0	5.77	1508052	5.10
MI_a	757.83	74316.0	7.16	1508052	5.17
FE_a	696.25	50608.0	185.06	59604	156.87
BY_x	29179.0	2788790	1009.40	528468	616.84

(the sum of the theoretical communication and data dependency overhead per worker in Table 6.9) should be approximately equal to the experimental result $T_{oe} = T_{sk} - T_e/k$ as listed in Table 6.10.

The **Sampling** cost T_{sk} is approximately the same on both systems. Note that the combined experimental overhead T_{oe} is greater than the theoretical estimation T_{ot}. Moreover, the scaled difference $(T_{oe} - T_{ot})/T_{sk}$ is larger on Anantham than that on System X. Nevertheless, C_m matches exactly (Table 6.9) the experimental results. One possibility is that the communication overhead could be underestimated because the small simulation program that generated the data points for modeling T_{cp} may incur less overhead than the full-size DIRECT optimization program does so with a large amount of memory allocated. There might also exist another system-dependent source of overhead other than the communication, such as memory access inefficiency, that may increase the overhead T_{oe} on Anantham.

With all the overhead terms analyzed, the isoefficiency function (Equation 6.9) for the vertical scheme may be expressed as follows:

$$W = \frac{E_p}{1 - E_p} \times \frac{T^1_{oc}(W, k) + T_{od}(k) + T_{os}}{T_f},$$

where $T^1_{oc}(k)$ is a linear function of k, $T_{od}(k)$ is approximately linear function of k, and T_{os} is a constant for a particular problem with specified $I_{\max}$ and resulting W. Therefore, W becomes

$$W = \frac{E_p(T_{cp}k(1 + I_{\max}) + T_{od}(k) + T_{os})/T_f}{1 - E_p - E_pT_{cp}/T_f}.$$

Firstly, observe that W grows linearly with k, meaning that the vertical scheme is scalable. Secondly, a larger ratio of T_{cp}/T_f on a particular system requires a faster growth of W to maintain the same E_p as more workers are used. Lastly, a larger T_f gives a better scalability.

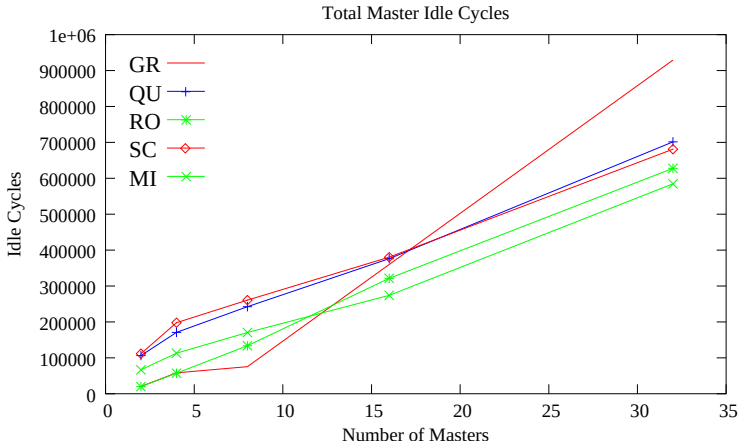

Figure 6.27. The total master idle cycles are calculated with the data of $F_{i,j}$, the function evaluations on master j at iteration i. $n = 2, 4, \ldots, 32$ masters are used for test problems with $I_{\max} = 122$.

6.4.2. Horizontal Scheme Scalability

When the objective function is computationally cheap, the horizontal scheme is more suitable than the vertical scheme as discussed in Section 6.3.1. Thus, $T_f \approx 2.6\text{E-}05$ was considered for all the artificial test problems in the scalability analysis of the horizontal scheme with multiple masters ($n > 1$) and no workers ($k = 0$) in a single domain.

The overhead includes T^2_{oc}, the communication overhead involved in the global convex hull computation during the parallel **Selection** and T'_{od}, the data dependency overhead among masters:

$$T'_o(H, W, n) = T^2_{oc}(H, n) + T'_{od}(H, W, n), \tag{6.13}$$

where H stands for the total work in the convex hull computation.

Two components of T^2_{oc} are (1) T_{ou}, the point-to-point communication overhead for updating the intermediate results and finalization, and (2) T_{oh}, the collective communication overhead for the parallel **Selection**. The messages for intermediate data update and termination process are from point to point using a fixed size buffer, thus

$$T_{ou}(n) = (I_{\max} + \frac{1}{2})(n-1)T_{cp}, \tag{6.14}$$

where T_{cp} is a constant. Therefore, $T_{ou}(n)$ grows linearly with n regardless of systems. The global collective communication is approximated with five phases and six messages from the second iteration as discussed in Section 6.3.2, thus

$$\begin{aligned} T_{oh} = \sum_{i}^{I_{\max}-1} & [3T_{ca}(8, n) + T_{ca}(8n, n) \\ & + T_{ca}(\sum_{j=1}^{n} LC_{i,j} \times S_{box}, n) \\ & + T_{ca}(GC_i \times S_{box}, n)]. \end{aligned} \tag{6.15}$$

All terms of T_{oh} grow linearly in $\mathcal{O}(n)$.

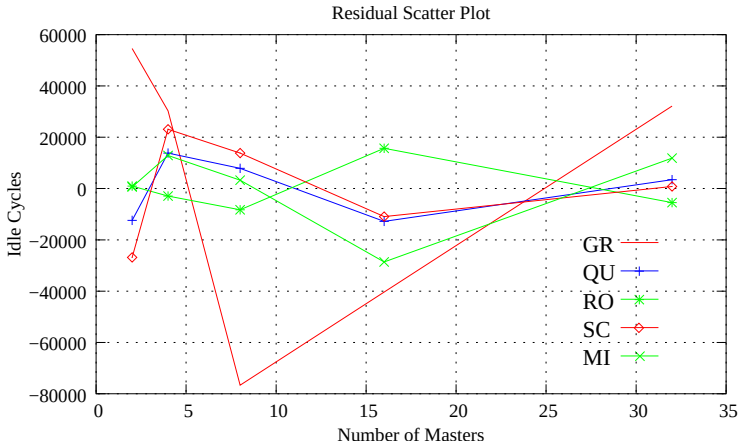

Figure 6.28. The scatter plot of residuals $\delta'_p(n)$ for test problems.

Section 6.2 has demonstrated that the horizontal scheme has significantly worse load balancing on function evaluation tasks than the vertical scheme. The further investigation here reveals that it is mostly caused by the data dependency overhead T'_{od}. Suppose $C_{i,j}$ is the number of global convex hull boxes assigned to master j at iteration i, and D_k is the number of longest dimensions for the convex hull box k on master j, then master j computes $F_{i,j} = \sum_{k=1}^{C_{i,j}}(2D_k)$ function evaluations at iteration i. The task imbalance among masters generates master idle cycles. The total number of master idle cycles is

$$X'_i = \sum_{j=1}^{n}(\max_{j=1}^{n} F_{i,j} - F_{i,j}) = \frac{T'_{od}}{T_f}. \tag{6.16}$$

Figure 6.27 shows the growth pattens of the total master idle cycles as the number of masters n increases five times from 2 to 32 for five test problems. The linear growth of X'_i is estimated in Table 6.11, similarly to Table 6.8 for the total worker idle cycles.

Table 6.11. Comparison of the growth rate θ', the residual standard error e, and the correlation coefficient R^2 for the estimated linear growth of the master idle cycles for test problems.

#	θ'	e	R^2
GR	31034.0	64390	0.979
QU	19310.3	13950	0.997
RO	20463.9	10850	0.999
SC	18058.1	22850	0.992
MI	16887.0	19480	0.993

First, observe that the growth rate θ' is much larger than θ in Table 6.8, indicating a faster growth of the data dependency overhead T'_{od} among masters than T_{od} among workers. Second, T'_{od} is highly problem-dependent because it grows at distinctly different rates for different problems. With a few data points, the residual error e is fairly large even though R^2 is reasonable. Figure 6.28 shows the residual scatter plot of the residual error function $\delta'_p(n)$ for the master idle cycles. The wide fluctuation of residual errors again implies the intractable property of T'_{od}.

Extending T_{cp} (Equation 6.5) and T_{ca} (Equation 6.3), the communication overhead T_{oc}^2 becomes

$$\begin{aligned} T_{oc}^2(H,n) &= T_{ou}(n) + T_{oh}(H,n) \\ &= [(I_{\max} + \frac{1}{2})T_{cp} \\ &+ (I_{\max} - 1)(6C_p + 8C_s)]n \end{aligned} \tag{6.17}$$

Compared with T_{oc}^1 in Equation 6.10, T_{oc}^2 grows faster in terms of n. Among these terms, T_{ou} (Equation 6.14 and T_{cp} in Equation 6.3) contributes very little to the overall overhead, as shown in Table 6.12, which compares T_{ou}, T_{oh} (applying Equation 6.15, Equation 6.5, and Equation 6.4 with the collected data for $LC_{i,j}$ and GC_i) and $T'_{od}(H,W,n)$ (applying Equation 6.16 with the collected data for $F_{i,j}$) using $n = 32$ masters and $I_{\max} = 122$ on System X and Anantham.

Table 6.12. Comparison (in seconds) of T_{ou}^x (on System X), T_{ou}^a (on Anantham), T_{oh}^x, T_{oh}^a, and T'_{od} using 32 masters. $I_{\max} = 122$. $N_d = 150$ and $T_f =$ 2.6E-05 second.

#	T_{ou}^x	T_{ou}^a	T_{oh}^x	T_{oh}^a	T'_{od}
GR	0.070	0.104	4.123	4.337	24.154
QU	0.070	0.104	2.893	3.059	18.235
RO_x	0.070	0.104	3.212	–	16.317
RO_a	0.070	0.104	–	2.975	16.369
SC	0.070	0.104	6.625	6.940	17.709
MI	0.070	0.104	1.969	2.098	15.200

On a particular system, T_{ou} is the same for different problems. T_{oh} is more considerable than T_{ou} and has minor differences on these two systems. When $T_f \geq$ 1.0E-04, T'_{od} is the dominant overhead resulting approximately the same overall overhead T'_o for a particular problem on System X and Anantham. If T_f is less than 1.0E-04, T_{oc} becomes comparable with T'_{od}.

Table 6.13. Verification experimental results of C_{cp}, C_{ca}, and T'_{od}.

#	C_{cp}	C_{ca}	T'_{od}
GR	7566	726	24.622
QU	7566	726	13.098
RO_x	7566	726	16.624
RO_a	7566	726	16.292
SC	7566	726	14.018
MI	7566	726	10.911

Several experiments were conducted using 32 masters (coupled processors on System X and Anantham) to verify the above estimation. On the root master, two messages counters C_{cp} and C_{ca} were used to keep track of the point-to-point one-way messaging during the intermediate update and the collective messaging during the **Selection** step respectively for all the test runs. The **Sampling** cost T_{si} on each of $i = 1,\ldots,32$ masters were measured. The experimental measurement of $T'_{od} = \sum_i^{32}(\max_i^{32} T_{si} - T_{si})$ is expected to be close to the theoretical results in Table 6.12. Table 6.13 lists the experimental results of C_{cp}, C_{ca}, and T'_{od}.

Both C_{cp} and C_{ca} were collected on the root master. Generally, $C_{cp} = 2I_{\max}(n-1)+2$ and $C_{ca} = 6(I_{\max}-1)$, where $n = 32$ and $I_{\max} = 122$. Another $n-3$ oneway messages were not counted by C_{cp}, because they were sent among non-root masters during final termination. C_{ca} exactly matches the number of global messages for collective communication. The experimental results for T'_{od} are close to the estimation especially for the GR and RO problems.

Derived from Equation (6.9), the isoefficiency function for the horizontal scheme is

$$W = \frac{E_p}{1-E_p} \times \frac{T_{oc}^2(H,n) + T'_{od}(H,W,n)}{T_f},$$

where $T_{oc}^2(H,n)$ is a linear function of n and $T'_{od}(H,W,n)$ is approximately a linear function of n. Because the horizontal scheme has a faster growth rate of both communication overhead and data dependency overhead, its scalability is worse than that of the vertical scheme. Remarkably, the data dependency is not only a dominant source of overhead for expensive objective functions, it is also highly problem-dependent and intractable. Furthermore, the difference in communication characteristics on System X and Anantham has little impact for expensive objective functions, but becomes considerable when the objective function cost T_f is low.

6.4.3. Scalability Experiments

Empirical studies on scalability were done for all five benchmark functions with a fixed cost $T_f = 0.1$, a growing problem dimension $N = 2^i$ ($i = 2, \ldots, 6$), and an increasing number of processors $p = 10 \cdot 2^{i-1}$ ($i = 1, \ldots, 5$). Since the problem structure changes as N grows, the traditionally defined scaled speedup is not applicable here. Since T_f is maintained approximately constant by using a microsecond precision utility function `gettimeofday` in C, the increase from 0.1 to the average cost per evaluation $\overline{T_e} = pT_p/N_e$ can be considered

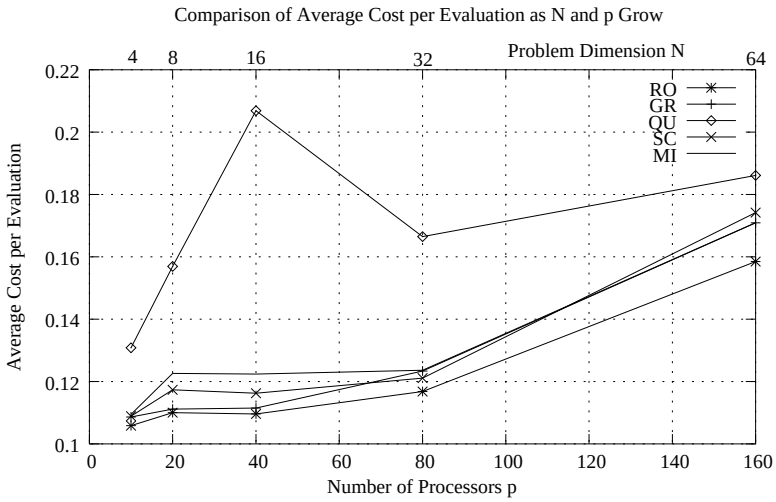

Figure 6.29. The growth of $\overline{T_e}$ as N and p increase for all five benchmark functions.

as the average overhead per function evaluation as both N and p increase, where T_p is the parallel execution time with p processors and N_e is the actual number of evaluations.

Figure 6.29 plots how $\overline{T_e}$ changes as N and p grow. For most problems, $\overline{T_e}$ grows slowly until N reaches 32 and p reaches 80. The larger increase in overhead for the QU problem could be related to its special problem structure that causes more worker idleness and computation during **Selection** and **Division**. Moreover, the growth in N may not produce more concurrent evaluation tasks proportionally. Therefore, doubling p every time when N is doubled is not guaranteed to maintain efficient performance. On the other hand, load balancing can be improved greatly for a fixed p as N and the iteration limit $I_{\max}$ or the evaluation limit L_e grows. An experiment in Section 6.1.2 has shown that the parallel efficiency curves for 100 processors reach more than 90%, 80%, and 70% when $I_{\max} = 30$, 20, and 10, respectively, as N increases from 10 to 50, 100, and 150 for the problem RO with the same cost $T_f = 0.1$.

The next scalability study varies the evaluation limit L_e as p grows for the problems FE and BY. The comparisons were also done with the number of iterations/evaluations fixed as p grows. The fixed speedup and scaled speedup are plotted in Figure 6.30. The fixed speedup follows the conventional definition $S_f = T(W, 1)/T(W, p)$, where W is the fixed work load, $T(W, 1)$ is the execution time on a single processor, and $T(W, p)$ is the parallel execution time on p processors. The scaled speedup is usually obtained as $S_s = pT(W_s, 1)/T(pW_s, p)$, where W_s is the base work for a single processor, $T(W_s, 1)$ is the execution time with a single processor on the work W_s, and $T(pW_s, p)$ is the parallel execution time with p processors and the linearly increased work pW_s. S_s needs to be redefined here because the stopping condition `MAX_EVL` is checked after all convex hull boxes have been sampled and subdivided, meaning the number of evaluations does not grow exactly linearly as DIRECT iterates. Therefore, define

$$S_s = \frac{pT(W_s, 1)}{T(W_p, p)(pW_s/W_p)},$$

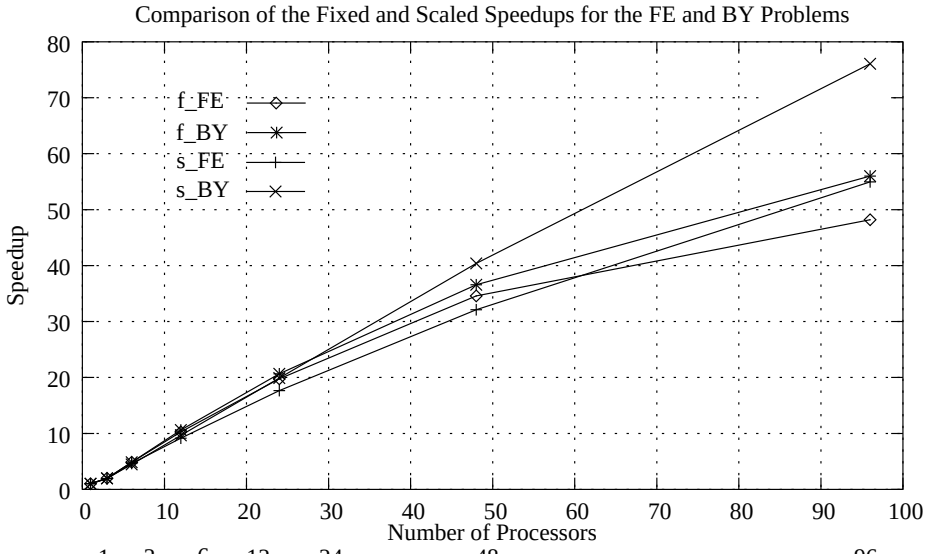

p	1	3	6	12	24	48	96
W_p(FE)	449	941	2465	5413	11339	23187	47051
W_p(BY)	287	571	1699	3095	7263	19059	40045

Figure 6.30. Comparison of the fixed and scaled speedups for the problems FE and BY as L_e and p grow. The actual work W_p is shown in the table below the plot.

where W_s represents the base number of evaluations on a single processor and $W_p > W_s$ is the increased number of evaluations as p grows. Hence, $T(pW_s, p)$ is approximated with $T(W_p, p)(pW_s/W_p)$.

In Figure 6.30, the fixed speedup is obtained with $W = 3251$ for the problem FE and $W = 1699$ for the problem BY. For the scaled speedup, $W_s = 449$ for the problem FE and $W_s = 287$ for the problem BY. The evaluation limits with p processors are listed in the table under the plot for both problems FE and BY. The scaled speedup is slightly worse than the fixed speedup when $p \leq 24$ for the problem BY and when $p \leq 48$ for the problem FE. Note also that the speedup for the problem BY is better than that for the problem FE, because the problem dimension and evaluation cost of the problem BY are higher.

CHAPTER 7: Real World Applications

Like other global optimization approaches of [26] and [32], DIRECT is being tested by parameter estimation for high dimensional nonlinear models. Moles et al. [68] applied DIRECT to a global nonlinear parameter estimation problem in systems biology. However, unnecessary overhead and complexity caused by inefficient implementation inside other software packages (e.g., Matlab) may obscure DIRECT's advanced features. Some computational biologists are attracted by DIRECT's unique strategy of balancing global and local search, its selection rules for potentially optimal regions according to a Lipschitz condition, and its easy-to-use black box interface.

The JigCell systems biology project [3] at Virginia Tech is such an example of applying DIRECT to a problem solving environment. Both global and local optimization techniques are used for biological pathway modeling. One of the most important tools developed for JigCell is the Parameter Estimator, which finds the optimal set of parameters to fit a mathematical pathway model to experimental data.

Section 7.1 describes the general modeling process and Section 7.2 discusses primitive optimization results from the work in [39]. More details and discussions can be found in the work done by Panning et al. [74] and Zwolak et al. [99].

7.1. Cell Cycle Modeling in Systems Biology

The ultimate goal of molecular cell biology is to understand how the information stored in the genome is read out and put into action as the physiological behavior of a living cell. At one end of this continuum, genes direct the synthesis of polypeptide chains, and at the other end, networks of interacting proteins govern how a cell moves, feeds, responds, and reproduces. The model presented here is of the latter type and can be represented as a system of ordinary differential equations (ODE).

The complexity of solving a parameter estimation problem depends on the scale of the ODE model, the size of the parameter space, and the process of the error function evaluation for experiments. The FE objective function costs about 3 seconds per function evaluation with three ODEs containing 16 parameters and the BY objective function takes approximately 11 seconds per evaluation with 36 ODEs containing 143 parameters. A sequential DIRECT would require a few days and even a few weeks to fully explore the parameter space. On a single machine, DIRECT will eventually fail due to limited memory capacity for the fast-growing intermediate data. These computationally intensive and memory demanding applications are the real motivation behind the design of the massively parallel DIRECT that copes with the memory and speed demand, and efficiently utilizes modern large scale parallel systems.

To further understand the modeling process, the FE model [99] [39] is described here as an example. The model describes the activity of MPF (maturation promoting factor) in frog

egg extracts. A frog egg extract is the cytoplasmic protein mix obtained by disrupting (or disintegrating) the membranes of hundreds of frog eggs and separating out the cytoplasm containing protein. The extract can be easily manipulated and assayed compared with intact frog eggs but it still has nearly the same chemical kinetics as an intact frog egg. MPF plays an important role in the chemical kinetics of frog eggs. Primarily the activity of MPF controls when the frog egg enters mitosis and subsequently divides. MPF is a dimer of Cdk1 and Cyclin and is at the center of the model.

The model includes two other proteins that regulate MPF activity: Wee1 and Cdc25. Wee1 inhibits MPF activation, and Cdc25 promotes MPF activation. In turn, MPF regulates Wee1 and Cdc25 creating feedback loops. These three proteins are the most important to cell division in frog eggs. The following system of ODEs describes their interactions:

$$\begin{aligned}\frac{dM}{dt} &= \big(v'_d(1-D) + v''_d D\big)(C_T - M) \\ &\quad - \big(v'_w(1-W) + v''_w W\big)M, \qquad (7.1)\\ \frac{dD}{dt} &= v_d\left(\frac{M(1-D)}{K_{md}+(1-D)} - \frac{\rho_d D}{K_{mdr}+D}\right), \qquad (7.2)\\ \frac{dW}{dt} &= v_w\left(-\frac{MW}{K_{mw}+W} + \frac{\rho_w(1-W)}{K_{mwr}+(1-W)}\right), \qquad (7.3)\end{aligned}$$

where

$$\begin{aligned} M &= \text{[MPF]/[total Cdk1]},\\ D &= \text{[Cdc25P]/[total Cdc25]},\\ W &= \text{[Wee1]/[total Wee1]},\\ C_T &= \text{[total cyclin]/[total Cdk1]}.\end{aligned}$$

M, D, W, and C_T represent scaled concentrations of active MPF, active Cdc25, active Wee1, and total cyclin in the extract, respectively. The parameters v'_d, v''_d, v'_w, v''_w, v_d, K_{md}, ρ_d, K_{mdr}, v_w, K_{mw}, ρ_w, and K_{mwr} are also scaled, making the system dimensionless.

The parameters of the model are unknown. They can be determined experimentally at a great cost to the experimentalist, and only to the theoretician's immediate benefit. The parameters can also be determined by comparing model simulations to experiments and adjusting the parameters until the model matches the experiments. In the present work, a formal objective function [99] has been defined in terms of the parameters and given to the parallel DIRECT to perform a global parameter estimation combined with a local ODR (nonlinear orthogonal distance regression) method.

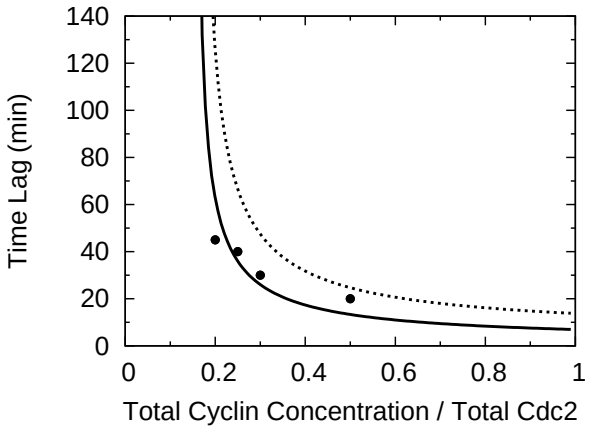

Figure 7.1. Single-start DIRECT result: time lag for MPF activation.

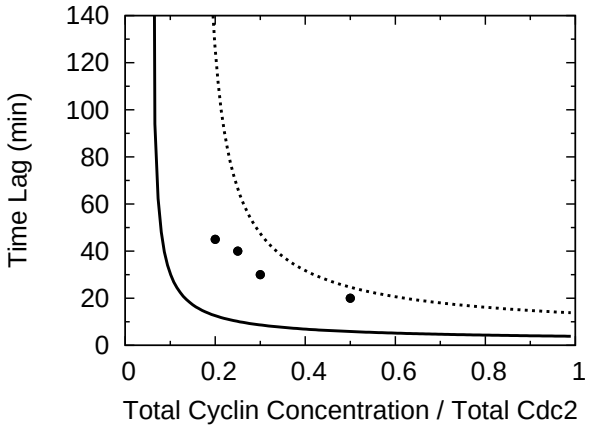

Figure 7.2. Multistart DIRECT result: time lag for MPF activation.

7.2. Simulation and Results

As discussed in Section 6.2.2, a multiple subdomain DIRECT search (multi-start) found lower function values than a single domain DIRECT search (single-start) for both the FE and BY problems. For the FE model, the corresponding parameter sets were plugged in the model to compare the simulation results and the experimental data.

Figures 7.1 through 7.4 compare the simulation results using the discovered parameter sets (solid lines) with the known set of experimental data (dots) as well as with the simulation results from the parameter sets in [69] and [87] (dotted lines). For the time lag plot, the parameter set by Moore [69] predicts the experimental data points better than that from the multistart DIRECT, although the latter gives a closer match in the case of phosphorylation of Wee1. This suggests that the present work explores some previously unexplored regions of parameter space, which may lead to new optimal parameter sets with different biological interpretations.

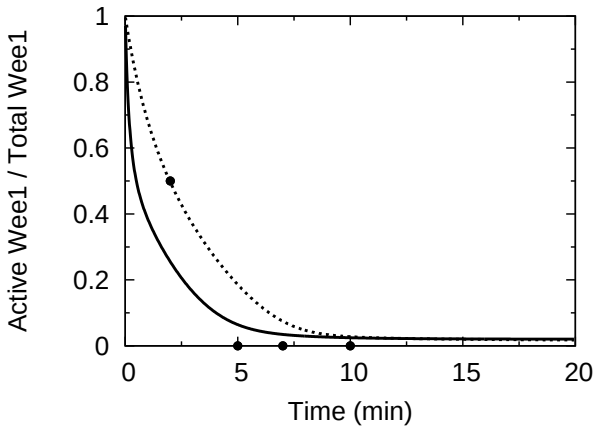

Figure 7.3. Single-start DIRECT result: phosphorylation of Wee1 during mitosis, when MPF is more active.

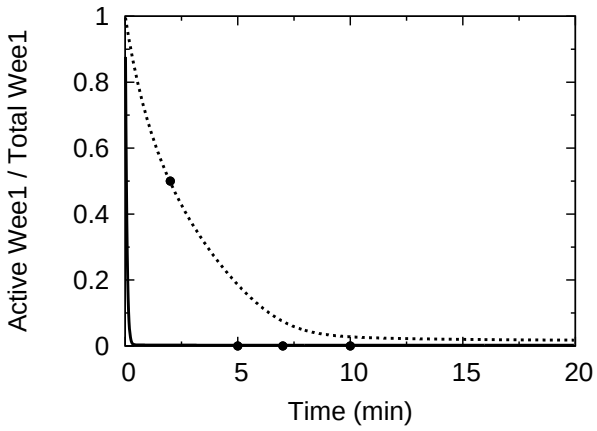

Figure 7.4. Multistart DIRECT result: phosphorylation of Wee1 during mitosis, when MPF is more active.

CHAPTER 8: Conclusion

The main design aspects for the data-distributed massively parallel DIRECT are (1) algorithm modifications that meet the needs of various applications and improve the performance on large scale parallel systems, (2) distributed dynamic data structures enhanced with a memory reduction technique for breaking the "curse of dimensionality", (3) a multilevel functional and data parallelism that eliminates system dependency, boosts concurrency, and mitigates data dependency, and (4) error handling strategies that detect certain errors at run time, reduce potential computation loss, and enable hot restarts for large scale runs.

The multilevel functional and data parallelism consists of three components, among which "domain decomposition" transforms the single start DIRECT into a multistart algorithm, "box subdivision" spreads data across multiple processors, and "function evaluation" distributes evaluation tasks to multiple processors. The implementation of the multilevel parallelism has evolved from the initial design pDIRECT_I to the improved design pDIRECT_II, which addresses the shortcomings of pDIRECT_I in program portability, system utilization, load balancing, and termination efficiency. pDIRECT_II adopts a pure message passing model to replace the mixed shared memory and message passing model that heavily depends on multiple software packages. The fixed worker assignment in pDIRECT_I has been replaced by a more efficient dynamic scheme, where (1) workers are shared globally by all the masters across subdomains, (2) active masters are randomly selected by workers, and (3) finished masters are converted to workers. These dynamic features reduce the processor idleness and offer an exact stopping condition unavailable in the initial design. Lastly, workers exit when all masters are finished, so the termination message is passed down only in the tree of masters, thus greatly simplifying the termination process proposed in pDIRECT_I.

For pDIRECT_II, important performance factors have been extensively studied using modeling and analysis tools such as bounding models, linear regression models, and isoefficiency functions. The analysis covers a broad range of performance metrics including optimization effectiveness, memory usage, parallel efficiency, load balancing, and scalability. Furthermore, this work has been applied to cell cycle modeling for frog egg extracts [99] and budding yeast [74], two real world applications in systems biology. The general modeling process of the frog egg cell cycle and the VTDIRECT95 package documentation will guide interested users to apply this work to other scientific applications.

The crucial performance factors proved to be the problem structure and configuration that directly affect the amount of data dependency overhead and memory requirement. The next most important factors are the scheme configuration parameters that determine four different parallel schemes—pure vertical, pure horizontal, hybrid single domain, and hybrid multiple subdomains. The vertical scheme outperforms the horizontal scheme in most cases, except for a small number of processors ($p < 5$) and cheap objective functions, in which case,

stacking function evaluations ($N_b > 1$) should be considered to reduce the communication overhead. The hybrid schemes are recommended for large scale optimization applications with high computational cost and memory requirement. The hybrid scheme with multiple subdomains has demonstrated its superiority in balancing workload, thus reducing overhead and improving the overall scalability.

On System X and Anantham, the empirical study with T_f varying in small time steps was conducted for both schemes to compare the resulting parallel performance under two types of computing environments differing in both hardware (i.e., CPU frequency, system architecture, and interconnect network) and software (i.e., operating systems, MPI supporting packages, and compilers). System X outperforms Anantham in most cases, except for a few cases under horizontal schemes when T_f is larger than 2.5E-04 second, the performance boundary value for the vertical and horizontal scheme on System X. The detailed analysis of overhead and scalability further verifies the experimental observations. Both theoretical and experimental studies have demonstrated that different system settings only matter when T_f is small. For expensive objective functions, the dominant impact on the parallel performance comes from the problem-dependent factors such as data dependency. However, higher network bandwidth and greater node availability on System X certainly provide a better computing environment for many large scale optimization applications.

Moreover, several important design considerations for the present work can be generalized for global search algorithms, as follows.

(1) Unnecessary data storage should be released dynamically to reduce the memory burden.
(2) Tasks should be dynamically distributed in the smallest possible chunks to ensure the best possible load balancing.
(3) Point sampling and evaluation can be decoupled to enhance the program concurrency.
(4) Domain decomposition not only results in better optimization solutions for problems with irregular structures, but also improves load balancing and scalability if using a large number of processors.

The new insights gained from the present work suggest a fresh research direction for conquering the biggest challenge—the data dependency of DIRECT. Advanced algorithm steps will be designed for **Sampling** to prefetch enough function evaluation tasks, generated from selected boxes that are not on the convex hull, so that the current idle worker cycles would be put to use. The function values at these extra sampling points may not necessarily contribute to the optimization process, so an optimal selection strategy would balance such waste with the benefit of idle cycle computations that *do* further the DIRECT search. Also, the optimal strategy would preserve the determinism of DIRECT, contrasted with nondeterministic methods that produce different solutions on different runs. Of paramount importance is that the proposed modification does not destroy DIRECT's global convergence property. Given the recent interest in DIRECT both in the mathematics and computer science communities, the prospects for significant progress are bright.

REFERENCES

1. K. Aida, W. Natsume, and Y. Futakata, "Distributed computing with hierarchical master-worker paradigm for parallel branch and bound algorithm", in *3rd IEEE/ACM International Symposium on Cluster Computing and the Grid (CCGRID'03)*, Tokyo, Japan, 2003.
2. I. Al-furaih, S. Aluru, S. Goil, and S. Ranka, "Parallel construction of multidimensional binary search trees", *IEEE Trans. on Parallel and Distributed Systems*, Vol. 11, No. 2, pp. 136–148, 2000.
3. N.A. Allen, C.A. Shaffer, M.T. Vass, N. Ramakrishnan, and L.T. Watson , "Improving the development process for Eukaryotic cell cycle models with a modeling support environment", *Simulation*, Vol. 79, No. 12, pp. 674–688, 2003.
4. M.D. Atkinson, J.-R. Sack, N. Santoro, and T. Strothotte, "Min-max heap and generalized priority queues", *Communications of the ACM*, Vol. 29, No. 10, pp. 996–1000, 1986.
5. C. Audet and J.E. Dennis Jr., "Mesh adaptive direct search algorithms for constrained optimization", *SIAM Journal on Optimization*, Vol. 17, No. 1, 2006.
6. K. Bae, J. Jiang, W.H. Tranter, C.R. Anderson, T.S. Rappaport, J. He, A. Verstak, L.T. Watson, N. Ramakrishnan, and C.A. Shaffer, "WCDMA STTD performance analysis with transmitter location optimization in indoor systems using ray tracing techniques", in *Proc. IEEE 2002 Radio and Wireless Conference (RAWCON 2002)*, Boston, MA, pp. 123–127, 2002.
7. C.A. Baker, "Parallel global aircraft configuration design space exploration", Technical Report MAD 2000-06-28, Virginia Polytechnic Institute and State University, Blacksburg, VA, 2000.
8. C.A. Baker, L.T. Watson, B. Grossman, R.T. Haftka, and W.H. Mason, "Parallel global aircraft configuration design space exploration", in *Proc. High Performance Computing Symposium 2000, A. Tentner (Ed.), Soc. for Computer Simulation Internat*, San Diego, CA, pp. 101–106, 2000.
9. C. Banino, O. Beaumont, L. Carter, J. Ferrante, A. Legrand, and Y. Robert, "Scheduling strategies for master-slave tasking on heterogeneous processor platforms", *IEEE Trans. on Parallel and Distributed Systems*, Vol. 15, No. 4, pp. 319–330, 2004.
10. M.C. Bartholomew-Biggs, S.C. Parkhurst, and S.P. Wilson, "Global optimization approaches to an aircraft routing problem", *EUR J. Operational Research*, Vol. 146, No. 2, pp. 417–431, 2003.
11. R. Batchu, Y.S. Dandass, A. Skjellum, and M. Beddhu, "MPI/FT: A model-based approach to low-overhead fault tolerant message-passing middleware", *Cluster Computing*, Vol. 7, pp. 303–315, 2004.
12. D.J. Becker, T. Sterling, D. Savarese, J.E. Dorband, U.A. Ranawake, and C.V. Packer, "Beowulf: A parallel workstation for scientific computation", in *International Conference on Parallel Processing*, pp. 11–14, 1995.
13. N.J. Boden, D. Cohen, R.E. Felderman, A.E. Kulawik, J.N. Seizovic, "Myrinet: A gigabit-per-second local area network", *IEEE Micro*, Vol. 15, No. 1, pp. 29–36, 1995.
14. P.T. Boggs, R.H. Byrd, J.R. Donaldson, and R.B. Schnabel, "Algorithm 676 — ODRPACK: Software for weighted orthogonal distance regression", *ACM Trans. Math. Software*, Vol. 15, No. 4, pp. 348–364, 1989.
15. A. Bouteiller, T. Herault, G. Krawezik, P. Lemarinier, and F. Cappello, "MPICH-V Project: A multiprotocal automatic fault-tolerant MPI", *International Journal of High Performance Computing and Applications*, Vol. 20, pp. 319–333, 2006.
16. E. Cantu-Paz, "A survey of parallel Genetic Algorithm", *Calculateurs Paralleles*, Paris Hermes, Vol. 10, No. 2, pp. 141–171, 1998.
17. R.G. Carter, J.M. Gablonsky, A. Patrick, C.T. Kelly, and O.J. Eslinger, "Algorithms for noisy problems in gas transmission pipeline optimization", *Optimization and Engineering*, Vol. 2, No. 2, pp. 139–157, 2001.
18. X. Chen and D. Turner, "Efficient message-passing within SMP systems", *Recent Advances in Parallel Virtual Machine and Message Passing Interface, Lecture Notes in Computer Science*, Springer, Berlin/Heidelberg, Vol. 2840, pp. 286–293, 2003.
19. J. Clausen, "Parallel branch and bound — principles and personal experiences", *Parallel Computing in Optimization*, Sverre Storoy (Ed.), Kluwer Academic Publishers, Norwell, MA, pp. 239–267, 1997.
20. S.E. Cox, W.E. Hart, R. Haftka, and L.T. Watson, "DIRECT algorithm with box penetration for improved local convergence", in *9th AIAA/ISSMO Symposium and Exhibit on Multidisciplinary Analysis and Optimization*, Atlanta, GA, AIAA Paper 2002–5581, 15 pages, 2002.

21. S. E. Cox, R. T. Haftka, C. Baker, B. Grossman, W. H. Mason, L. T. Watson, "Global multidisciplinary optimization of a high speed civil transport", in *Proc. Aerospace Numerical Simulation Symposium '99*, Tokyo, Japan, pp. 23–28, 1999.
22. S. Cox, R.T. Haftka, C. Baker, B. Grossman, W. Mason and L. T. Watson, "A comparison of optimization methods for the design of a high speed civil transport", *Journal of Global Optimization*, Vol. 21, No. 4, December, 2001.
23. P. Dalgaard, *Introductory Statistics with R*, Springer, New York, 2002.
24. T. Decker and W. Krandick, "Isoefficiency and the parallel Descartes method", in *Proceedings of Dagstuhl Seminar "Symbolic Algebraic Methods and Verification Methods"*, Lecture Notes in Computer Science, Springer-Verlag, London, UK, pp. 55–69, 2001.
25. J.E. Dennis and V. Torczon, "Direct search methods on parallel machines", *SIAM J. on Optimization*, Vol. 1, pp. 448–474, 1991.
26. W.R. Esposito and C.A. Floudas, "Global optimization in parameter estimation of nonlinear algebraic models via the Error-In-Variables approach", *Ind Eng. Chemistry and Research*, Vol. 37, pp. 1841–1858, 1998.
27. G.E. Fagg, A. Bukovsky, and J.J. Dongarra, "HARNESS and fault tolerant MPI", *Parallel Computing*, Vol. 27, pp. 1479–1495, 2001.
28. D.E. Finkel and C.T. Kelly, "An adaptive restart implementation of DIRECT", CRCS-TR04-30, Center for Research in Scientific Computation, North Carolina State University, Raleigh, NC, 2004.
29. J.M. Gablonsky, "Modifications of the DIRECT algorithm", PhD thesis, Department of Mathematics, North Carolina State University, Raleigh, NC, 2001.
30. J.M. Gablonsky, "An implementation of the DIRECT algorithm", Technical Report CRSC-TR98-29, Center for Research in Scientific Computation, North Carolina State University, Raleigh, NC, 1998.
31. J.M. Gablonsky and C.T. Kelley, "Locally-biased form of the DIRECT algorithm", *J. of Global Optimization*, Vol. 21, No. 1, pp. 27–37, 2001.
32. C. Gau and M.A. Stadtherr, "Nonlinear parameter estimation using interval analysis", in *AIchE Symposium*, Vol. 94, No. 320, pp 445-450, 1999.
33. A. Grama, A. Gupta, G. Karypis, and V. Kumar, *Introduction to Parallel Computing*, Pearson Education Limited, 2nd Edition, 2003.
34. R. Graham, "An efficient algorithm for determining the convex hull of a finite planar point set", *Info. Proc. Letters*, Vol. 1, pp. 132–133, 1972.
35. W. Gropp and E. Lusk, "Fault tolerance in message passing interface programs", *International Journal of High Performance Computing Applications*, Vol. 18, pp. 363–372, 2004.
36. W. Gropp, E. Lusk, and R. Thakur, *Using MPI-2: Advanced features of the message-passing interface*, The MIT Press, Cambridge, Massachusetts, London, England, 1999.
37. Z. Hafidi, E.G. Talbi, and J.M. Geib, "MARS: Adaptive scheduling of parallel applications in a multiuser heterogeneous environment", in *European School of Computer Science ESPPE'96: Parallel Programming Environments for High Performance Computing*, Alpe d'Huez, France, pp. 119–122, 1996.
38. J. He, "Global Optimization of Transmitter Placement for Indoor Wireless Communication Systems", M.S. Thesis, Department of Computer Science, Virginia Polytechnic Institute and State University, Blacksburg, VA, 2002.
39. J. He, M. Sosonkina, C.A. Shaffer, J.J. Tyson, L.T. Watson, and J.W. Zwolak, "A hierarchical parallel scheme for global parameter estimation in systems biology", in *Proc. 18th Internat. Parallel & Distributed Processing Symp., CD-ROM, IEEE Computer Soc.*, Los Alamitos, CA, 2004.
40. J. He, M. Sosonkina, C.A. Shaffer, J.J. Tyson, L.T. Watson, and J.W. Zwolak, "A hierarchical parallel scheme for a global search algorithm", in *Proc. High Performance Computing Symposium, Advanced Simulation Technologies Conference, A. Tentner (Ed.), Society for Modeling and Simulation International*, Arlington, VA, pp. 43–50, 2004.
41. J. He, M. Sosonkina, L.T. Watson, A. Verstak, and J.W. Zwolak, "Data-distributed parallelism with dynamic task allocation for a global search algorithm", in *Proc. High Performance Computing Symposium 2005, M. Parashar and L. Watson (eds.), Soc. for Modeling and Simulation Internat.*, San Diego, CA, pp. 164–172, 2005.
42. J. He, A. Verstak, L.T. Watson, T.S. Rappaport, C.R. Anderson, N. Ramakrishnan, C.A. Shaffer, W.H. Tranter, K. Bae, and J. Jiang, "Global optimization of transmitter placement in wireless communication systems", in *Proc. High Performance Computing Symposium, A. Tentner (ed.), Soc. for Modeling and Simulation International*, San Diego, CA, pp. 328–333, 2002.

43. J. He, A. Verstak, L.T. Watson, and M. Sosonkina, "Performance studies of a parallel global search algorithm on System X", in *2006 Spring Simulation Multiconf., High Performance Computing Symp., J.A. Hamilton, Jr., R. MacDonald, and M.J. Chinni (eds.), Soc. for Modeling and Simulation Internat.*, San Diego, CA, pp. 209–214, 2006.
44. J. He, A. Verstak, M. Sosonkina, and L.T. Watson, "Performance modeling and analysis of a massively parallel DIRECT: Part 2", Technical Report TR-07-02, Department of Computer Science, Virginia Polytechnic Institute and State University, Blacksburg, VA, 2007.
45. J. He, A. Verstak, L.T. Watson, and M. Sosonkina, "Performance modeling and analysis of a massively parallel DIRECT: Part 1", Technical Report TR-07-01, Department of Computer Science, Virginia Polytechnic Institute and State University, Blacksburg, VA, 2007.
46. J. He, A. Verstak, L.T. Watson, and M. Sosonkina, "Design and implementation of a massively parallel version of DIRECT", *Computational Optimization and Applications*, to appear.
47. J. He, A. Verstak, L.T. Watson, C.A. Stinson, N. Ramakrishnan, C.A. Shaffer, T.S. Rappaport, C.R. Anderson, K. Bae, J. Jiang, and W.H. Tranter, "Globally optimal transmitter placement for indoor wireless communication systems", *IEEE Transactions on Wireless Communications*, Vol. 3, No. 6, pp. 1906–1911, 2004.
48. J. He, A. Verstak, L.T. Watson, C.A. Stinson, N. Ramakrishnan, C.A. Shaffer, T.S. Rappaport, C.R. Anderson, K. Bae, J. Jiang, and W.H. Tranter, "S^4W: Globally optimized design of wireless communication systems", Computer Science Technical Report TR-02-16, Virginia Polytechnic Institute and State University, Blacksburg, VA, 2002.
49. J. He, L.T. Watson, N. Ramakrishnan, C.A. Shaffer, A. Verstak, J. Jiang, K. Bae, and W.H. Tranter, "Dynamic data structures for a direct search algorithm", *Computational Optimization and Applications*, Vol. 23, No. 1, pp. 5–25, 2002.
50. J. He, L.T. Watson, and M. Sosonkina, "Algorithm XXX: VTDIRECT95: Serial and parallel codes for the global optimization algorithm DIRECT", *Submitted to ACM Trans. on Mathematical Software*, October, 2007.
51. K. Holmqvist, A. Migdalas, and P.M. Pardalos, "Parallelized heuristics for combinatorial search", *Parallel Computing in Optimization*, Sverre Storoy (Eds.), Kluwer Academic Publisher, Norwell, MA, pp 269–294, 1997.
52. R. Horst, P.M. Pardalos, and N.V. Thoai, *Introduction to Global Optimization*, Second Edition, Kluwer Academic Publishers, Dordrecht, Boston, London, 2000.
53. K. Huang and F. Wang, "Design patterns for parallel computations of master-slave model", in *International Conference on Information, Communications and Signal Processing, ICICS'97*, Singapore, September, 1997.
54. V.K. Janakiram, D.P. Agrawal, and R. Mehrotra, "A randomized parallel backtracking algorithm", *IEEE Trans. Comput*, Vol. 37, No. 12, pp. 1665–1676, 1988.
55. D.R. Jones, "The DIRECT global optimization algorithm", *Encyclopedia of Optimization, Vol. 1*, Kluwer Academic Publishers, Dordrecht, Boston, London, pp. 431–440, 2001.
56. D.R. Jones, C.D. Perttunen, and B.E. Stuckman, "Lipschitzian optimization without the Lipschitz constant", *Journal of Optimization Theory and Applications*, Vol. 79, No. 1, pp. 157–181, 1993.
57. V. Kumar and A. Gupta, "Analyzing scalability of parallel algorithms and architectures", *J. of Parallel and Distributed Computing*, Vol. 22, No. 3, pp. 379–391, 1994.
58. R.M. Lewis, V. Torczon, and M.W. Trosset, "Direct search methods: then and now", *Journal of Computational and Applied Mathematics*, Vol. 124, pp. 191–207, 2000.
59. J. Liu, B. Chandrasekaran, W. Yu, J. Wu, D. Buntinas, S. Kini, D.K. Panda, "Microbenchmark performance comparison of high-speed cluster interconnects", *IEEE Micro*, Vol. 24, No. 1, pp. 42–51, 2004.
60. J. Liu, J. Wu, S.P. Kini, P. Wyckoff, and D.K. Panda, "High performance RDMA-based MPI implementation over InfiniBand", *International J. of Parallel Programming*, Vol. 32, No. 3, pp. 167–198, 2004.
61. K. Ljungberg, S. Holmgren, and Ö Carlborg, "Simultaneous search for multiple QTL using the global optimization algorithm DIRECT", *Bioinformatics (Oxford, England)*, Vol. 20, No. 12, pp. 1887–1895, 2004.
62. S. Louca, N. Neophytou, A. Lachanas, and P. Evripidou, "MPI-FT: Portable fault tolerance scheme for MPI", *Parallel Processing Letters*, Vol. 10, pp. 371–382, 2000.

63. J. Luthi, S. Majumdar, G. Kotsis, and G. Haring, "Performance bounds for distributed systems with workload variabilities and uncertainties", *Parallel Computing*, Vol. 22, No. 13, pp. 1789–1806, 1997.
64. U. Manber, *Introduction to Algorithms: a Creative Approach*, Addison-Wesley, Reading, MA, 1989.
65. M.T. McMahon and L.T. Watson, "A distributed genetic algorithm with migration for the design of composite laminate structures", *Parallel Algorithms and Applications*, Vol. 14, pp. 329–362, 2000.
66. A. Migdalas, P.M. Pardalos, and S. Storoy (Eds.) , *Parallel computing in optimization*, Kluwer Academic Publishers, Norwell, MA, 1997.
67. D. Misha, C.A. Shaffer, N. Ramakrishnan, L.T. Watson, K. Bae, J. He, A. Verstak, and W.H. Tranter, "S^4W: A problem solving environment for wireless system design", *Software Practice and Experience*, Vol. 37, No. 14, pp. 1539–1558, 2007.
68. C.G. Moles, P. Mendes, and J.R. Banga, "Parameter estimation in biochemical pathways: a comparison of global optimization methods", *Genome Res.*, Vol. 13, pp. 2467–2474, 2003.
69. J. Moore, "Private Communication", *August*, 1997.
70. E. Nardelli, F. Barillari, and M. Pepe, "Distributed searching of multi-dimensional data: a performance evaluation study", *Journal of Parallel and Distributed Computing*, Vol. 49, pp. 111–134, 1998.
71. S.A. Nelson and P.Y. Papalambros, "A modification to Jones' global optimization algorithm for fast local convergence", in *7th AIAA/USAF/NASA/ISSMO Symposium on Multidisciplinary Analysis and Optimization*, St. Louis, MO, pp. 341–348, 1998.
72. J. Nieplocha and B. Carpenter, "ARMCI: A portable remote memory copy library for distributed array libraries and compiler run-time systems", in *3rd Workshop on Runtime Systems for Parallel Programming (RTSPP) of International Parallel Processing Symposium*, IPPS/SDP'99, CDROM, 1999.
73. D.K. Panda and MVAPICH team, "MVAPICH 0.9.8 User and Tuning Guide", *Network-based Computing Laboratory*, Department of Computer Science and Engineering, Ohio State University, Columbus, Ohio, 2006.
74. T. D. Panning, L. T. Watson, N. A. Allen, K. C. Chen, C. A. Shaffer, and J. J. Tyson, "Deterministic global parameter estimation for a model of the budding yeast cell cycle", *J. Global Optim.*, to appear.
75. K. Parzyszek, J. Nieplocha, and R.A. Kendall, "A generalized portable SHMEM library for high performance computing", in *12th IASTED International Conference Parallel and Distributed Computing and Systems (PDCS)*, pp. 401–406, 2000.
76. J.S. Plank, "An overview of checkpointing in uniprocessor and distributed systems, focusing on implementation and performance", Technical Report UT-CS-97-372, University of Tennessee, Knoxville, Tennessee, 1997.
77. H. Pohlheim, "GEATbx: Genetic and Evolutionary Algorithm Toolbox for Use with Matlab–Documentation", Technical University Ilmenau, Germany, 1996.
78. J.J. Pombo, J.C. Cabaleiro, and T.F. Pena, "Parallel complete remeshing for adaptive schemes", in *International Conference on Parallel Processing Workshops*, pp. 73–78, 2001.
79. V.N. Rao, and V. Kumar, "Concurrent access of priority queues", *IEEE Trans. Comput.*, Vol. 37, No. 12, pp. 1657–1665, 1988.
80. Y. Saad, *Iterative methods for sparse linear systems*, SIAM, Philadelphia, PA, 2nd edition, 2003.
81. H. Samet, *Design and analysis of spatial data structures*, Addison-Wesley, Reading, MA, 1990.
82. Ya.D. Sergeyev and D. Kvasov, "Global search based on efficient diagonal partitions and a set of Lipschitz constants", *SIAM J. on Optimization*, Vol. 16, No. 3, pp. 910–937, 2006.
83. C.A. Shaffer, *A practical introduction to data structures and algorithm analysis*, Prentice-Hall, Upper Saddle River, NJ, 1997.
84. R.R. Skidmore, A. Verstak, N. Ramakrishnan, T.S. Rappaport, L.T. Watson, J. He, S. Varadarajan, C.A. Shaffer, J. Chen, K. Bae, J. Jiang, and W.H. Tranter, "Towards integrated PSEs for wireless communications: experiences with the S^4W and SitePlanner projects", *ACM SIGMOBILE Mobile Computing and Communication Review*, Vol. 8, pp. 20–34, 2004.
85. M. Sosonkina, D.C.S. Allison, and L.T. Watson, "Scalability analysis of parallel GMRES implementations", *Parallel Algorithms and Applications*, Vol. 17, pp. 285–299, 2002.
86. E.G. Talbi, Z. Hafidi, and J.M. Geib, "A parallel adaptive tabu search approach", *Parallel Computing*, Vol. 24, pp. 2003–2019, 1998.
87. Z. Tang, T.R. Coleman, and W.G. Dunphy, "Two distinct mechanisms for negative regulation of the Wee1 protein kinase", *EMBO J.*, Vol. 12, No. 9, pp. 3427–36, 1993.

88. V. Torczon, "On the convergence of the multidirectional search algorithm", *SIAM Journal on Optimization*, Vol. 1, No. 1, pp. 123–145, 1991.
89. V. Torczon, "PDS: Direct search methods for unconstrained optimization on either sequential or parallel machines", CRPC (Center for Research on Parallel Computation, Rice University), TR92206, Houston, Texas, 1992.
90. S.S. Vadhlyar, G.E. Fagg, and J.J. Dongarra, "Towards an accurate model for collective communications", *International J. of High Performance Computing Applications*, Vol. 18, No. 1, pp. 159–167, 2004.
91. A. Verstak, J. He, L.T. Watson, N. Ramakrishnan, C.A. Shaffer, T.S. Rappaport, C.R. Anderson, K. Bae, J. Jiang, and W.H. Tranter, "S^4W: Globally optimized design of wireless communication systems", in *16th Internat. Parallel & Distributed Processing Symp., CD-ROM, IEEE Computer Soc.*, Los Alamitos, CA, 8 pages, 2002.
92. E. Vieth, "Fitting piecewise linear regression functions to biological responses", *Journal of applied physiology*, Vol. 67, No. 1, pp. 390–396, 1989.
93. L.T. Watson and C.A. Baker, "A fully-distributed parallel global search algorithm", *Engineering Computations*, Vol. 18, No. 1/2, pp. 155–169, 2001.
94. L.T. Watson, M. Sosonkina, R.C. Melville, A.P. Morgan, and H.F. Walker, "Algorithm 777: HOMPACK90: A suite of FORTRAN 90 codes for globally convergent homotopy algorithms", *ACM Transactions on Mathematical Software*, Vol. 23, pp. 514–549, 1997.
95. B. Wilkinson and M. Allen, *Parallel Programming—Techniques and Applications using Networked Workstations and Parallel Computers*, Prentice Hall, Upper Saddle River, NJ, 1999.
96. M.S. Wu, R. Kendall, K. Wright, and Z. Zhang, "Performance Modeling and Tuning Strategies of Mixed Mode Collective Communications", in *SC '05: Proceedings of the 2005 ACM/IEEE conference on Supercomputing*, pp. 45–55, 2005.
97. J. Zhou, X. Deng, and P. Dymond, "A 2-D parallel convex hull algorithm with optimal communication phases", *Parallel Computing*, Vol. 27, No. 3, pp. 243–255, 2001.
98. H. Zhu and D.B. Bogy, "DIRECT algorithm and its application to slider air-bearing surface optimization", *IEEE Transactions on Magnetics*, Vol. 38, No. 5, pp. 2168–2170, 2002.
99. J.W. Zwolak, J.J. Tyson, and L.T. Watson, "Globally optimised parameters for a model of mitotic control in frog egg extracts", *IEE Systems Biology*, Vol. 152, No. 2, pp. 81–92, 2005.

APPENDIX A: Test Functions

Table A.1. Test functions selected from GEATbx [77].

Name	Description
GR	Griewank: $f = 1 + \sum_{i=1}^{N} {x_i}^2/500 - \prod_{i=1}^{N} \cos(x_i/\sqrt{i}))$, $-20.0 \leq x_i \leq 30.0,\ f(0,\ldots,0) = 0.0$
QU	Quartic: $f = \sum_{i=1}^{N} 2.2 \times (x_i + 0.3)^2 - (x_i - 0.3)^4$,$-2.0 \leq x_i \leq 3.0$, $f(3,\ldots,3) = -29.816N$
RO	Rosenbrock's Valley: $f = \sum_{i=1}^{N} 100(x_{i+1} - x_i^2)^2 + (1 - x_i)^2$, $-2.048 \leq x_i \leq 2.048,\ f(1,\ldots,1) = 0$
SC	Schwefel: $f = -\sum_{i=1}^{N} x_i \sin(\sqrt{\lvert x_i \rvert})$, $-500 \leq x_i \leq 500,\ f\big(420.9(1,\ldots,1)\big) \approx -418.9N$
MI	Michalewicz: $f = -\sum_{i=1}^{N} \sin(x_i) \times \sin(\frac{ix_i^2}{\pi})^{20}$, $0 \leq x_i \leq \pi,\ f(\bar{x}) = 0$ for $\bar{x} \in \{0,\pi\}^N$
SB	Six-hump Camel Back: $f = (4 - 2.1 * x_1^2 + x_1^4/3)x_1^2 + x_1x_2 + (-4 + 4 * x_2^2)x_2^2$, $-3 \leq x_1 \leq 3,\ -2 \leq x_2 \leq 2$,$f(\bar{x}) = -1.0316$ at $\bar{x} = (-0.0898, 0.7126)$ and $(0.0898, -0.7126)$
BR	Branin rcos: $f = (x_2 - \frac{5.1}{4-\pi^2}x_1^2 + \frac{5}{\pi}x1 - 6)^2 + 10(1 - \frac{1}{8-\pi})\cos(x_1) + 10$, $-5 \leq x_1 \leq 10,\ 0 \leq x_2 \leq 15$,$f(\bar{x}) = 0.397887$ at $\bar{x} = (-\pi, 12.275)$, $(\pi, 2.275)$, and $(9.42478, 2.475)$

Figure A.1. Griewank function (left) and Quartic function (right).

Figure A.2. Rosenbrock's Valley function (left) and Schwefel's function (right).

Figure A.3. Michalewicz's function (left) and Six-hump Camel Back function (right).

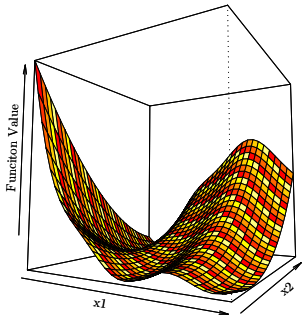

Figure A.4 . Branin rcos function.

APPENDIX B: VTDIRECT95

VTDIRECT95 is a Fortran 95 implementation of D.R. Jones' deterministic global optimization algorithm DIRECT [56] introduced in Chapter 2. The package includes both a serial code and a data-distributed massively parallel code for different problem scales and optimization (exploration vs. exploitation) goals. As discussed in Chapter 3, dynamic data structures are used to organize local data, handle unpredictable memory requirements, reduce the memory usage, and share the data across multiple processors. The parallel code employs a multilevel functional and data parallelism (presented in Chapter 4) to boost concurrency and mitigate the data dependency, thus improving the load balancing and scalability. In addition, checkpointing features (described in Chapter 5) are integrated into both versions to provide fault tolerance and hot restarts. The package organization, portability, and usage are described in this chapter.

B.1. Package Organization

Figure B.1 shows the high level organization of VTDIRECT95. The module `VTdirect_MOD` declares the user called driver subroutine `VTdirect` for the serial code. Correspondingly, the module `pVTdirect_MOD` declares the user called parallel driver subroutine `pVTdirect`, the subroutine `pVTdirect_init` for MPI initialization, the subroutine `pVTdirect_finalize` for MPI finalization, as well as the data types, parameters, and auxiliary functions used exclusively in the parallel code.

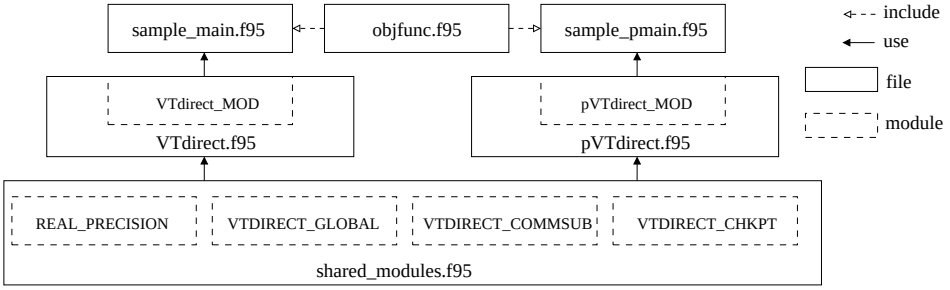

Figure B.1. The module/file dependency map.

The two driver subroutines `VTdirect` and `pVTdirect` share the modules: (1) `REAL_PRECISION` from HOMPACK90 ([94]) for specifying the real data type, (2) `VTDIRECT_GLOBAL` containing definitions of derived data types, parameters, and module procedures, (3) `VTDIRECT_COMMSUB` containing the subroutines and functions common to both the serial and parallel versions, and (4) `VTDIRECT_CHKPT` defining data types and module procedures for the checkpointing feature. These shared modules are merged in the file `shared_modules.f95` as shown in Figure B.1. `sample_main` and `sample_pmain` are sample main programs that call `VTdirect` and `pVTdirect`, respectively, to optimize five test

objective functions defined in `objfunc.f95` and verify the installation. The dependencies between the package components are depicted in Figure B.1.

In the sample serial main program `sample_main` each test objective function illustrates a different way of calling the driver subroutine `VTdirect`. The calls illustrate the four different stopping rules—maximum number of iterations `MAX_ITER`, maximum number of function evaluations `MAX_EVL`, minimum box diameter `MIN_DIA`, and minimum relative decrease in objective function value `OBJ_CONV`. For the last objective function, a multiple best box (MBB) output is illustrated. Details of the arguments are in comments at the beginning of the subroutine `VTdirect`. Different parallel schemes are used in the test cases for `pVTdirect`, called by the sample parallel main program `sample_pmain`. Both sample main programs print to standard out the stopping rule satisfied, the minimum objective function value, the minimum box diameter, and the number of iterations, function evaluations, and the minimum vector(s). In addition, the test output for pVTdirect lists the number of masters per subdomain and the number of subdomains.

Different computation precision and different compiled code on different systems may require different numbers of iterations or evaluations to reach the desired solution accuracy (1.0E-03) specified in the test programs. If a test program fails to locate the optimum value or the optimum point given the stopping conditions in the supplied namelist input file, the stopping conditions can be adjusted accordingly.

B.2. Portability Issues

The module `REAL_PRECISION` from HOMPACK90 [94] is used to define real arithmetic for "precision portability" across different systems. In the `REAL_PRECISION` module, `R8` is the selected `KIND` value corresponding to real numbers with at least 13 decimal digits of precision, covering 60-bit (Cray) and 64-bit (IEEE 754 Standard) real arithmetic.

Another portability issue arises under the parallel computing environment. Although MPI is well known for its portability across machines, its latest standard has not proposed a portable way of matching the data types specified with Fortran 95 `KIND` values. The `REAL (KIND=R8)` real number may be considered as double precision on one system but as single precision on another system. This data type matching problem is addressed here by calling `INQUIRE` to obtain the byte size for the `R8` type and using `MPI_BYTE` to transfer a buffer holding `R8` values, assuming the same byte ordering on all the involved machines. No performance degradation has been observed for this approach.

B.3. Usage Guide

One of the virtues of DIRECT, shared by VTDIRECT95, is that it only has one tuning parameter (ϵ) beyond the problem definition and stopping condition. Using VTDIRECT95 basically takes three simple steps. First, define the objective function with an input argument for the point coordinates (`c`), an output argument for evaluation status (`iflag`), and an output variable for the returned function value (`f`). A nonzero return value for `iflag` is used to indicate that `c` is infeasible or `f` is undefined at `c`. The user written objective function is a FUNCTION procedure that must conform to the interface:

```
INTERFACE
  FUNCTION Obj_Func(c, iflag) RESULT(f)
    USE REAL_PRECISION, ONLY: R8
    REAL(KIND = R8), DIMENSION(:), INTENT(IN)::  c
    INTEGER, INTENT(OUT)::  iflag
    REAL(KIND = R8)::  f
  END FUNCTION Obj_Func
END INTERFACE
```

Second, allocate the required arrays and specify appropriate input parameters to call one of the driver subroutines. In the parallel case, the MPI initialization and finalization subroutines need to be called before and after calling the parallel driver subroutine (pVTdirect), unless MPI is initialized and finalized elsewhere in the same application. The required arrays include the input lower (`L`) and upper (`U`) bounds, and an output array for the optimum vector (`X`). Additionally, in the parallel version, the return status is also an array, required to be allocated beforehand, to hold statuses returned from subdomains, even if only one domain exists, in which case the size of the status array is one. If the user desires to specify the optional input argument `BOX_SET`, an array of boxes must be allocated and an optional weight array `W` for dimensional scaling may also be allocated.

All other input parameters specified in the argument list of the driver subroutine are conveniently read in from a NAMELIST file, as illustrated in the sample main programs. Using namelist files is an elegant way of varying input parameters as needed, without recompiling the program. The namelist file `pdirectRO.nml` shown below is to test `pVTdirect` for optimizing the 4-dimensional problem RO. The parameters are grouped into four categories (NAMELISTs): parallel scheme `PSCHEME`, problem configuration `PROBLEM`, optimization parameters `OPTPARM`, and checkpointing option `CHKPTOP`. This example uses two subdomains and two masters per subdomain, and the stopping condition is when the minimum box diameter reaches 1.0E-05. The checkpointing feature is activated when `chkpt_start` equals 1 (saving) or 2 (recovery). The program will terminate if the checkpoint file errors occur as explained in the section on error handling (Chapter 5). It is the user's responsibility to maintain the checkpoint files, including renaming or removing old files.

```
&PSCHEME n_subdomains=2 n_masters=2 bin=1 /

&PROBLEM N=4
    LB(1:4)=-2.048,-2.048,-2.048,-2.048
    UB(1:4)=2.048,2.048,2.048,2.048 /

&OPTPARM iter_lim=0 eval_lim=0 diam_lim=1.0E-5 objf_conv=0.0
    eps_fmin=0.0 c_switch=1 min_sep=0.0 weight(1:4)=1,1,1,1
    n_optbox=1 /

&CHKPTOP chkpt_start=0 /
```

Finally, the last step is to interpret the return status, collect the results, and deallocate the arrays as needed. The return status consists of two digits. The tens digit indicates the general status: 0 for a successful run, 1 for an input parameter error, 2 for a memory allocation error or failure, and 3 for a checkpoint file error. The stopping condition for a successful run is further indicated in the units digit, which also points to the exact source of error if a nonzero status is returned. For example, a return status of 33 means the checkpoint file header does not match with the current setting. All the error codes and interpretations can be found in the source code documentation. A successful run returns the optimum value and vector(s) in the user-prepared variables and arrays. In order to receive a report on the actual number of iterations/evaluations, or minimum box diameter, these optional arguments must be present in the argument list. The final results of calling `pVTdirect` are merged on processor 0 (the root master), so `proc_id` is returned to designate the root to report the results. VTDIRECT95 is designed so that the optimization results may be directly fed to another procedure or process, the typical situation in large scale scientific computing.

Appendix C: Shared Modules

The shared modules `REAL_PRECISION`, `VTDIRECT_GLOBAL` that defines data types, parameters, and module procedures used by both `VTdirect` and `pVTdirect`, `VTDIRECT_COMMSUB` that declares the subroutines and functions shared by `VTdirect` and `pVTdirect`, and `VTDIRECT_CHKPT` that defines data types and module procedules for the checkpointing feature used in both `VTdirect` and `pVTdirect` are listed below.

```
MODULE REAL_PRECISION  ! From HOMPACK90.
  ! This is for 64-bit arithmetic.
  INTEGER, PARAMETER:: R8=SELECTED_REAL_KIND(13)
END MODULE REAL_PRECISION
MODULE VTDIRECT_GLOBAL
USE REAL_PRECISION
IMPLICIT NONE
!
!HyperBox: Defines an n-dimensional box.
!  val  - Function value at the box center.
!  c    - The center point coordinates.
!  side - Box side lengths for all dimensions.
!  diam - Box diameter squared.
!
TYPE HyperBox
  REAL(KIND = R8) :: val
  REAL(KIND = R8), DIMENSION(:), POINTER :: c
  REAL(KIND = R8), DIMENSION(:), POINTER :: side
  REAL(KIND = R8) :: diam
END TYPE HyperBox
!
!BoxLink: Contains 1-D array of hyperboxes, linked to each column of
!         BoxMatrix when needed.
!  Line - 1-D array of boxes.
!  ind  - Index of last box in array 'Line'.
!  next - The pointer to the next BoxLink.
!  prev - The pointer to the previous BoxLink.
!
TYPE BoxLink
  TYPE(HyperBox), DIMENSION(:), POINTER :: Line
  INTEGER :: ind
  TYPE(BoxLink), POINTER :: next
  TYPE(BoxLink), POINTER :: prev
END TYPE BoxLink
!
!P_BoxLink: Contains a pointer to a BoxLink for a column in BoxMatrix.
!  p - Pointer to a BoxLink.
!
TYPE P_BoxLink
  TYPE(BoxLink), POINTER :: p
END TYPE P_BoxLink
!
!BoxLine: Contains 1-D array of newly sampled hyperboxes.
!  Line - 1-D array of boxes.
!  ind  - Index of last box in array 'Line'.
!  dir  - Directions in which box centers are sampled.
```

```
!
TYPE BoxLine
  TYPE(HyperBox), DIMENSION(:), POINTER :: Line
  INTEGER :: ind
  INTEGER, DIMENSION(:), POINTER :: dir
END TYPE BoxLine
!
!BoxMatrix: Contains 2-D array of hyperboxes.
!  M       - 2-D array of boxes.
!  ind     - An array holding the number of boxes in all the columns in 'M'.
!  child   - The pointer to the next BoxMatrix with the smaller diameters.
!  sibling - The pointer array for all columns, pointing to the next
!            BoxLinks with the same diameters.
!  id      - Identifier of this box matrix among all box matrices.
!
TYPE BoxMatrix
  TYPE(HyperBox), DIMENSION(:,:), POINTER :: M
  INTEGER, DIMENSION(:), POINTER :: ind
  TYPE(BoxMatrix), POINTER :: child
  TYPE(P_BoxLink), DIMENSION(:), POINTER :: sibling
  INTEGER :: id
END TYPE BoxMatrix
!
! P_Box: Contains a pointer to a hyperbox.
!
TYPE P_Box
  TYPE (HyperBox), POINTER :: p_box
END TYPE P_Box
!
!int_vector : A list holding integer values.
!  dim      - The index of the last element in the list.
!  elements - The integer array.
!  flags    - The integer array holding the status for 'elements'.
!             Bit 0: status of convex hull processing.
!  next     - The pointer to the next integer vector list.
!  prev     - The pointer to the previous integer vector list.
!  id       - Identifier of this integer vector list among all lists.
!
TYPE int_vector
  INTEGER :: dim
  INTEGER, DIMENSION(:), POINTER :: elements
  INTEGER, DIMENSION(:), POINTER :: flags
  TYPE(int_vector), POINTER :: next
  TYPE(int_vector), POINTER :: prev
  INTEGER :: id
END TYPE int_vector
!
!real_vector: A list holding real values.
!  dim      - The index of the last element in the list.
!  elements - The real array.
!  next     - The pointer to the next real vector list.
!  prev     - The pointer to the previous real vector list.
!  id       - Identifier of this real vector list among all lists.
!
TYPE real_vector
  INTEGER :: dim
```

```
  REAL(KIND = R8), DIMENSION(:), POINTER :: elements
  TYPE(real_vector), POINTER :: next
  TYPE(real_vector), POINTER :: prev
  INTEGER :: id
END TYPE real_vector
!
!ValList: a list for sorting the wi for all dimensions i corresponding
!  to the maximum side length. wi = min f(c+delta*ei), f(c-delta*ei),
!  the minimum of objective function values at the center point c +
!  delta*ei and the center point c - delta*ei, where delta is one-third of
!  this maximum side length and ei is the ith standard basis vector.
!  dim - The index of the last element in the list.
!  val - An array holding the minimum function values.
!  dir - An array holding the sampling directions corresponding to the
!        function values in array 'val'.
!
TYPE ValList
  INTEGER :: dim
  REAL(KIND = R8), DIMENSION(:), POINTER :: val
  INTEGER, DIMENSION(:), POINTER :: dir
END TYPE
! Parameters.
! Argument input error.
INTEGER, PARAMETER :: INPUT_ERROR = 10
! Allocation failure error.
INTEGER, PARAMETER :: ALLOC_ERROR = 20
! File I/O error.
INTEGER, PARAMETER :: FILE_ERROR = 30
! Stop rule 1: maximum iterations.
INTEGER, PARAMETER :: STOP_RULE1 = 0
! Stop rule 2: maximum evaluations.
INTEGER, PARAMETER :: STOP_RULE2 = 1
! Stop rule 3: minimum diameter.
INTEGER, PARAMETER :: STOP_RULE3 = 2
! Stop rule 4: minimum relative change in objective function.
INTEGER, PARAMETER :: STOP_RULE4 = 3
! 'flags' bits for 'setInd' of type 'int_vector'.
INTEGER, PARAMETER :: CONVEX_BIT = 0
! Bit 0: if set, the first box on the corresponding column is in the convex
!        hull box set.
! Global variables.
INTEGER :: col_w, row_w ! Factors defining reasonable memory space for
  ! each box matrix allocation.
INTEGER :: N_I          ! Local copy of 'N'.
REAL(KIND = R8) :: EPS4N
TYPE(Hyperbox), POINTER :: tempbox ! Box for swapping heap elements.
! Interfaces.
INTERFACE ASSIGNMENT (=)
  MODULE PROCEDURE AssgBox
END INTERFACE
INTERFACE insNode
  MODULE PROCEDURE insNodeI
  MODULE PROCEDURE insNodeR
END INTERFACE insNode
INTERFACE rmNode
  MODULE PROCEDURE rmNodeI
```

```
  MODULE PROCEDURE rmNodeR
END INTERFACE rmNode
CONTAINS
SUBROUTINE AssgBox(x, y)
IMPLICIT NONE
! Copy the contents of box 'y' to box 'x'.
!
! On input:
! y - Box with type 'HyperBox'.
!
! On output:
! x - Box with type 'HyperBox' having contents of box 'y'.
!
TYPE(HyperBox), INTENT(IN) :: y
TYPE(HyperBox), INTENT(INOUT) :: x
x%val = y%val
x%diam = y%diam
x%c = y%c
x%side = y%side
RETURN
END SUBROUTINE AssgBox
SUBROUTINE insNodeR(n, pt, index, Set)
IMPLICIT NONE
! Insert a real number 'pt' at the indexed position 'index' of 'Set'.
!
! On input:
! n     - The maximum length of the real array in each node of 'Set'.
! pt    - The real number to be inserted to 'Set'.
! index - The position at which to insert 'pt' in a node of 'Set'.
! Set   - A linked list of type(real_vector) nodes.
!
! On output:
! Set   - 'Set' has an added real number and modified 'dim' component.
!
INTEGER, INTENT(IN) :: n
REAL(KIND = R8), INTENT(IN) :: pt
INTEGER, INTENT(IN) :: index
TYPE(real_vector), INTENT(INOUT), TARGET :: Set
! Local variables.
TYPE(real_vector), POINTER :: p_set ! Pointer to a node of 'Set'.
! Insert 'pt' into 'Set'.
IF (Set%dim < n ) THEN
  ! The head node is not full. There are no other nodes.
  ! Update 'dim'.
  Set%dim = Set%dim + 1
  IF (index == Set%dim) THEN
    ! The desired position is at end, so insert 'pt' at end.
    Set%elements(Set%dim) = pt
  ELSE
    ! The desired position is not at end, so shift elements before
    ! insertion.
    Set%elements(index+1:Set%dim) = Set%elements(index:Set%dim-1)
    Set%elements(index) = pt
  END IF
ELSE
  ! The head node is full. Check other nodes.
```

```
  p_set => Set%next
  ! To shift elements, find the last node which is not full.
  DO WHILE(p_set%dim == n)
    p_set => p_set%next
  END DO
  ! Found the last node 'p_set' which is not full.
  ! Update 'dim' of 'p_set'. Shift element(s) inside this node, if any.
  p_set%dim = p_set%dim + 1
  ! Loop shifting until reaching the node 'Set' at which to insert 'pt'.
  DO WHILE(.NOT. ASSOCIATED(p_set, Set))
    ! Shift element(s) inside this node,  if any.
    p_set%elements(2:p_set%dim) = p_set%elements(1:p_set%dim-1)
    ! Shift the last element from the previous node to this one.
    p_set%elements(1) = p_set%prev%elements(n)
    ! Finished shifting this node. Go to the previous node.
    p_set => p_set%prev
  END DO
  ! Reached the original node 'Set'.
  IF (index == Set%dim) THEN
    ! The desired position is at end, so insert 'pt' at end.
    Set%elements(Set%dim) = pt
  ELSE
    ! The desired position is not at end, so shift elements before
    ! insertion.
    Set%elements(index+1:Set%dim) = Set%elements(index:Set%dim-1)
    Set%elements(index) = pt
  END IF
END IF
RETURN
END SUBROUTINE insNodeR
SUBROUTINE insNodeI(n, pt, index, Set)
IMPLICIT NONE
! Insert an integer number 'pt' at the indexed position 'index' of 'Set'.
!
! On input:
! n        - The maximum length of the integer array in each node of 'Set'.
! pt       - The integer number to be inserted to 'Set'.
! index    - The position at which to insert 'pt'.
! Set      - A linked list of type(int_vector) nodes.
!
! On output:
! Set   - 'Set' has an added integer number and modified 'dim' component.
INTEGER, INTENT(IN) :: n
INTEGER, INTENT(IN) :: pt
INTEGER, INTENT(IN) :: index
TYPE(int_vector), INTENT(INOUT), TARGET :: Set
! Local variables.
TYPE(int_vector), POINTER :: p_set ! Pointer to a node of 'Set'.
LOGICAL :: setflags ! The flag to operate on component 'flags'.
! Assign 'setflags'.
setflags = ASSOCIATED(Set%flags)
! Insert 'pt' into 'Set'.
IF (Set%dim < n ) THEN
  ! The head node is not full. There are no other nodes.
  Set%dim = Set%dim + 1
  IF (index == Set%dim) THEN
```

```
    ! The desired position is at end, so insert 'pt' at end.
    Set%elements(Set%dim) = pt
    ! Clear the 'flags'.
    IF (setflags) Set%flags(Set%dim) = 0
ELSE
    ! The desired position is not at end, so shift elements before
    ! insertion.
    Set%elements(index+1:Set%dim) = Set%elements(index:Set%dim-1)
    IF (setflags) THEN
      ! Shift the 'flags'.
      Set%flags(index+1:Set%dim) = Set%flags(index:Set%dim-1)
      ! Clear the 'flags'.
      Set%flags(index) = 0
    END IF
    ! Insert 'pt'.
    Set%elements(index) = pt
  END IF
ELSE
  ! The head node is full. There must be other nodes.
  p_set => Set%next
  ! To shift elements, find the last node which is not full.
  DO WHILE(p_set%dim == n)
    p_set => p_set%next
  END DO
  ! Found the last node 'p_set' which is not full.
  ! Update 'dim' of 'p_set'. Shift element(s), if any.
  p_set%dim = p_set%dim + 1
  ! Loop shifting until reaching the original node 'Set'.
  DO WHILE(.NOT. ASSOCIATED(p_set, Set))
    ! Shift element(s) inside this node, if any.
    p_set%elements(2:p_set%dim) = p_set%elements(1:p_set%dim-1)
    ! Shift the last element from the previous node to this one.
    p_set%elements(1) = p_set%prev%elements(n)
    IF (setflags) THEN
      ! Shift the 'flags'.
      p_set%flags(2:p_set%dim) = p_set%flags(1:p_set%dim-1)
      p_set%flags(1) = p_set%prev%flags(n)
    END IF
    ! Finished shifting this node. Go to the previous node.
    p_set => p_set%prev
  END DO
  ! Reached the original node 'Set'.
  IF (index == Set%dim) THEN
    ! The desired position is at end, so insert 'pt' at end.
    Set%elements(Set%dim) = pt
    ! Clear the 'flags'.
    IF (setflags) Set%flags(Set%dim) = 0
  ELSE
    ! The desired position is not at end, so shift elements before
    ! insertion.
    Set%elements(index+1:Set%dim) = Set%elements(index:Set%dim-1)
    IF (setflags) THEN
      ! Shift the 'flags'.
      Set%flags(index+1:Set%dim) = Set%flags(index:Set%dim-1)
      ! Clear the 'flags'.
      Set%flags(index) = 0
```

```
    END IF
    ! Insert 'pt'.
    Set%elements(index) = pt
  END IF
END IF
RETURN
END SUBROUTINE insNodeI
SUBROUTINE rmNodeI(n, offset, index, Set)
IMPLICIT NONE
! Remove an integer entry at position 'index' from the integer array
! in the node at 'offset' links from the beginning of the linked list
! 'Set'.
!
! On input:
! n        - The maximum length of the integer array in each node of 'Set'.
! offset   - The offset of the desired node from the first node of 'Set'.
! index    - The position at which to delete an integer from the integer
!            array in the node.
! Set      - A linked list of type(int_vector) nodes.
!
! On output:
! Set    - The desired node of 'Set' has the indexed integer entry removed
!          and the 'dim' component modified.
!
INTEGER, INTENT(IN) :: n
INTEGER, INTENT(IN) :: offset
INTEGER, INTENT(IN) :: index
TYPE(int_vector), INTENT(INOUT), TARGET :: Set
! Local variables.
INTEGER :: i  ! Loop counter.
TYPE(int_vector), POINTER :: p_set  ! Pointer to a node of 'Set'.
LOGICAL :: setflags ! The flag to operate on component 'flags'.
! Assign 'setflags'.
setflags = ASSOCIATED(Set%flags)
! Find the desired node.
p_set => Set
DO i = 1, offset
  p_set => p_set%next
END DO
IF (index < p_set%dim) THEN
  ! It's not the last entry in 'p_set', so shift elements.
  p_set%elements(index:p_set%dim-1) = p_set%elements(index+1:p_set%dim)
  ! Shift the 'flags'.
  IF (setflags) p_set%flags(index:p_set%dim-1) = p_set%flags(index+1:p_set%dim)
END IF
IF (p_set%dim < n) THEN
  ! There are not other elements in next node, so remove the indexed
  ! entry directly from 'Set' by updating 'dim'.
  p_set%dim = p_set%dim - 1
ELSE
  ! There might be nodes in which to shift elements.
  ! Check if any element(s) in next node to shift.
  IF (ASSOCIATED(p_set%next)) THEN
    p_set => p_set%next
    DO
      IF (p_set%dim > 0) THEN
```

```
        ! There are elements to shift.
        ! Shift one element from p_next into its previous node.
        p_set%prev%elements(n) = p_set%elements(1)
        ! Shift elements inside p_next.
        p_set%elements(1:p_set%dim-1) = p_set%elements(2:p_set%dim)
        IF (setflags) THEN
          ! Shift the 'flags'.
          p_set%prev%flags(n) = p_set%flags(1)
          p_set%flags(1:p_set%dim-1) = p_set%flags(2:p_set%dim)
        END IF
      ELSE
        ! There are no elements to shift. Update 'dim' of previous node.
        p_set%prev%dim = p_set%prev%dim - 1
        EXIT
      END IF
      ! Move on to the next node, if any. If there are no more nodes, update
      ! 'dim'.
      IF (ASSOCIATED(p_set%next)) THEN
        p_set => p_set%next
      ELSE
        p_set%dim = p_set%dim - 1
        EXIT
      END IF
    END DO
  ELSE
    ! There are no more nodes. Update 'dim' of 'p_set'.
    p_set%dim = p_set%dim - 1
  END IF
END IF
RETURN
END SUBROUTINE rmNodeI
SUBROUTINE rmNodeR(n, offset, index, Set)
IMPLICIT NONE
! Remove a real entry at position 'index' from the real array
! in the node at 'offset' links from the beginning of the linked list
! 'Set'.
!
! On input:
! n      - The maximum length of the real array in each node of 'Set'.
! offset - The offset of the desired node from the first node of 'Set'.
! index  - The position at which to delete a real entry from the real
!          array in the node.
! Set    - A linked list of type(real_vector) nodes.
!
! On output:
! Set    - The desired node of 'Set' has the indexed real entry removed
!          and the 'dim' component modified.
!
INTEGER, INTENT(IN) :: n
INTEGER, INTENT(IN) :: offset
INTEGER, INTENT(IN) :: index
TYPE(real_vector), INTENT(INOUT), TARGET :: Set
! Local variables.
INTEGER :: i  ! Loop counter.
TYPE(real_vector), POINTER :: p_set  ! Pointer to a node of 'Set'.
! Find the desired node.
```

```
p_set => Set
DO i = 1, offset
  p_set => p_set%next
END DO
IF (index < p_set%dim)THEN
  ! It's not the last entry in 'p_set', so shift elements.
  p_set%elements(index:p_set%dim-1) = p_set%elements(index+1:p_set%dim)
END IF
IF (p_set%dim < n) THEN
  ! There are not other elements in next node, so remove the indexed
  ! entry directly from 'Set' by updating 'dim'.
  p_set%dim = p_set%dim - 1
ELSE
  ! There might be nodes in which to shift elements.
  ! Check if any element(s) in next node to shift.
  IF (ASSOCIATED(p_set%next)) THEN
    p_set => p_set%next
    DO
      IF (p_set%dim > 0) THEN
        ! There are elements to shift.
        ! Shift one element from p_next into its previous node.
        p_set%prev%elements(n) = p_set%elements(1)
        ! Shift elements inside p_next.
        p_set%elements(1:p_set%dim-1) = p_set%elements(2:p_set%dim)
      ELSE
        ! There are no elements to shift. Update 'dim' of previous node.
        p_set%prev%dim = p_set%prev%dim - 1
        EXIT
      END IF
      ! Move on to the next node if any. If there are no more nodes, update
      ! 'dim'.
      IF (ASSOCIATED(p_set%next)) THEN
        p_set => p_set%next
      ELSE
        p_set%dim = p_set%dim - 1
        EXIT
      END IF
    END DO
  ELSE
    ! There are no  more nodes. Update 'dim' of 'p_set'.
    p_set%dim = p_set%dim - 1
  END IF
END IF
RETURN
END SUBROUTINE rmNodeR
END MODULE VTDIRECT_GLOBAL
MODULE VTDIRECT_COMMSUB
USE VTDIRECT_GLOBAL
INTERFACE OPERATOR (.lexLT.) ! Lexicographic comparison operator.
  MODULE PROCEDURE lexOrder
END INTERFACE
CONTAINS
SUBROUTINE binaryS(p_rset, diam, pos, found)
IMPLICIT NONE
! Using a binary search, match the squared diameter 'diam' with an
! element in the node 'p_rset' of 'setDia', and return the position
```

```
! 'pos' if a match is found. If there is no match, return the right
! 'pos' at which to insert 'diam'. When 'pos' is returned as 0, 'diam'
! should be inserted after all others. If 'pos' is not 0, 'diam' could
! be inserted at the position 'pos' of 'p_rset' depending on 'found'.
! See insMat().
! On input:
! p_rset - A pointer to one of the nodes in 'setDia'.
! diam   - The diameter squared to match against.
!
! On output:
! pos   - The position in 'p_rset' for a match or insertion.
! found - Status indicating whether 'diam' is found in 'p_rest' or not.
!
TYPE(real_vector), INTENT(IN) :: p_rset
REAL(KIND = R8), INTENT(IN) :: diam
INTEGER, INTENT(OUT) :: pos
LOGICAL, INTENT(OUT) :: found
! Local variables.
INTEGER :: low, mid, up
! Initialization for searching.
found = .FALSE.
! Initialize limits outside bounds of array for binary search.
low = 0
up = p_rset%dim + 1
IF (p_rset%dim > 0) THEN
  ! Check with the first and the last.
  IF (p_rset%elements(1) <= diam) THEN
    ! 'diam' is the biggest.
    IF (ABS(p_rset%elements(1) - diam)/MAX(diam, p_rset%elements(1)) <= EPS4N) THEN
      ! 'diam' is the same as the first one.
      found = .TRUE.
    END IF
    pos = 1
    RETURN
  ELSE
    IF (p_rset%elements(up-1) >= diam) THEN
      IF (ABS(p_rset%elements(up-1) - diam)/MAX(p_rset%elements(up-1), diam) &
         <= EPS4N) THEN
        ! 'diam' is the smallest one. Same as the last one in 'p_rset'.
        found = .TRUE.
        pos = up-1
      ELSE
        ! 'diam' is smaller than all in 'p_rset'. Set 'pos' 0 to insert
        ! 'diam' after all others.
        found = .FALSE.
        pos = 0
      END IF
      RETURN
    ELSE
      ! 'diam' falls in between the biggest and the smallest. Apply binary
      ! search.
      DO WHILE((low + 1) < up)
        mid = (low + up) / 2
        IF (ABS(diam - p_rset%elements(mid))/           &
          MAX(diam, p_rset%elements(mid)) <= EPS4N) THEN
          ! 'diam' found.
```

```
          up = mid
          EXIT
        END IF
        IF (diam < p_rset%elements(mid))THEN
          low = mid
        ELSE
          up = mid
        END IF
      END DO
      ! Check if it's found.
      mid = up
      IF (ABS(diam - p_rset%elements(mid))/MAX(diam, p_rset%elements(mid)) &
         <= EPS4N) THEN
        ! Found it, so assign 'mid' to 'pos' in order to insert the
        ! associated box in the same column as 'mid'.
        found = .TRUE.
        pos = mid
      ELSE
        found = .FALSE.
        IF (diam > p_rset%elements(mid) )THEN
          ! 'diam' is bigger than the one at 'mid'. Set 'pos' to be 'mid'
          ! in order to insert 'diam' before 'mid'.
          pos = mid
        ELSE
          ! 'diam' is smaller than the one at 'mid'. Set 'pos' to be one
          ! after 'mid' in order to insert 'diam' after 'mid'.
          pos = mid + 1
        END IF
      END IF
    END IF
  END IF
ELSE
  ! 'p_rset' is empty. Set 'pos'=0 to insert 'diam' at the end of 'p_rset'.
  found = .FALSE.
  pos = 0
END IF
RETURN
END SUBROUTINE binaryS
SUBROUTINE checkblinks(col, b, status)
IMPLICIT NONE
! Check if this column needs a new box link. Create one if needed.
!
! On input:
! col - The local column index.
! b   - The current link of box matrices.
!
! On output:
! b      - 'b' has the newly added box link for 'col' if needed.
! status - Return status.
!          0   Successful.
!          1   Allocation error.
!
INTEGER, INTENT(IN) :: col
TYPE(BoxMatrix), INTENT(INOUT) :: b
INTEGER, INTENT(OUT) :: status
! Local variables.
```

```
TYPE(BoxLink), POINTER :: newBoxLink, p_link
INTEGER :: i
! Set normal status.
status = 0
IF ((b%ind(col) == row_w) .AND. (.NOT. ASSOCIATED(b%sibling(col)%p))) THEN
  ! When the M part of the box column is full and there are no box links:
  ! Make a new box link linked to it. Allocate a new one.
  ALLOCATE(newBoxLink, STAT = status)
  IF (status /= 0) RETURN
  CALL initLink(newBoxLink, status)
  IF (status /= 0) RETURN
  ! This is the first box link that does not have previous link.
  NULLIFY(newBoxLink%prev)
  ! Link it as 'sibling' of this column.
  b%sibling(col)%p => newBoxLink
ELSE ! There is at least one box link.
  IF (b%ind(col) > row_w) THEN
    ! Find the last box link 'p_blink'.
    p_link => b%sibling(col)%p
    DO i=1,(b%ind(col)-1)/row_w-1
      p_link => p_link%next
    END DO
    IF ((p_link%ind == row_w) .AND. (.NOT. ASSOCIATED(p_link%next))) THEN
      ! It's full.
      ! Need a new box link. Allocate a new one.
      ALLOCATE(newBoxLink, STAT = status)
      IF (status /= 0) RETURN
      CALL initLink(newBoxLink, status)
      IF (status /= 0) RETURN
      ! Link the new box link to the last one as the next link.
      p_link%next => newBoxLink
      ! Link the last box link to the new one as the previous link.
      newBoxLink%prev => p_link
    END IF
  END IF
END IF
RETURN
END SUBROUTINE checkblinks
FUNCTION findpt(b, col, i_last, index, p_last) RESULT(p_index)
IMPLICIT NONE
! Find the pointer for the box 'index' in the column 'col' of box
! matrix 'b'. If this box 'index' is in one of the box links, record
! the pointer to the box link holding this box 'index' in 'p_last'
! and compute the box position offset 'i_last'. These two records will
! be used to resume chasing the pointers for the heap elements closer
! to the bottom.
!
! On input:
! b      - Box matrix holding the box column 'col' with the box 'index'.
! col    - Column index.
! i_last - Box position offset used in finding the starting box position
!          from the box link 'p_last'.
! index  - Box index.
! p_last - Pointer to the last box link that has been chased so far.
!
! On output:
```

```
! i_last - Updated 'i_last'.
! p_last - Updated 'p_last'.
!
TYPE(BoxMatrix), INTENT(IN), TARGET :: b
INTEGER, INTENT(IN) :: col
INTEGER, INTENT(INOUT) :: i_last
INTEGER, INTENT(IN) :: index
TYPE(BoxLink), POINTER :: p_last
TYPE(HyperBox), POINTER :: p_index
! Local variables.
TYPE(BoxLink), POINTER :: p_l   ! Pointer to a box link.
INTEGER :: i
IF (.NOT. ASSOCIATED(p_last)) THEN
  ! 'p_last' has not been set, so start from the first box matrix 'b'.
  IF (index <= row_w) THEN
    ! The box 'index' is in 'M' array of 'b'.
    p_index => b%M(index,col)
  ELSE
    ! Chase to the box link that this box belongs to.
    p_l => b%sibling(col)%p
    DO i = 1, (index-1)/row_w -1
      p_l => p_l%next
    END DO
    ! Found the box link that holds the box 'index'.
    p_index => p_l%Line(MOD(index-1, row_w)+1)
    ! Set 'p_last' and 'i_last'.
    p_last => p_l
    i_last = ((index-1)/row_w)*row_w
  END IF
ELSE
  ! Start from 'p_last', because it is the last box link that has been
  ! processed.
  p_l => p_last
  DO i = 1, (index-i_last-1)/row_w
    p_l => p_l%next
  END DO
  ! Found the box link that holds the box 'index'.
  p_index => p_l%Line(MOD(index-1,row_w)+1)
  ! Set 'p_last' and 'i_last'.
  p_last => p_l
  i_last = ((index-1)/row_w)*row_w
END IF
RETURN
END FUNCTION findpt
SUBROUTINE initLink(newBoxLink, iflag)
IMPLICIT NONE
! Initialize a new box link.
!
! On input:
!   newBoxLink - A new box link.
!
! On output:
!   newBoxLink - 'newBoxLink' with initialized structures.
!   iflag      - Return status.
!                0   Normal.
!                1   Allocation failure.
```

```
!
TYPE(BoxLink), INTENT(INOUT) :: newBoxLink
INTEGER, INTENT(OUT) :: iflag
! Local variables.
INTEGER :: i
! Initialize 'iflag'.
iflag = 0
! Allocate 'Line' of the new BoxLink.
ALLOCATE(newBoxLink%Line(row_w),STAT = iflag)
IF (iflag /= 0) RETURN
DO i = 1, row_w
  ALLOCATE(newBoxLink%Line(i)%c(N_I),STAT = iflag)
  IF (iflag /= 0) RETURN
  ALLOCATE(newBoxLink%Line(i)%side(N_I),STAT = iflag)
  IF (iflag /= 0) RETURN
END DO
! Nullify pointers 'next' and 'prev'.
NULLIFY(newBoxLink%next)
NULLIFY(newBoxLink%prev)
! Initialize the counter for boxes.
newBoxLink%ind = 0
RETURN
END SUBROUTINE initLink
SUBROUTINE  insBox(box, col, b, iflag)
IMPLICIT NONE
! Insert 'box' in column 'col' of box matrices 'b'. If all positions
! in 'col' are full, make a new box link linked to the end of
! this column.
!
! On input:
! box   - The box to be inserted.
! col   - The global column index at which to insert 'box'.
! b     - The head link of box matrices.
!
! On output:
! b     - 'b' has a newly added 'box'.
! iflag - Return status.
!          0   Normal.
!          1   Allocation failure.
!
TYPE(HyperBox), INTENT(IN) :: box
INTEGER, INTENT(IN) :: col
TYPE(BoxMatrix), INTENT(INOUT), TARGET :: b
INTEGER, INTENT(OUT) :: iflag
! Local variables.
INTEGER :: b_id, i, mycol, status
TYPE(BoxLink), POINTER :: p_blink
TYPE(BoxMatrix), POINTER :: p_b
! Initialize 'iflag' as a normal return.
iflag = 0
! Locate the box matrix in which to insert 'box'.
mycol = col
IF (mycol <= col_w) THEN
  p_b => b
ELSE
  b_id = (mycol-1)/col_w + 1
```

```
  mycol = MOD(mycol-1, col_w) + 1
  p_b => b
  DO i=1, b_id-1
    p_b => p_b%child
  END DO
END IF
! Insert the box at the end of column 'mycol' of box matrix 'p_b'.
IF (p_b%ind(mycol) < row_w) THEN
  ! There is no box links.
  p_b%M(p_b%ind(mycol)+1, mycol) = box
ELSE
  ! There are box links. Chase to the last box link.
  p_blink => p_b%sibling(mycol)%p
  DO i = 1, p_b%ind(mycol)/row_w - 1
    p_blink => p_blink%next
  END DO
  p_blink%ind = p_blink%ind + 1
  p_blink%Line(p_blink%ind) = box
END IF
! Update 'ind' of the column ('ind' of 'p_b' counts all the boxes in
! this column including the ones in its box links.).
p_b%ind(mycol) = p_b%ind(mycol) + 1
! Siftup the box in the heap.
CALL siftup(p_b, mycol, p_b%ind(mycol))
! Add a new box link if needed.
CALL checkblinks(mycol, p_b, status)
IF (status /=0) THEN ; iflag = 1 ; END IF
RETURN
END SUBROUTINE insBox
SUBROUTINE insMat(box, b, setDia, setInd, setFcol, status, isConvex)
IMPLICIT NONE
! Retrieve all box matrices to find the place at which to insert 'box'.
! Insert it in the column with the same squared diameter, or a new
! column if the squared diameter is new. In the same column, the smaller
! 'val', the earlier the position.
!
! On input:
! box     - The box to be inserted.
! b       - The head link of box matrices.
! setDia  - A linked list holding different squared diameters.
! setInd  - A linked list holding the column indices corresponding to
!           'setDia'.
! setFcol - A linked list holding free columns of box matrices.
! isConvex- A flag to indicate if 'box' is on the convex hull.
!
! On output:
! b       - 'b' has the newly added 'box' and updated counters.
! setDia  - 'setDia' has a newly added squared diameter if any and
!           updated 'dim' if modified.
! setInd  - 'setInd' has a newly added column index if needed and
!           updated 'dim' if modified.
! setFcol - 'setFcol' has a column index removed if needed and updated
!           'dim' if modified.
! status  - Status of processing.
!            0    Normal.
!            1    Allocation failures of type 'BoxMatrix'.
```

```
!            2    Allocation failures of type 'BoxLink'.
!            3    Allocation failures of type 'real_vector' or 'int_vector'.
!
!
TYPE(HyperBox), INTENT(IN) :: box
TYPE(BoxMatrix), INTENT(INOUT), TARGET :: b
TYPE(real_vector), INTENT(INOUT), TARGET :: setDia
TYPE(int_vector), INTENT(INOUT), TARGET :: setInd
TYPE(int_vector), INTENT(INOUT), TARGET :: setFcol
INTEGER, INTENT(OUT) :: status
INTEGER, INTENT(IN) :: isConvex
! Local variables.
INTEGER :: b_id, b_pos, i, iflag, j, pos
LOGICAL :: found
TYPE(BoxMatrix), POINTER :: p_b
TYPE(int_vector), POINTER :: p_iset
TYPE(real_vector), POINTER :: p_rset
! Initialization for msearchSet().
pos = 0
found = .FALSE.
NULLIFY(p_rset)
iflag = 0
status = 0
! Locate a node of 'setDia' into which 'diam' can be inserted.
p_rset => msearchSet(setDia, box%diam)
CALL binaryS(p_rset, box%diam, pos, found)
IF (found) THEN
  ! A match is found in 'p_rset' of 'setDia'.
  ! Find the corresponding node in 'setInd' to match 'p_rset'.
  p_iset => setInd
  DO i = 1, p_rset%id-1
    p_iset => p_iset%next
  END DO
  ! Insert 'box' in the column indexed by 'pos' in a node of 'setInd'.
  CALL insBox(box, p_iset%elements(pos), b, iflag)
  IF (iflag == 1 ) THEN ; status = 2 ; RETURN ; END IF
  IF (isConvex == 1) THEN ! Set 'CONVEX_BIT'.
    p_iset%flags(pos) = IBSET(p_iset%flags(pos), CONVEX_BIT)
  END IF
ELSE
  ! No match is found. It's a new squared diameter.
  IF (pos == 0)THEN
    ! Obtain a free column from 'setFcol' to insert 'box' after all
    ! other columns.
    IF (setFcol%dim > 0)THEN
      ! 'setFcol' is not empty, so pop a column from the top of 'setFcol'
      ! nodes.
      IF (setFcol%dim < col_w) THEN
        ! The head node is not full, therefore it must be the top node.
        i = setFcol%elements(setFcol%dim)
        ! Update 'dim'.
        setFcol%dim = setFcol%dim - 1
      ELSE
        ! There might be other nodes with element(s).
        p_iset => setFcol%next
        IF (ASSOCIATED(p_iset)) THEN
```

```
      ! Chase to the top node of 'setFcol' with element(s).
      DO WHILE(p_iset%dim == col_w)
        p_iset => p_iset%next
      END DO
      ! The top node could be 'p_iset' or its 'prev'.
      IF (p_iset%dim /= 0) THEN
        i = p_iset%elements(p_iset%dim)
        p_iset%dim = p_iset%dim - 1
      ELSE
        i = p_iset%prev%elements(p_iset%prev%dim)
        p_iset%prev%dim = p_iset%prev%dim - 1
      END IF
    ELSE
      ! There are no more nodes with elements. Pop a column from the
      ! head node of 'setFcol'.
      i = setFcol%elements(setFcol%dim)
      ! Update 'dim'.
      setFcol%dim = setFcol%dim -1
    END IF
  END IF
ELSE
  ! There are no free columns, so make a new box matrix.
  CALL newMat(b, setDia, setInd, setFcol, iflag)
  IF (iflag /= 0) THEN ; status = iflag ; RETURN ; END IF
  ! Pop a column from the top of 'setFcol' for use.
  i = setFcol%elements(setFcol%dim)
  CALL rmNode(col_w, 0, setFcol%dim, setFcol)
END IF
! Found the global column index 'i' at which to insert 'box'. Convert
! it to a local column index 'b_pos' and locate the box
! matrix 'p_b' at which to insert 'box'.
IF (i <= col_w) THEN
  p_b => b
  b_pos = i
ELSE
  b_id = (i-1)/col_w + 1
  b_pos = MOD(i-1, col_w) + 1
  p_b => b
  DO j = 1, b_id -1
    p_b => p_b%child
  END DO
END IF
! Insert 'box' at the beginning of the new column 'b_pos'.
p_b%M(1,b_pos) = box
! Locate the nodes in both 'setDia' and 'setInd' at which to insert
! the new squared diameter and the column index 'i' at the end of
! both linked lists ('pos' is 0).
IF (setDia%dim < col_w)THEN
  ! There are no more nodes with elements. Assign the head node
  ! to 'p_rset'.
  p_rset => setDia
ELSE
  ! There are other nodes to check.
  p_rset => setDia%next
  IF (ASSOCIATED(p_rset)) THEN
    ! Chase to the end of the linked list.
```

```
      DO WHILE(p_rset%dim == col_w)
        p_rset => p_rset%next
      END DO
    ELSE
      ! There are no more nodes. Assign the head node to 'p_rset'
      p_rset => setDia
    END IF
  END IF
  ! Found the node 'p_rset' of 'setDia' to insert.
  CALL insNode(col_w, box%diam, p_rset%dim+1, p_rset)
  ! Find the corresponding node in 'setInd' at which to insert the
  ! column index 'i'.
  p_iset => setInd
  DO j =1, p_rset%id -1
    p_iset => p_iset%next
  END DO
  CALL insNode(col_w, i, p_iset%dim+1, p_iset)
  ! Set 'CONVEX_BIT'.
  IF (isConvex == 1) p_iset%flags(p_iset%dim) = &
    IBSET(p_iset%flags(p_iset%dim), CONVEX_BIT)
  ! Update 'ind' of col 'b_pos' in 'p_b'.
  p_b%ind(b_pos) = 1
ELSE
  ! 'pos' is not 0. 'p_rset' points to the right node of 'setDia' to
  ! insert the new squared diameter.
  ! Obtain a free column from 'setFcol' to insert a new column before the
  ! column indexed by the returned 'pos'.
  IF (setFcol%dim > 0)THEN
    ! 'setFcol' is not empty, so pop a column from the top of 'setFcol'
    ! nodes.
    IF (setFcol%dim < col_w) THEN
    ! The head node is not full, so it must be the top.
      i = setFcol%elements(setFcol%dim)
      setFcol%dim = setFcol%dim - 1
    ELSE
      ! There might be nodes with free columns.
      p_iset => setFcol%next
      IF (ASSOCIATED(p_iset)) THEN
        ! Chase to the top of 'setFcol' links.
        DO WHILE(p_iset%dim == col_w)
          p_iset => p_iset%next
        END DO
        ! The top node could be 'p_iset' or its 'prev'.
        IF (p_iset%dim /= 0) THEN
          i = p_iset%elements(p_iset%dim)
          p_iset%dim = p_iset%dim - 1
        ELSE
          i = p_iset%prev%elements(p_iset%prev%dim)
          p_iset%prev%dim = p_iset%prev%dim - 1
        END IF
      ELSE
        ! There are no more nodes with elements. Pop a column from the
        ! head node of 'setFcol'.
        i = setFcol%elements(setFcol%dim)
        setFcol%dim = setFcol%dim -1
      END IF
```

```
      END IF
    ELSE
      ! There are no free columns, so make a new box matrix.
      CALL newMat(b, setDia, setInd, setFcol, iflag)
      IF (iflag /= 0) THEN ; status = iflag ; RETURN ; END IF
      ! Pop a column for use.
      i = setFcol%elements(setFcol%dim)
      CALL rmNode(col_w, 0, setFcol%dim, setFcol)
    END IF
    ! Found the global column index 'i' at which to insert 'box'.
    ! Convert it to a local column index 'b_pos' and locate the
    ! box matrix 'p_b' in which to insert 'box'.
    IF (i <= col_w) THEN
      p_b => b
      b_pos = i
    ELSE
      b_id = (i-1)/col_w + 1
      b_pos = MOD(i-1, col_w) + 1
      p_b => b
      DO j = 1, b_id -1
        p_b => p_b%child
      END DO
    END IF
    ! Add 'box' to be the first on column 'b_pos' of 'p_b'.
    p_b%M(1,b_pos) = box
    ! Insert the new squared diameter at the position 'pos' in 'p_rset'
    ! of 'setDia'.
    CALL insNode(col_w, box%diam, pos, p_rset)
    ! Insert the corresponding column index 'i' at the same position 'pos'
    ! in a node of 'setInd'.
    p_iset => setInd
    DO j = 1, p_rset%id -1
      p_iset => p_iset%next
    END DO
    CALL insNode(col_w, i, pos, p_iset)
    IF (isConvex == 1) p_iset%flags(pos) = &
      IBSET(p_iset%flags(pos), CONVEX_BIT)
    ! Update 'ind' of box matrix 'p_b'.
    p_b%ind(b_pos) = 1
  END IF
END IF
RETURN
END SUBROUTINE insMat
FUNCTION lexOrder(a, b) RESULT (smaller)
IMPLICIT NONE
! Compare box centers 'a' and 'b' lexicographically. If 'a' is
! lexicographically smaller than 'b', return .TRUE. .  Define operator
! .lexLT. .
!
! On input:
! a - center of a box.
! b - center of a box.
!
! On output:
! smaller - .TRUE.   'a' is smaller than 'b' lexicographically.
!           .FALSE.  Otherwise.
```

```
!
REAL(KIND = R8), DIMENSION(:), INTENT(IN) :: a
REAL(KIND = R8), DIMENSION(:), INTENT(IN) :: b
LOGICAL :: smaller
! Local variables.
INTEGER :: i
! Initialize 'smaller'.
smaller = .FALSE.
! Loop for comparing coordinates of 'a' and 'b'.
DO i = 1,SIZE(a)
  IF (a(i) < b(i)) THEN
    smaller = .TRUE.
    EXIT
  ELSE IF (a(i) == b(i)) THEN
    CONTINUE
  ELSE ! a(i) > b(i)
    EXIT
  END IF
END DO
RETURN
END FUNCTION lexOrder
FUNCTION msearchSet(setDia, diam) RESULT(p_rset)
IMPLICIT NONE
! Find the right node in 'setDia' in which to insert 'diam'.
!
! On input:
! setDia - A linked list holding different squared diameters.
! diam   - A diameter squared to be inserted in a node in 'setDia'.
!
! On output:
! p_rset - Pointer to the right node of 'setDia'.
!
TYPE(real_vector), INTENT(IN), TARGET :: setDia
REAL(KIND = R8), INTENT(IN) :: diam
TYPE(real_vector), POINTER :: p_rset
! Local variables.
TYPE(real_vector), POINTER :: p_setDia
! Initialize 'p_setDia'.
p_setDia => setDia
DO
  IF (p_setDia%dim > 0) THEN
    ! There are elements to be compared with 'diam'.
    IF (diam >= p_setDia%elements(1)) THEN
      ! 'diam' is the biggest. Return this node as 'p_rset'.
      p_rset => p_setDia
      EXIT
    ELSE
      IF ((diam >= p_setDia%elements(p_setDia%dim)) .OR.     &
         ((ABS(diam - p_setDia%elements(p_setDia%dim))       &
         /MAX(diam, p_setDia%elements(p_setDia%dim))) <= EPS4N) ) THEN
        ! 'diam' is within the range of elements in this node.
        p_rset => p_setDia
        EXIT
      ELSE
        ! 'diam' is smaller than the last element. Go on to the next
        ! node, if any.
```

```
        IF (ASSOCIATED(p_setDia%next)) THEN
          p_setDia => p_setDia%next
        ELSE
          ! There are no more nodes. Return this pointer.
          p_rset => p_setDia
          EXIT
        END IF
      END IF
    END IF
  ELSE
    ! It's empty. Return this pointer.
    p_rset => p_setDia
    EXIT
  END IF
END DO
RETURN
END FUNCTION msearchSet
SUBROUTINE newMat(b, setDia, setInd, setFcol, iflag)
IMPLICIT NONE
! Make a new box matrix and its associated linked lists for holding
! different squared diameters, column indices, and free columns.
! Link them to existing structures.
!
! On input:
! b       - The head link of box matrices.
! setDia  - Linked list holding different squared diameters of
!           current boxes.
! setInd  - Linked list holding column indices of box matrices.
! setFcol - Linked list holding free columns of box matrices.
!
! On output:
! b       - 'b' has a box matrix link added at the end.
! setDia  - 'setDia' has a node added at the end.
! setInd  - 'setInd' has a node added at the end.
! setFcol - 'setFcol' has a node added at the end.
! iflag   - Return status.
!           0   Normal.
!           1   Allocation failures of type 'BoxMatrix'.
!           3   Allocation failures of type 'real_vector' or 'int_vector'.
!
TYPE(BoxMatrix), INTENT(INOUT), TARGET :: b
TYPE(real_vector), INTENT(INOUT), TARGET :: setDia
TYPE(int_vector), INTENT(INOUT), TARGET :: setInd
TYPE(int_vector), INTENT(INOUT), TARGET :: setFcol
INTEGER, INTENT(OUT) :: iflag
! Local variables.
INTEGER :: alloc_err, i, j
TYPE(BoxMatrix), POINTER :: new_b, p_b
TYPE(int_vector), POINTER :: n_setFcol, n_setInd, p_setFcol, p_setInd
TYPE(real_vector), POINTER :: n_setDia, p_setDia
! Initialize iflag for normal return.
iflag = 0
! Allocate a new box matrix.
ALLOCATE(new_b, STAT=alloc_err)
IF (alloc_err /= 0) THEN; iflag = 1; RETURN; END IF
! Allocate its associated arrays.
```

```
ALLOCATE(new_b%M(row_w, col_w), STAT=alloc_err)
IF (alloc_err /= 0) THEN; iflag = 1; RETURN; END IF
ALLOCATE(new_b%ind(col_w), STAT=alloc_err)
IF (alloc_err /= 0) THEN; iflag = 1; RETURN; END IF
! Clear the box counter for each column.
new_b%ind(:) = 0
! Nullify pointers for a child link and box links.
NULLIFY(new_b%child)
ALLOCATE(new_b%sibling(col_w), STAT=alloc_err)
IF (alloc_err /= 0) THEN; iflag = 1; RETURN; END IF
DO i = 1, col_w
  NULLIFY(new_b%sibling(i)%p)
END DO
DO i = 1, row_w
  DO j = 1, col_w
    ALLOCATE(new_b%M(i,j)%c(N_I), STAT=alloc_err)
    IF (alloc_err /= 0) THEN; iflag = 1; RETURN; END IF
    ALLOCATE(new_b%M(i,j)%side(N_I), STAT=alloc_err)
    IF (alloc_err /= 0) THEN; iflag = 1; RETURN; END IF
  END DO
END DO
! Find the last box matrix to link with the new one.
p_b => b
DO WHILE(ASSOCIATED(p_b%child))
  p_b => p_b%child
END DO
! Found the last box matrix p_b. Link it to new box matrix 'b'.
p_b%child => new_b
! Set up 'id' for new_b.
new_b%id = p_b%id + 1
! Allocate new 'setDia', 'setInd' and 'setFcol' for 'new_b'.
! Find the corresponding nodes of 'setDia', 'setInd' and 'setFcol'.
p_setDia => setDia
p_setInd => setInd
p_setFcol => setFcol
DO i=1, p_b%id-1
  p_setDia => p_setDia%next
  p_setInd => p_setInd%next
  p_setFcol => p_setFcol%next
END DO
! Allocate a new node for 'setDia'. Initialize its structure.
ALLOCATE(n_setDia, STAT=alloc_err)
IF (alloc_err /= 0) THEN; iflag = 3; RETURN; END IF
ALLOCATE(n_setDia%elements(col_w), STAT=alloc_err)
IF (alloc_err /= 0) THEN; iflag = 3; RETURN; END IF
NULLIFY(n_setDia%next)
NULLIFY(n_setDia%prev)
n_setDia%id = p_setDia%id +1
n_setDia%dim = 0
! Allocate a new node for 'setInd'. Initialize its structure.
ALLOCATE(n_setInd, STAT=alloc_err)
IF (alloc_err /= 0) THEN; iflag = 3; RETURN; END IF
ALLOCATE(n_setInd%elements(col_w), STAT=alloc_err)
IF (alloc_err /= 0) THEN; iflag = 3; RETURN; END IF
ALLOCATE(n_setInd%flags(col_w), STAT=alloc_err)
IF (alloc_err /= 0) THEN; iflag = 3; RETURN; END IF
```

```
n_setInd%flags(:)= 0
NULLIFY(n_setInd%next)
NULLIFY(n_setInd%prev)
n_setInd%id = p_setInd%id + 1
n_setInd%dim = 0
! Allocate a new node for 'setFcol'. Initialize its structure.
ALLOCATE(n_setFcol, STAT=alloc_err)
IF (alloc_err /= 0) THEN; iflag = 3; RETURN; END IF
ALLOCATE(n_setFcol%elements(col_w), STAT=alloc_err)
IF (alloc_err /= 0) THEN; iflag = 3; RETURN; END IF
NULLIFY(n_setFcol%next)
NULLIFY(n_setFcol%prev)
n_setFcol%id = p_setFcol%id + 1
n_setFcol%dim = 0
! Link them to the end of existing sets.
p_setDia%next => n_setDia
n_setDia%prev => p_setDia
p_setInd%next => n_setInd
n_setInd%prev => p_setInd
p_setFcol%next => n_setFcol
n_setFcol%prev => p_setFcol
! Fill up 'setFcol' with new columns from the new box matrix.
! Starting from the last column, push free columns to the top of 'setFcol'.
DO i = 1, col_w
  setFcol%elements(i) = new_b%id*col_w - (i-1)
END DO
setFcol%dim = col_w
RETURN
END SUBROUTINE newMat
SUBROUTINE siftdown(b, col, index)
IMPLICIT NONE
! Sift down the heap element at 'index' through the heap column 'col' in
! the box matrix 'b'.
!
! On input:
! b     - Box matrix holding the box column 'col' for siftdown.
! col   - Column index.
! index - Index of the box to be sifted down.
!
! On output:
! b     - Box matrix with the elements rearranged by siftdown.
!
TYPE(BoxMatrix), INTENT(INOUT), TARGET :: b
INTEGER, INTENT(IN) :: col, index
! Local variables.
INTEGER :: i           ! Loop counters.
INTEGER :: i_last      ! Index of the last box that has been processed
                       ! in the previous iteration.
INTEGER :: i_last_backup  ! i_last's backup used to go back to i_last,
                          ! which may be updated in the current iteration.
INTEGER :: left, right    ! Indices for the left and right children.
TYPE(BoxLink), POINTER :: p_last        ! Pointer to the last box link
                                        ! that has been processed.
TYPE(BoxLink), POINTER :: p_last_backup ! Pointer backup for 'p_last'.
TYPE(HyperBox), POINTER :: p_i          ! Pointer to the heap parent box.
TYPE(HyperBox), POINTER :: p_left, p_right  ! Pointers to the left and right
```

```
                                          ! child boxes.
! Exit if it is an empty column.
IF (b%ind(col) == 0) RETURN
! Initialization.
NULLIFY(p_last)
i_last=0
! Starting siftdown operation from the box 'index'
i = index
DO
! Find the indices for the left and right children.
left = 2*i
right = 2*i + 1
! If 'i' is a leaf, exit.
IF (left > b%ind(col)) EXIT
! Find the pointers to the the ith box and its left child. Record the
! pointer 'p_last' and index 'i_last' for the currently processed box
! link.
  p_i => findpt(b, col, i_last, i, p_last)
  p_left => findpt(b, col, i_last, left, p_last)
  IF (left < b%ind(col)) THEN
    ! Backup the pointer 'p_last' and the index 'i_last', because they will
    ! be updated when finding the pointer to the right child. If the right
    ! child is in the correct place in the heap, restore the pointer
    ! 'p_last' and the index 'i_last'.
    p_last_backup => p_last
    i_last_backup = i_last
    p_right => findpt(b, col, i_last, right, p_last)
    IF (p_left%val > p_right%val) THEN
      p_left => p_right
      left = left + 1
    ELSE
      IF (p_left%val == p_right%val) THEN
        ! When values are equal, smaller lex order wins.
        IF (p_right%c .lexLT. p_left%c) THEN
          p_left => p_right
          left = left + 1
        ELSE
          ! Restore 'p_last' and 'i_last' to the values before finding
          ! the pointer for the right child.
          p_last => p_last_backup
          i_last = i_last_backup
        END IF
      ELSE
        ! Restore 'p_last' and 'i_last' to the values before finding
        ! the pointer for the right child.
        p_last => p_last_backup
        i_last = i_last_backup
      END IF
    END IF
  END IF
  ! If the boxes are in the correct order, exit.
  IF (p_i%val < p_left%val) EXIT
  IF ((p_i%val == p_left%val) .AND. (p_i%c .lexLT. p_left%c)) EXIT
  ! Swap the boxes pointed to by 'pi' and 'p_left'.
  tempbox = p_i
  p_i = p_left
```

```
  p_left = tempbox
  ! Continue siftdown operation from the left child of 'i'.
  i = left
END DO
RETURN
END SUBROUTINE siftdown
SUBROUTINE siftup(b, col, index)
IMPLICIT NONE
! Sift up the heap element at 'index' through the heap column 'col' in
! the box matrix 'b'.
!
! On input:
! b     - Box matrix holding the box column 'col' for siftup.
! col   - Column index.
! index - Index of the box to be sifted up.
!
! On output:
! b     - Box matrix with the elements rearranged by siftup.
!
TYPE(BoxMatrix), INTENT(INOUT), TARGET :: b
INTEGER, INTENT(IN) :: col, index
! Local variables.
INTEGER :: i, j      ! Loop counters.
INTEGER :: parent    ! Index for the parent.
INTEGER :: e_idi, e_idp, l_idi, l_idp
TYPE(BoxLink), POINTER :: p_blinki, p_blinkp ! Pointers for the box link.
TYPE(HyperBox), POINTER :: p_i  ! Pointer to the box indexed as 'i'.
TYPE(HyperBox), POINTER :: p_p  ! Pointer to the parent box.
! Exit if it is an empty column.
IF (b%ind(col) == 0) RETURN
! Starting siftup operation from the box 'index'.
i = index
IF (i == 1) RETURN ! Exit if there is only one box in the column.
l_idi = (i-1)/row_w  ! If 0, it's inside the box matrix M.
e_idi = MOD(i-1,row_w)+1
! Locate the box 'i'.
IF (l_idi == 0) THEN
  p_i => b%M(i, col)
ELSE
  ! Chase to the box link that this box belongs to.
  p_blinki => b%sibling(col)%p
  DO j = 1, l_idi-1
    p_blinki => p_blinki%next
  END DO
  ! Found the box link that holds the box 'i'.
  p_i => p_blinki%Line(e_idi)
END IF
DO WHILE (i /= 1) ! If the root has been reached, exit.
  ! Find the index for the parent.
  parent = i/2
  ! Compute link id and element id for the parent.
  l_idp = (parent-1)/row_w
  e_idp = MOD(parent-1,row_w)+1
  ! Locate the box 'parent'.
  IF (l_idp == 0) THEN
    p_p => b%M(parent, col)
```

```
  ELSE
    p_blinkp => b%sibling(col)%p
    DO j = 1, l_idp-1
      p_blinkp => p_blinkp%next
    END DO
    p_p => p_blinkp%Line(e_idp)
  END IF
  ! Found the boxes 'parent' and 'i'. Compare their 'val's. If box 'i' has
  ! a smaller 'val', swap box 'i' with box 'parent'. Otherwise, box 'i'
  ! moves up to point to the box 'parent' and repeats the comparison and
  ! swaps (if needed), until box 'i' becomes the root.
  IF ((p_i%val < p_p%val) .OR. &
     ((p_i%val == p_p%val) .AND. (p_i%c .lexLT. p_p%c))) THEN
    tempbox = p_i
    p_i = p_p
    p_p = tempbox
    l_idi = l_idp
    e_idi = e_idp
    i = parent
    p_i => p_p
    IF (l_idi /= 0) p_blinki => p_blinkp
  ELSE
    i = 1
  END IF
END DO
RETURN
END SUBROUTINE siftup
END MODULE VTDIRECT_COMMSUB
MODULE VTDIRECT_CHKPT
USE VTDIRECT_GLOBAL
USE VTDIRECT_COMMSUB
!
! Definitions of derived data types.
!
! LogNode: Defines a checkpoint log node that contains a box's center
! coordinates and the objective function value there.
!   c   - Point coordinates.
!   val - The function value at 'c'.
!
TYPE LogNode
  REAL(KIND = R8), DIMENSION(:), POINTER :: c
  REAL(KIND = R8) :: val
END TYPE LogNode
!
! LogList: Contains a list of checkpoint logs. These logs are listed in
! the order that they were written to the checkpoint file when recovering
! in the case of the sequential run of VTdirect or the parallel run of
! pVTdirect with the same number of masters that generated the checkpoint
! logs. When the number of masters is different from that in the run that
! generated the checkpoint logs, these logs in the list are sorted in
! lexicographical order to facilitate a binary search to look up the function
! values.
!   idx  - Index to a log node during recovery, index of last log node
!          during construction.  idx is initialized to 0; if the logs are
!          all recovered and the list is deallocated, idx is set to -1.
!   list - List of log nodes.
```

```
!
TYPE LogList
  INTEGER :: idx
  TYPE(LogNode), DIMENSION(:), POINTER :: list
END TYPE LogList
!
! Definitions of global parameters, and variables.
!
INTEGER, PARAMETER :: CHKSUNIT=444 ! Logical unit number for a checkpoint
! file, or a base logical unit number for a set of checkpoint files when
! multiple files are kept open to recover the checkpoint logs from
! multiple masters in the parallel code pVTdirect. To avoid conflicts
! with other logical units in the same application, this value should
! be adjusted accordingly.
INTEGER, PARAMETER :: CHKRUNIT=CHKSUNIT+1 ! The second base logical unit
! number is needed for writing to a set of new checkpoint files when
! restarting with a number of masters different from that in the run that
! generated the checkpoint file (only in pVTdirect).
INTEGER, PARAMETER :: INITLEN = 1000 ! The initial length of the log list.
TYPE(LogList) :: fList  ! The list of checkpoint logs.
CONTAINS
!
! Internal subroutines and functions.
!
RECURSIVE FUNCTION bFindlex(c, s, e) RESULT (ans)
IMPLICIT NONE
! Do a recursive binary search for 'c' starting at position 's' and ending at
! position 'e' in the log list sorted in lexicographical order.
!
! On input:
! c  - Point coordinates.
! s  - Starting position.
! e  - Ending position.
!
! On output:
! ans - The position that c matches. If 0, 'c' is not found.
!
REAL(KIND = R8), DIMENSION(:), INTENT(IN) :: c
INTEGER, INTENT(IN) :: s, e
INTEGER :: ans
! Local variables.
INTEGER :: mid  ! The middle position.
! When 's' and 'e' meet, check if 'c' is found.
IF (s == e) THEN
  IF (ALL(c == fList%list(s)%c)) THEN
    ans = s
  ELSE ! 'c' is not found in the list.
    ans = 0
  END IF
ELSE
  ! Compute 'mid' to recursively search the list in two divided portions.
  mid = CEILING((s+e)*0.5_R8)
  IF (c .lexLT. fList%list(mid)%c) THEN
    ans = bFindlex(c, s, mid-1)
  ELSE
    ans = bFindlex(c, mid, e)
```

```
  END IF
END IF
RETURN
END FUNCTION bFindlex
SUBROUTINE cleanList()
IMPLICIT NONE
! Deallocate the list structure of logs to release the memory and set a flag.
!
! On input: None.
!
! On output: None.
!
! Local variable.
INTEGER :: i
! Deallocate all log nodes in the list.
DO i = 1, SIZE(fList%list)
  DEALLOCATE(fList%list(i)%c)
END DO
DEALLOCATE(fList%list)
! Set a flag that the log list has been deallocated.
fList%idx = -1
RETURN
END SUBROUTINE cleanList
SUBROUTINE enlargeList(len, copy)
IMPLICIT NONE
! Enlarge the current log list to size 'len'. The stored logs are
! preserved when 'copy' is .TRUE..
!
! On input:
! len  - The larger size of the list.
! copy - A switch indicating whether to copy the original content in
!        the list.  If .TRUE., the original logs will be copied to a
!        temporary buffer and then stored at the beginning of the
!        enlarged list.
!
! On output:
! fList%list - A larger list.
!
INTEGER, INTENT(IN) :: len
LOGICAL, INTENT(IN) :: copy
! Local variables.
INTEGER :: i
TYPE(LogNode), DIMENSION(:), ALLOCATABLE :: tmplist
! Exit if 'len' is not larger.
IF (len <= SIZE(fList%list)) RETURN
! Allocate 'tmplist' to temporarily store original logs.
IF (copy) THEN
  ALLOCATE(tmplist(fList%idx))
  DO i = 1, fList%idx
    ALLOCATE(tmplist(i)%c(N_I))
    tmplist(i)%c = fList%list(i)%c
    tmplist(i)%val = fList%list(i)%val
  END DO
END IF
! Deallocate the current list.
CALL cleanList()
```

```
! Reallocate the list with size 'len'.
CALL initList(len)
! Copy back the original list and deallocate the log nodes in 'tmplist'.
IF (copy) THEN
  DO i = 1, SIZE(tmplist)
    fList%list(i)%c = tmplist(i)%c
    fList%list(i)%val = tmplist(i)%val
    fList%idx = fList%idx + 1
    DEALLOCATE(tmplist(i)%c)
  END DO
  ! Deallocate 'tmplist'.
  DEALLOCATE(tmplist)
END IF
RETURN
END SUBROUTINE enlargeList
FUNCTION idxList() RESULT (ans)
IMPLICIT NONE
! Return the used size 'idx' of the list.
!
! On input: None.
!
! On output:
! ans - 'idx' of 'fList'.
!
INTEGER :: ans
ans = fList%idx
RETURN
END FUNCTION idxList
FUNCTION inList(c, val) RESULT(ans)
IMPLICIT NONE
! Recover the function value 'val' at 'c' in the order it was recorded
! at the list. 'inList' is called by VTdirect, and by pVTdirect only when
! the number of masters for the recovery run is the same as that for
! the run that generated the checkpoint file.
!
! On input:
! c  -  Point coordinates.
!
! On output:
! val - The function value at 'c'.
! ans - .TRUE. if 'val' is found.
!       .FALSE. if 'c' is not matched.
!
REAL(KIND = R8), DIMENSION(:), INTENT(IN) :: c
REAL(KIND = R8), INTENT(OUT) :: val
LOGICAL :: ans
! Initialize 'ans'.
ans = .FALSE.
! Update the index to the newest recovered log.
fList%idx = fList%idx + 1
! Exit when idx is out of range.
IF ((fList%idx > SIZE(fList%list)).OR.(fList%idx < 1)) RETURN
IF (ALL(c == fList%list(fList%idx)%c)) THEN
  ! Found 'c' and return 'val'.
  val = fList%list(fList%idx)%val
  ans = .TRUE.
```

```
ELSE
END IF
RETURN
END FUNCTION inList
SUBROUTINE initList(len)
IMPLICIT NONE
! Initialize the list of checkpoint logs.
!
! On input:
! len  - The number of log nodes to be initialized.
!
! On output:
! fList%list - Initialized list.
!
INTEGER, INTENT(IN) :: len
! Local variable.
INTEGER :: i
! Allocate 'fList' and 'len' number of log nodes.
ALLOCATE(fList%list(len))
DO i = 1, len
  ALLOCATE(fList%list(i)%c(N_I))
END DO
! Initialize 'idx'.
fList%idx = 0
RETURN
END SUBROUTINE initList
SUBROUTINE insList(c, val)
IMPLICIT NONE
! Insert 'c' and 'val' to the log list and update the index.
!
! On input:
! c    - Point coordinates.
! val  - The function value at 'c'.
!
! On output:
! fList%list - The updated log list.
!
REAL(KIND = R8), DIMENSION(:), INTENT(IN) :: c
REAL(KIND = R8), INTENT(IN) :: val
! Enlarge the list to be twice the current size if needed.
IF (fList%idx + 1 > SIZE(fList%list)) THEN
  CALL enlargeList(2*SIZE(fList%list), .TRUE.)
END IF
! Increase 'idx'.
fList%idx = fList%idx + 1
! Add 'c' and 'val'.
fList%list(fList%idx)%c = c
fList%list(fList%idx)%val = val
RETURN
END SUBROUTINE insList
FUNCTION lookupTab(c, val) RESULT(ans)
IMPLICIT NONE
! Do a binary search for 'c' to retrieve the corresponding function value
! 'val' in the table of logs sorted in lexicographical order.
! 'lookupTab' is only called by pVTdirect when the number of masters in
! the recovery run has changed from that in the run that generated the
```

```
! checkpoint logs.
!
! On input:
! c  -  Point coordinates.
!
! On output:
! val - The function value at 'c'.
! ans - .TRUE. if 'c' is found.
!       .FALSE. if 'c' is not found.
!
REAL(KIND = R8), DIMENSION(:), INTENT(IN) :: c
REAL(KIND = R8), INTENT(OUT) :: val
LOGICAL :: ans
! Local variables.
INTEGER :: i
! Initialize 'ans'.
ans = .FALSE.
! Do a binary search for 'c' in the table of logs sorted lexicographically.
i = bFindlex(c, 1, fList%idx)
IF (i /= 0) THEN
  ! 'c' is found, return 'val'.
  val = fList%list(i)%val
  ans = .TRUE.
END IF
RETURN
END FUNCTION lookupTab
FUNCTION moreList() RESULT (ans)
IMPLICIT NONE
! Return the recovery status of the log list 'fList'.
!
! On input: None.
!
! On output:
! ans - .TRUE. if the list has more logs to recover.
!       .FALSE. if the list has no more logs to recover.
!
LOGICAL :: ans
! Initialize 'ans'.
ans = .TRUE.
IF (fList%idx == -1) ans = .FALSE.
RETURN
END FUNCTION moreList
SUBROUTINE resetList()
IMPLICIT NONE
! Reset the index of the function value list to 0, preparing for
! recovery.
!
! On input: None.
!
! On output: Reset index in the function value list.
!
fList%idx = 0
RETURN
END SUBROUTINE resetList
SUBROUTINE siftdownList(pos, len)
IMPLICIT NONE
```

```
! Sift down the log at position 'pos' in the list with 'len' logs.
!
! On input:
! pos - Position of the log to be sifted down.
! len - The length of the list.
!
! On output:
! fList%list - A log list with the log at position 'pos' sifted down.
!
INTEGER, INTENT(IN) :: pos, len
! Local variables.
INTEGER :: i, left
IF (len == 0) RETURN ! Exit if there are no logs in the list.
i = pos  ! Let 'i' start at the log at 'pos'.
DO
  left = 2*i  ! Find the 'left' child of the log at 'i'.
  IF (left > len) EXIT ! Exit when log 'i' is a leaf.
  ! Find the larger one of the left and right (left+1) children.
  IF (left+1 <= len) THEN
    ! Let 'left' point to the right child (if present) if it is larger.
    IF (fList%list(left)%c .lexLT. fList%list(left+1)%c) left = left + 1
  END IF
  ! Compare 'left' child with the parent 'i'. Exit when 'i' is larger.
  IF (fList%list(left)%c .lexLT. fList%list(i)%c) EXIT
  ! Because 'i' is smaller, swap logs at 'i' and 'left'.
  CALL swapList(i, left)
  i = left ! Move down 'i'.
END DO
RETURN
END SUBROUTINE siftdownList
FUNCTION sizeList() RESULT (ans)
IMPLICIT NONE
! Return the size of the list.
!
! On input: None.
!
! On output:
! ans - Size of the log list 'fList'.
!
INTEGER :: ans
ans = SIZE(fList%list)
RETURN
END FUNCTION sizeList
SUBROUTINE sortList()
IMPLICIT NONE
! Sort the logs in the list.
!
! On input: None.
!
! On output:
! fList   - Sorted list of checkpoint logs.
!
! Local variables.
INTEGER :: i
! Heapify the entire list to be a maxheap.
DO i = fList%idx/2, 1, -1
```

```
  CALL siftdownList(i, fList%idx)
END DO
! Sort the list in ascending lexicographical order.
DO i=1, fList%idx
  ! Swap the largest one at the beginning with the one at end of the list.
  CALL swapList(1, fList%idx-(i-1))
  ! Sift down the first one.
  CALL siftdownList(1, fList%idx-i)
END DO
RETURN
END SUBROUTINE sortList
SUBROUTINE swapList(i, j)
IMPLICIT NONE
! Swap logs at positions 'i' and 'j' in the list.
!
! On input:
! i - Position of the first log to be swapped.
! j - Position of the second log to be swapped.
!
! On output:
! fList%list - Log list with positions 'i' and 'j' swapped.
!
INTEGER, INTENT(IN) :: i, j
! Local variables.
REAL(KIND = R8), DIMENSION(N_I) :: tmpc
REAL(KIND = R8) :: tmpf
IF (i == j) RETURN ! Exit when 'i' equals 'j'.
! Copy log 'i' to temporary variables.
tmpc = fList%list(i)%c
tmpf = fList%list(i)%val
! Copy log 'j' to 'i'.
fList%list(i)%c = fList%list(j)%c
fList%list(i)%val = fList%list(j)%val
! Copy back log 'i' to log 'j'
fList%list(j)%c = tmpc
fList%list(j)%val = tmpf
RETURN
END SUBROUTINE swapList
END MODULE VTDIRECT_CHKPT
```

Appendix D: Comments for VTdirect_MOD

The comments for the module VTdirect_MOD that declares subroutines and functions used in the serial VTDIRECT implementation are listed from the source code as below.

```
MODULE VTdirect_MOD
USE VTDIRECT_GLOBAL  ! Module (shared_modules.f95) for data types,
  ! parameters, global variables, interfaces, and internal subroutines.
USE VTDIRECT_COMMSUB ! Module (shared_modules.f95) for subroutines
  ! commonly used by VTdirect and pVTdirect.
USE VTDIRECT_CHKPT   ! Module (shared_modules.f95) for data types,
  ! subroutines, functions, global variables used by checkpointing.
CONTAINS
SUBROUTINE VTdirect(N, L, U, OBJ_FUNC, X, FMIN, STATUS, SWITCH, &
                    MAX_ITER, MAX_EVL, MIN_DIA, OBJ_CONV, EPS, &
                    MIN_SEP, W, BOX_SET, NUM_BOX, RESTART)
IMPLICIT NONE
! This is a serial implementation of the DIRECT global unconstrained
! optimization algorithm described in:
!
!    D.R. Jones, C.D. Perttunen, and B.E. Stuckman, Lipschitzian
!    optimization without the Lipschitz constant, Journal of Optimization
!    Theory and Applications, Vol. 79, No. 1, 1993, pp. 157-181.
!
! The algorithm to minimize f(x) inside the box L <= x <= U is as follows:
!
!    1. Normalize the search space to be the unit hypercube. Let c_1 be
!       the center point of this hypercube and evaluate f(c_1).
!    2. Identify the set S of potentially optimal rectangles.
!    3. For all rectangles j in S:
!       3a. Identify the set I of dimensions with the maximum side length.
!           Let delta equal one-third of this maximum side length.
!       3b. Sample the function at the points c +- delta*e_i for all i
!           in I, where c is the center of the rectangle and e_i is the
!           ith unit vector.
!       3c. Divide the rectangle containing c into thirds along the
!           dimensions in I, starting with the dimension with the lowest
!           value of f(c +- delta*e_i) and continuing to the dimension
!           with the highest f(c +- delta*e_i).
!    4. Repeat 2.-3. until stopping criterion is met.
!
! On input:
!
! N is the dimension of L, U, and X.
!
! L(1:N) is a real array giving lower bounds on X.
!
! U(1:N) is a real array giving upper bounds on X.
!
! OBJ_FUNC is the name of the real function procedure defining the
!    objective function f(x) to be minimized. OBJ_FUNC(C,IFLAG) returns
!    the value f(C) with IFLAG=0, or IFLAG/=0 if f(C) is not defined.
!    OBJ_FUNC is precisely defined in the INTERFACE block below.
!
! Optional arguments:
```

```
!
! SWITCH =
!    1   select potentially optimal boxes on the convex hull of the
!        (box diameter, function value) points (default).
!    0   select as potentially optimal the box with the smallest function
!        value for each diameter that is above the roundoff level.
!        This is an aggressive selection procedure that generates many more
!        boxes to subdivide.
!
! MAX_ITER is the maximum number of iterations (repetitions of Steps 2-3)
!    allowed; defines stopping rule 1. If MAX_ITER is present but <= 0
!    on input, there is no iteration limit and the number of iterations
!    executed is returned in MAX_ITER.
!
! MAX_EVL is the maximum number of function evaluations allowed; defines
!    stopping rule 2. If MAX_EVL is present but <= 0 on input, there is no
!    limit on the number of function evaluations, which is returned in
!    MAX_EVL.
!
! MIN_DIA is the minimum box diameter allowed; defines stopping rule 3.
!    If MIN_DIA is present but <= 0 on input, a minimum diameter below
!    the roundoff level is not permitted, and the box diameter of the
!    box containing the smallest function value FMIN is returned in
!    MIN_DIA.
!
! OBJ_CONV is the smallest acceptable relative improvement in the minimum
!    objective function value 'FMIN' between iterations; defines
!    stopping rule 4. OBJ_CONV must be positive and greater than the round
!    off level.  If absent, it is taken as zero.
!
! EPS is the tolerance defining the minimum acceptable potential
!    improvement in a potentially optimal box.  Larger EPS values
!    eliminate more boxes from consideration as potentially optimal,
!    and bias the search toward exploration.  EPS must be positive and
!    greater than the roundoff level.  If absent, it is taken as
!    zero.  EPS > 0 is incompatible with SWITCH = 0.
!
! MIN_SEP is the specified minimal (weighted) distance between the
!    center points of the boxes returned in the optional array BOX_SET.
!    If absent or invalid, MIN_SEP is taken as 1/2 the (weighted) diameter
!    of the box [L, U].
!
! W(1:N) is a positive real array.  The distance between two points X
!    and Y is defined as SQRT(SUM( (X-Y)*W*(X-Y) )).  If absent, W is
!    taken as all ones.
!
! BOX_SET is an empty array (TYPE HyperBox) allocated to hold the desired
!    number of boxes.
!
! RESTART =
!    0, checkpointing is off (default).
!    1, all function evaluations are logged to a file.
!    2, the program restarts from the checkpoint file 'vtdirchkpt.dat'
!       and new function evaluation logs will be appended to the end of
!       the file.
!
```

```
! On output:
!
! X(1:N) is a real vector containing the sampled box center with the
!    minimum objective function value FMIN.
!
! FMIN is the minimum function value.
!
! STATUS is a return status flag. The units decimal digit specifies
!    which stopping rule was satisfied on a successful return. The tens
!    decimal digit indicates a successful return, or an error condition
!    with the cause of the error condition reported in the units digit.
!
! Tens digit =
!  0 Normal return.
!    Units digit =
!     1   Stopping rule 1 (iteration limit) satisfied.
!     2   Stopping rule 2 (function evaluation limit) satisfied.
!     3   Stopping rule 3 (minimum diameter reached) satisfied. The
!         minimum diameter corresponds to the box for which X and
!         FMIN are returned.
!     4   Stopping rule 4 (relative change in 'FMIN') satisfied.
!  1 Input data error.
!    Units digit =
!     0   N < 2.
!     1   Assumed shape array L, U, W, or X does not have size N.
!     2   Some lower bound is >= the corresponding upper bound.
!     3   MIN_DIA, OBJ_CONV, or EPS is invalid or below the roundoff level.
!     4   None of MAX_EVL, MAX_ITER, MIN_DIA, and OBJ_CONV are specified;
!         there is no stopping rule.
!     5   Invalid SWITCH value.
!     6   SWITCH = 0 and EPS > 0 are incompatible.
!     7   RESTART has an invalid value.
!  2 Memory allocation error or failure.
!    Units digit =
!     0   BoxMatrix type allocation.
!     1   BoxLink or BoxLine type allocation.
!     2   int_vector or real_vector type allocation.
!     3   HyperBox type allocation.
!     4   BOX_SET is allocated with a wrong problem dimension.
!  3 Checkpoint file error.
!    Units digit =
!     0   Open error. If RESTART==1, an old checkpoint file vtdirchkpt.dat
!         may be present and needs to be removed. If RESTART==2,
!         vtdirchkpt.dat does not exist.
!     1   Read error.
!     2   Write error.
!     3   The file header does not match with the current setting.
!     4   A log is missing in the file for recovery.
!
! Optional arguments:
!
! MAX_ITER (if present) contains the number of iterations.
!
! MAX_EVL (if present) contains the number of function evaluations.
!
! MIN_DIA (if present) contains the diameter of the box associated with
```

```
!    X and FMIN.
!
! MIN_SEP (if present) is unchanged if it was a reasonable value on
!    input. Otherwise, it is reset to the default value.
!
! W (if present) is unchanged if it was positive on input. Any
!    non-positive component is reset to one.
!
! BOX_SET (if present) is an array of TYPE (HyperBox) containing the
!    best boxes with centers separated by at least MIN_SEP.
!    The number of returned boxes NUM_BOX <= SIZE(BOX_SET) is as
!    large as possible given the requested separation.
!
! NUM_BOX (if present) is the number of boxes returned in the array
!    BOX_SET(1:).
!
```

Appendix E: Comments for pVTdirect_MOD

The comments for the module pVTdirect_MOD that defines data types, subroutines, and functions used in the parallel VTDIRECT implementation are listed from the source code as below.

```
MODULE pVTdirect_MOD
USE VTDIRECT_GLOBAL  ! Module (shared_modules.f95) for data types,
  ! parameters, global variables, interfaces, and internal subroutines.
USE VTDIRECT_COMMSUB ! Module (shared_modules.f95) for subroutines
  ! used by VTdirect and pVTdirect in common.
USE VTDIRECT_CHKPT   ! Module (shared_modules.f95) for data types,
  ! subroutines, functions, global variables used by checkpointing.
INCLUDE "mpif.h"     ! MPI library functions.
!
!OptResults: Contains the search results for a subdomain.
!  fmin      - Minimum function value.
!  x         - The point coordinates associated with 'fmin'.
!  max_iter  - Number of iterations.
!  max_evl   - Number of evaluations.
!  min_dia   - Minimum diameter.
!  status    - Search return status.
!
TYPE OptResults
  REAL(KIND = R8) :: fmin
  REAL(KIND = R8), DIMENSION(:), POINTER :: x
  INTEGER :: max_iter
  INTEGER :: max_evl
  REAL(KIND = R8) :: min_dia
  INTEGER :: status
END TYPE OptResults
! MPI message types.
! A nonblocking function evaluation request.
INTEGER, PARAMETER :: NONBLOCK_REQ = 1
! A blocking function evaluation request.
INTEGER, PARAMETER :: BLOCK_REQ = 2
! Point(s) responding to a nonblocking request.
INTEGER, PARAMETER :: POINT_NBREQ = 3
! Point(s) responding to a blocking request.
INTEGER, PARAMETER :: POINT_BREQ = 4
! No more point for evaluation.
INTEGER, PARAMETER :: NO_POINT = 5
! Returned point function value(s).
INTEGER, PARAMETER :: FUNCVAL = 6
! All search work is done.
INTEGER, PARAMETER :: MYALL_DONE = 7
! Updating the global counter for the blocked workers.
INTEGER, PARAMETER :: COUNT_DONE = 8
! Search results.
INTEGER, PARAMETER :: RESULT_DATA = 9
! Converting a master to a worker.
INTEGER, PARAMETER :: BE_WORKER = 11
! Termination.
INTEGER, PARAMETER :: TERMINATE = 13
! Updating intermediate search results.
```

```
INTEGER, PARAMETER :: UPDATES = 14
! MPI error.
INTEGER, PARAMETER :: DMPI_ERROR = 40
CONTAINS
SUBROUTINE pVTdirect_finalize()
! MPI finalization.
!
! On input: None.
!
! On output: None.
!
! Local variable.
INTEGER :: ierr
CALL MPI_FINALIZE(ierr)
RETURN
END SUBROUTINE pVTdirect_finalize
SUBROUTINE pVTdirect_init(iflag)
! MPI initialization.
!
! On input: None.
!
! On output:
! iflag - Initialization status.
!
INTEGER, INTENT(OUT) :: iflag
iflag = 0
CALL MPI_INIT(iflag)
IF (iflag /= MPI_SUCCESS) THEN
  iflag = DMPI_ERROR
END IF
RETURN
END SUBROUTINE pVTdirect_init
SUBROUTINE pVTdirect(N, L, U, OBJ_FUNC, X, FMIN, PROCID, STATUS, &
                     SWITCH, MAX_ITER, MAX_EVL, MIN_DIA, OBJ_CONV, EPS, &
                     MIN_SEP, W, BOX_SET, NUM_BOX, N_SUB, N_MASTER, &
                     BINSIZE, RESTART)
IMPLICIT NONE
! This is a parallel implementation of the DIRECT global
! unconstrained optimization algorithm described in:
!
!    D.R. Jones, C.D. Perttunen, and B.E. Stuckman, Lipschitzian
!    optimization without the Lipschitz constant, Journal of Optimization
!    Theory and Application, Vol. 79, No. 1, 1993, pp. 157-181.
!
! The algorithm to minimize f(x) inside the box L <= x <= U is as follows:
!
!    1. Normalize the search space to be the unit hypercube. Let c_1 be
!       the center point of this hypercube and evaluate f(c_1).
!    2. Identify the set S of potentially optimal rectangles.
!    3. For all rectangles j in S:
!       3a. Identify the set I of dimensions with the maximum side length.
!           Let delta equal one-third of this maximum side length.
!       3b. Sample the function at the points c +- delta*e_i for all i
!           in I, where c is the center of the rectangle and e_i is the ith
!           unit vector.
!       3c. Divide the rectangle containing c into thirds along the
```

```
!           dimensions in I, starting with the dimension with the lowest
!           value of f(c +- delta*e_i) and continuing to the dimension
!           with the highest f(c +- delta*e_i).
!    4. Repeat 2.-3. until stopping criterion is met.
!
! On input:
!
! N is the dimension of L, U, and X.
!
! L(1:N) is a real array giving lower bounds on X.
!
! U(1:N) is a real array giving upper bounds on X.
!
! OBJ_FUNC is the name of the real function procedure defining the
!    objective function f(x) to be minimized. OBJ_FUNC(C,IFLAG) returns
!    the value f(C) with IFLAG=0, or IFLAG/=0 if f(C) is not defined.
!    OBJ_FUNC is precisely defined in the INTERFACE block below.
!
! Optional arguments:
!
! SWITCH =
!    1   select potentially optimal boxes on the convex hull of the
!        (box diameter, function value) points (default).
!    0   select as potentially optimal the box with the smallest function
!        value for each diameter that is above the roundoff level.
!        This is an aggressive selection procedure that generates many more
!        boxes to subdivide.
!
! MAX_ITER is the maximum number of iterations (repetitions of Steps 2-3)
!    allowed; defines stopping rule 1. If MAX_ITER is present but <= 0
!    on input, there is no iteration limit and the number of iterations
!    executed is returned in MAX_ITER.
!
! MAX_EVL is the maximum number of function evaluations allowed; defines
!    stopping rule 2. If MAX_EVL is present but <= 0 on input, there is no
!    limit on the number of function evaluations, which is returned in
!    MAX_EVL.
!
! MIN_DIA is the minimum box diameter allowed; defines stopping rule 3.
!    If MIN_DIA is present but <= 0 on input, a minimum diameter below
!    the roundoff level is not permitted, and the box diameter of the
!    box containing the smallest function value FMIN is returned in
!    MIN_DIA.
!
! OBJ_CONV is the smallest acceptable relative improvement in the minimum
!    objective function value 'FMIN' between iterations; defines
!    stopping rule 4. OBJ_CONV must be positive and greater than the round
!    off level.  If absent, it is taken as zero.
!
! EPS is the tolerance defining the minimum acceptable potential
!    improvement in a potentially optimal box.  Larger EPS values
!    eliminate more boxes from consideration as potentially optimal,
!    and bias the search toward exploration.  EPS must be positive and
!    greater than the roundoff level.  If absent, it is taken as
!    zero.  EPS > 0 is incompatible with SWITCH = 0.
!
```

```
! MIN_SEP is the specified minimal (weighted) distance between the
!    center points of the boxes returned in the optional array BOX_SET.
!    If absent or invalid, MIN_SEP is taken as 1/2 the (weighted) diameter
!    of the box [L, U].
!
! W(1:N) is a positive real array.  It is used in computing the distance
!    between two points X and Y as SQRT(SUM( (X-Y)*W*(X-Y) )) or scaling the
!    dimensions W*(U-L) for domain decomposition.  If absent, W is taken as
!    all ones.
!
! BOX_SET is an empty array (TYPE HyperBox) allocated to hold the desired
!    number of boxes.
!
! N_SUB is the specified number of subdomains that run the DIRECT search
!    in parallel. If absent or invalid (out of the range [1,32]), it is
!    taken as 1 (default).
!
! N_MASTER is the specified number of masters per subdomain. If absent or
!    invalid, it is taken as 1 (default).
!
! BINSIZE is the number of function evaluations per task to be sent at one
!    time. If absent, it is taken as 1 (default).
!
! RESTART
!    0, checkpointing is off (default).
!    1, function evaluations are logged to a file 'pvtdirchkpt.dat*' tagged
!       with the subdomain ID and the master ID.
!    2, the program restarts from checkpoint files on all masters and new
!       function evaluation logs will be appended to the end of the files.
!       When 'N_MASTER' has changed for the recovery run, at every
!       iteration, each master reads all the checkpoint logs for that
!       iteration from all checkpoint files. A new set of checkpoint files
!       is created to record the function evaluation logs.
!
! On output:
!
! X(1:N) is a real vector containing the sampled box center with the
!    minimum objective function value FMIN.
!
! FMIN is the minimum function value.
!
! PROCID is the assigned processor ID that is used for printing out the
!    final results.
!
! STATUS is an array of return status flags for 'N_SUB' subdomains. For
!    the final search result, the units decimal digit of the ith element
!    of the array represents the return status of subdomain i; the units
!    decimal digit tens decimal digit indicates a successful return, or an
!    error condition with the cause of the error condition reported in the
!    units digit. During the search process, the first array element is used
!    for intermediate status on each processor.
!
! Tens digit =
!  0 Normal return.
!    Units digit =
!     1   Stopping rule 1 (iteration limit) satisfied.
```

```
!     2   Stopping rule 2 (function evaluation limit) satisfied.
!     3   Stopping rule 3 (minimum diameter reached) satisfied. The
!         minimum diameter corresponds to the box for which X and
!         FMIN are returned.
!     4   Stopping rule 4 (relative change in 'FMIN') satisfied.
!  1 Input data error.
!    Units digit =
!     0   N < 2.
!     1   Assumed shape array L, U, or X does not have size N.
!     2   Some lower bound is >= the corresponding upper bound.
!     3   MIN_DIA, OBJ_CONV, or EPS is invalid or below the roundoff level.
!     4   None of MAX_EVL, MAX_ITER, MIN_DIA, and OBJ_CONV are specified;
!         there is no stopping rule.
!     5   Invalid SWITCH value.
!     6   SWITCH = 0 and EPS > 0 are incompatible.
!     7   RESTART has an invalid value.
!     8   Problem with the parallel scheme: the requested number of
!         processors is too small, or the worker to master ratio is less
!         than 2, or BOX_SET is specified for the multiple masters case.
!     9   BINSIZE has an invalid value.
!  2 Memory allocation error or failure.
!    Units digit =
!     0   BoxMatrix type allocation.
!     1   BoxLink or BoxLine type allocation.
!     2   int_vector or real_vector type allocation.
!     3   HyperBox type allocation.
!     4   BOX_SET is allocated with a wrong problem dimension.
!  3 Checkpoint file error.
!     0   Open error. If RESTART==1, an old checkpoint file may be present
!         and needs to be removed. If RESTART==2, the file may not exist.
!     1   Read error.
!     2   Write error.
!     3   The file header does not match with the current setting.
!     4   A log is missing in the file for recovery.
!  4 MPI error.
!     0   Initialization error.
!     1   MPI_COMM_RANK error.
!     2   MPI_COMM_GROUP error.
!     3   MPI_COMM_SIZE error.
!     4   MPI_GROUP_INCL error.
!     5   MPI_COMM_CREATE error.
!     6   MPI_GROUP_RANK error.
!     7   At least one processor aborts.
! Optional arguments:
!
! MAX_ITER (if present) contains the number of iterations.
!
! MAX_EVL (if present) contains the number of function evaluations.
!
! MIN_DIA (if present) contains the diameter of the box associated with
!         X and FMIN.
!
! MIN_SEP (if present) is unchanged if it was a reasonable value on
!         input. Otherwise, it is reset to the default value.
!
! W (if present) is unchanged if it was positive on input. Any
```

```
!   non-positive component is reset to one.
!
! BOX_SET (if present) is an array of TYPE (HyperBox) containing the
!          best boxes with centers separated by at least MIN_SEP.
!          The number of returned boxes NUM_BOX <= SIZE(BOX_SET) is as
!          large as possible given the requested separation.
!
! NUM_BOX (if present) is the number of boxes returned in the array
!         BOX_SET(1:).
!
! N_SUB (if present) is the actual number of subdomains.
!
! N_MASTER (if present) is the actual number of masters.
!
```

VITA

Jian He was born on September 19th, 1975 in Sichuan Province, China. She earned a bachelor's degree in Computer Engineering in July 1996 from Nanjing University of Science and Technology, Nanjing, China. From 1996 to 1999, Jian worked in the software team that successfully developed and deployed the first WSR-98D Doppler weather radar system at METSTAR Meteorological Radar System Company, a joint venture set up by Lockheed Martin Corporation and China Meteorological Administration in Beijing, China.

Motivated by her work experience in weather radar systems, Jian began graduate study in physics at the University of Wisconsin, Milwaukee in August 1999. Meantime, her research interest was developing towards generic modeling and computational techniques. In August 2000, she accepted a graduate research assistantship offered by Professor Layne T. Watson in computer science and mathematics at Virginia Polytechnic Institute and State University, also known as Virginia Tech. Since then, Jian has been working on research projects that exploit computing resources to solve complex engineering and scientific problems. In October 2002, she received the Master of Science degree in computer science and continued her study in pursuit of the Doctor of Philosophy degree. In Fall 2007, she successfully defended her Ph.D. work in the area of parallel global optimization. During her graduate studies, Jian did a summer internship in the Advanced Computations Department led by Dr. Kwok Ko at the Stanford Linear Accelerator Center, where she worked on dynamic flux balance analysis of metabolic networks.

Jian actively participated in research collaborations and presented her work in technical conferences and seminars. She was awarded outstanding graduate research awards for both her master's and doctoral work at Virginia Tech.